

1D-00548

TECHNICAL MEMORANDUM

---

**Results of a Geophysics Study to Characterize Geology  
at Naval Air Station Memphis, Millington, Tennessee**

---

In support of a RCRA Facility Investigation  
CTO-016, contract No. N62467-89-D-0318

for

**The Department of the Navy**  
Southern Division Naval Facilities Engineering Command  
North Charleston, South Carolina

by

**EnSafe/Allen & Hoshall**

5720 Summer Trees Dr., Suite 8, Memphis, TN 38134 • (901)383-9115

27 January 1995

## Table of Contents

Executive Summary . . . . .	iii
1.0 Introduction . . . . .	1
2.0 Site Background . . . . .	2
2.1 Geology . . . . .	2
2.2 Hydrology and Potential For Inter-Aquifer Contamination . . . . .	4
2.3 Development of a Geological Database . . . . .	5
3.0 Geophysical Application . . . . .	7
3.1 Description of TEM . . . . .	7
3.2 Field Application and Logistics . . . . .	8
3.3 Data Processing . . . . .	9
3.4 QA/QC Summary . . . . .	10
4.0 Data Interpretation . . . . .	11
4.1 Comparison of Surface and Downhole Geophysics . . . . .	11
4.2 TEM Formation Picks at Control Points . . . . .	24
4.3 TEM Picks Away From Control Points . . . . .	27
4.4 Cross-Section Interpretations . . . . .	28
4.5 Plan-View Interpretations . . . . .	36
5.0 Conclusions . . . . .	67
6.0 References . . . . .	68

## List of Figures

Fig. 1.	Location of Naval Air Station Memphis. . . . .	2
Fig. 2.	Typical shallow geology at NAS Memphis. The Cockfield and Cook Mountain formations act as a confining layer to the Memphis Sand aquifer. . . . .	3
Fig. 3.	Comparison of downhole resistivity log and surface TEM model results, test hole No. 1 (V-74). . . . .	13
Fig. 4.	Comparison of downhole resistivity log and surface TEM model results, test hole No. 2 (U-98). . . . .	15
Fig. 5.	Comparison of downhole resistivity log and surface TEM model results, test hole No. 3 (V-75). . . . .	17
Fig. 6.	Comparison of downhole resistivity log and surface TEM model results, test hole No. 4 (U-99). . . . .	19
Fig. 7.	Comparison of downhole resistivity log and surface TEM model results, test hole No. 5 (V-76). . . . .	21
Fig. 8.	Location of cross-sections shown in Plates 1 to 3. . . . .	28

## List of Tables

Table 1	Geological Database, NAS Memphis . . . . .	6
Table 2	Comparison of Drillhole and TEM Depth Picks . . . . .	25

## List of Plates

Plate 1	Joint Geophysics/Geology Interpretation TEM CROSS-SECTION A-A . .	29
Plate 2	Joint Geophysics/Geology Interpretation TEM CROSS-SECTION B-B . .	31
Plate 3	Joint Geophysics/Geology Interpretation TEM CROSS-SECTION C-C . .	33
Plate 4	Map of Surface Figures, Geophysics Investigation . . . . .	37
Plate 5	Surface Topography, NAS Memphis . . . . .	39
Plate 6	Top of Memphis Sand . . . . .	41
Plate 7	Top of Cook Mountain . . . . .	43
Plate 8	Thickness of Cook Mountain . . . . .	45
Plate 9	Top of Cockfield . . . . .	47
Plate 10	Thickness of Cockfield . . . . .	49
Plate 11	Thickness of confining layer . . . . .	51
Plate 12	Top of Fluival Unit . . . . .	53
Plate 13	Thickness of Fluvial Unit . . . . .	55
Plate 14	Base of Loess Conductor . . . . .	57
Plate 15	Top of Loess Conductor . . . . .	59
Plate 16	Thickness of Loess Conductor . . . . .	61

---

## **Executive Summary**

To prepare for future transfer of property on the northside of NAS Memphis, EnSafe/Allen & Hoshall recently conducted a geophysics study of the area. The purpose of the work was to generate a geologic conceptual model to help understand the potential for downward migration of near-surface contaminants into industrial and domestic water supplies. The geophysics results are based on an integration of surface geophysics data with results from five recent test holes and past drilling.

The study indicates that a confining layer of clay, which protects the Memphis Sand drinking water supply from near-surface contaminants, is present throughout the area. Thin areas or "pinchouts" in the clay are not indicated in the data, nor are faults. Based on these findings, the confining layer appears to be an effective barrier to downward migration of near-surface contamination to the Memphis Sand aquifer in the immediate area. However, shallower aquifers, which produce some non-potable industrial water, are not similarly protected. These waters will be tested during upcoming environmental investigations at the site.

---

**This page intentionally left blank.**

## **1.0 Introduction**

The northside of Naval Air Station Memphis (NAS Memphis) will be transferred to civilian control after a Resource Conservation and Recovery Act (RCRA) facility investigation (RFI) of 28 contaminated sites, known as solid waste management units (SWMUs). The goal of the RFI is to characterize the nature and extent of any contamination found and to recommend any necessary remediation procedures. Ensafe/Allen & Hoshall (E/A&H) has been retained under the Comprehensive Long-Term Environmental Action-Navy (CLEAN) contract to perform RFI characterization.

To provide a better understanding of potential contaminant pathways, the present study was commissioned to map subsurface geology. Five test boreholes were drilled and logged by the United States Geological Survey (USGS), and 90 geophysical soundings were performed by E/A&H. This Technical Memorandum integrates the findings to produce a single geologic interpretation of the area. Specific results from the USGS work will be reported separately and will serve as the sole authorized USGS interpretation.

The specific objectives of the geophysics work were to:

- ▶ Map the subsurface stratigraphy in three dimensions to evaluate features of importance in contaminant movement or retention, especially to potable water aquifers.
- ▶ Provide evidence of geologic structures which might affect contaminant movement.
- ▶ Integrate the geophysics results with previous drilling data and other information to provide a coherent geologic conceptual model.

The need for vertical penetration in the 70-meter (m) range and the large area needed to be characterized narrowed the choice of appropriate geophysical techniques to reflection seismics, audiofrequency magnetotellurics, and transient electromagnetics. Transient electromagnetics was selected as the best technique to fulfill the intended objectives.



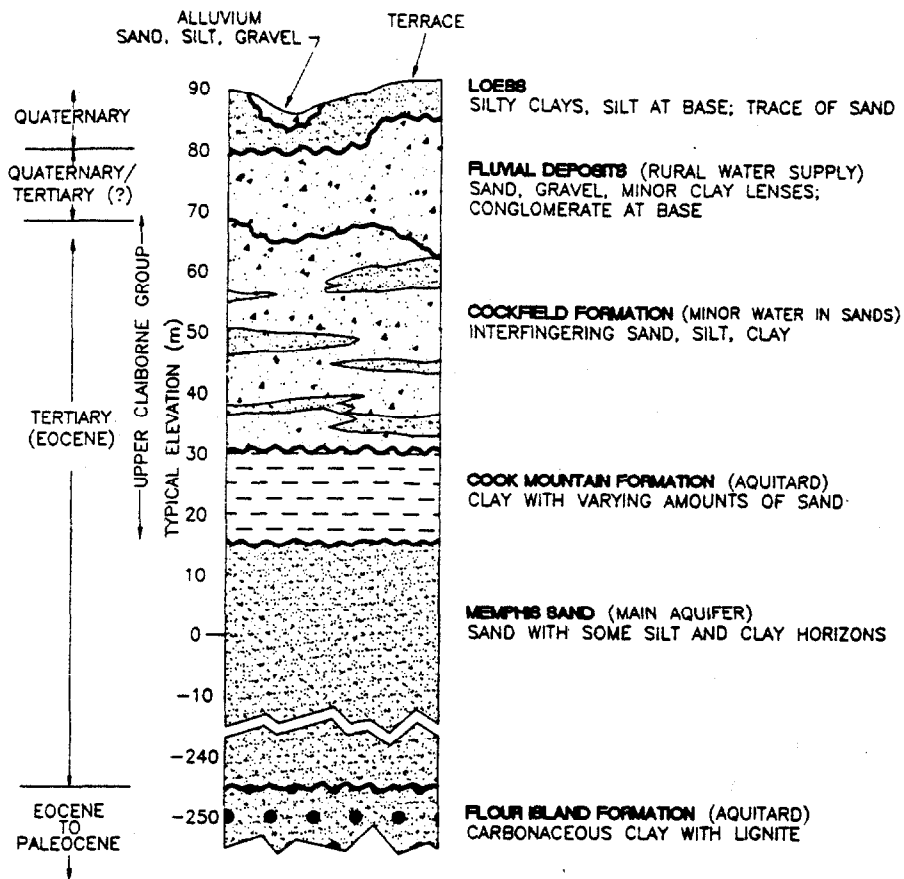


Fig. 2. Typical shallow geology at NAS Memphis. The Cockfield and Cook Mountain formations act as a confining layer to the Memphis Sand aquifer.

Above the Cook Mountain is the Cockfield Formation, a sequence of interfingering fine sand, silt, clay, and lignite lenses. It is heavily eroded locally, causing its top elevation and thickness to vary considerably over relatively short distances.

Quaternary/Tertiary fluvial deposits overlie the Cockfield, and consist of sand and clay, with gravels at their base. They commonly form terrace deposits, with or without a topographic expression at the surface (Parks, personal communication, 1994; see also Parks, 1992). These deposits occur along old downcut river channels and may be extensively eroded.

At the surface at NAS Memphis are loess deposits of Pleistocene age. These deposits include silt, silty clay, and traces of sand. Gravel and coarse sand are often found at the base. In some surface drainages, a thin cover of local alluvium may be present.

## **2.2 Hydrology and Potential For Inter-Aquifer Contamination**

Water-bearing units in the strata above the Memphis Sand are generally thin and discontinuous. Some water is present in the lower loess, but permeabilities are low and the unit is not sufficient to serve as a water supply. The fluvial unit supplies water to rural areas and to water the golf courses at NAS Memphis. Groundwater is semi-confined and flows southeast.

Some domestic wells are screened within the Cockfield (Parks, 1990), and regionally flow is to the south (Parks and Carmichael, 1990). However, water production at NAS Memphis is limited because of a high clay content. In this area, the Cockfield is regarded as an aquitard, and together with the Cook Mountain Formation is part of the Jackson-Upper Claiborne confining sequence which overlies the Memphis Sand.

The Memphis Sand is a high-producing, high-quality aquifer. Two of the five current production wells at NAS Memphis are screened in this unit, which is locally about 260 m thick. The other three wells are in the Fort Pillow Sand, located beneath a confining layer below the Memphis Sand. The Memphis Sand is confined at the base by the Flour Island Formation, and at the top by the Cook Mountain Formation clays.

While the Upper-Claiborne confining layers constrain the main aquifer to the Memphis Sand, they do not always form a uniformly effective confining layer to downward migration of surface contamination. For example, Graham and Parks (1986) and Parks and Lounsbury (1975) present several lines of evidence that the aquifer may be supplied by near-surface sources, suggesting potential vertical communication to the aquifer. Mirecki and Parks (1994) identified a window in the confining clay over the Memphis Sand at the Shelby County Landfill, 28 km south of NAS Memphis, and confirmed inter-aquifer communication by identifying landfill contaminants in the Memphis Sand aquifer.

Faults have long been suspected in the area. Faulting might provide contaminant migration pathways if the fault zone is more porous, or can cause formation thinning by erosion on upthrown blocks. Based on borehole logs and stratigraphic descriptions in wells throughout Shelby County, Kingsbury and Parks (1993) interpret north-northeast and east-southeast sets of normal faults extending from depth up through at least the top of the Memphis Sand (the discontinuous depositional nature of the overlying units makes it difficult to determine if the faults extend further toward the surface). At the Memphis Sand, the throw on these faults is

estimated to range up to approximately 50 m. However, the existence of faults is still controversial, and alternative explanations such as erosional features are viable ones.

To date, there has been no evidence of an erosional window or significant faulting in the confining sequence at NAS Memphis. The Cook Mountain, representing the most effective confining unit, has been encountered in all borings, although its thickness can vary over relatively short distances (Parks, 1990). Insufficient drillhole control exists to characterize locally important structures and formational thicknesses. Facies, which could present a migration pathway through chance spatial alignments of sandy units, are poorly mapped in the NAS Memphis area. Faults might also present a direct migration path, and these too are poorly mapped on a small scale. Clearly, identifying stratigraphic windows and faults is an important part of the geophysical investigation.

### **2.3 Development of a Geological Database**

As a part of this report, E/A&H has assembled a geologic database from historic drilling on and off the NAS Memphis property. Sources include published literature, various environmental reports and documents, and NAS Memphis drilling records from engineering and production wells. Added to this are various borehole geophysical logs obtained by the USGS and a consistent suite of lithologic and geophysical logs from five test holes drilled by the USGS as a part of the geologic conceptual model development.

Formation picks were made based on drilling logs and geophysical logs. Drilling logs which were judged too general or which had poor lithologic descriptions were omitted from the process; these unfortunately included about a dozen deep test holes and all the NAS Memphis production wells.

The data were reviewed by E/A&H and USGS personnel (Kingsbury, 1994) to check for unusual or erroneous picks. In some cases, previously published picks were revised based on recent drilling information. Although this review was informal, it probably was sufficiently thorough to correct most problems in the data. Remaining errors are likely to be small.

The geologic database is presented in Table 1. Sources are footnoted. Note that the confining unit is present in all the wells in the database.

Table 1  
 Geological Database, NAS Memphis

Boring	State Plane (NAD82)		Formation Tops (m)					Thickness Confining Unit (m)
	East (feet)	North (feet)	Surface Elev. (m)	Fluvial	Cock- field	Cook Mtn.	Memphis Sand	
TH-1 (V-74)	819325 <sup>a</sup>	389939 <sup>a</sup>	87.0 <sup>a</sup>	76.6 <sup>a</sup>	67.2 <sup>a</sup>	27.9 <sup>a</sup>	-	-
TH-2 (U-98)	812941 <sup>a</sup>	394378 <sup>a</sup>	86.6 <sup>a</sup>	72.9 <sup>a</sup>	57.9 <sup>a</sup>	32.3 <sup>a</sup>	-	-
TH-3 (V-75)	816308 <sup>a</sup>	397764 <sup>a</sup>	99.3 <sup>a</sup>	94.1 <sup>a</sup>	89.4 <sup>a</sup>	38.9 <sup>a</sup>	-	-
TH-4 (U-99)	811592 <sup>a</sup>	391410 <sup>a</sup>	81.6 <sup>a</sup>	69.4 <sup>a</sup>	60.9 <sup>a</sup>	50.5 <sup>a</sup>	36.5 <sup>a</sup>	24.4
TH-5 (V-76)	814576 <sup>a</sup>	391713 <sup>a</sup>	88.5 <sup>a</sup>	79.4 <sup>a</sup>	62.3 <sup>a</sup>	31.2 <sup>a</sup>	-	-
U-54	806880 <sup>b</sup>	390601 <sup>b</sup>	80.8 <sup>b</sup>	69. <sup>b</sup>	58.2 <sup>b</sup>	-	25.3 <sup>b</sup>	32.9
U-55	807798 <sup>b</sup>	390767 <sup>b</sup>	80.8 <sup>b</sup>	67. <sup>b</sup>	51.5 <sup>b</sup>	43.6 <sup>b</sup>	35.6 <sup>b</sup>	15.9
U-58	810797 <sup>b</sup>	389029 <sup>b</sup>	80.8 <sup>b</sup>	67. <sup>b</sup>	60.7 <sup>b</sup>	39. <sup>b</sup>	27.8 <sup>b</sup>	32.9
U-59	811084 <sup>b</sup>	387904 <sup>b</sup>	80.8 <sup>b</sup>	69.8 <sup>b</sup>	51.2 <sup>b</sup>	41. <sup>b</sup>	32.0 <sup>b</sup>	19.2
U-60	812895 <sup>b</sup>	389654 <sup>b</sup>	89.0 <sup>b</sup>	80.5 <sup>b</sup>	62.2 <sup>b</sup>	47.5 <sup>b</sup>	26.8 <sup>b</sup>	35.4
V-4	814039 <sup>b</sup>	391329 <sup>b</sup>	86.3 <sup>b</sup>	-	62.5 <sup>b</sup>	37.5 <sup>b</sup>	23.8 <sup>b</sup>	38.7
V-9	822273 <sup>b</sup>	387766 <sup>b</sup>	83.2 <sup>b</sup>	72.5 <sup>b</sup>	64.9 <sup>b</sup>	38.0 <sup>b</sup>	29. <sup>b</sup>	35.9
V-10	822430 <sup>b</sup>	387557 <sup>b</sup>	82.6 <sup>b</sup>	-	63.4 <sup>b</sup>	47. <sup>b</sup>	32.9 <sup>b</sup>	30.5
V-24	822395 <sup>b</sup>	401421 <sup>b</sup>	114.3 <sup>b</sup>	106. <sup>b</sup>	93.3 <sup>b</sup>	35.7 <sup>b</sup>	26.8 <sup>b</sup>	66.5
Lake House (V-77)	819356 <sup>a</sup>	398903 <sup>a</sup>	98.6 <sup>a</sup>	92.5 <sup>a</sup>	87.6 <sup>a</sup>	-	-	-
Runway	814094 <sup>a</sup>	395619 <sup>a</sup>	89.5 <sup>a</sup>	77.8 <sup>a</sup>	-	-	-	-
GM-1	817358 <sup>a</sup>	383664 <sup>a</sup>	81.4 <sup>c</sup>	67.9 <sup>c</sup>	-	-	-	-
GM-2	816430 <sup>a</sup>	382564 <sup>a</sup>	80.7 <sup>c</sup>	71.6 <sup>c</sup>	-	-	-	-
GM-3	815798 <sup>a</sup>	382699 <sup>a</sup>	81.6 <sup>c</sup>	72.5 <sup>c</sup>	-	-	-	-
GM-5	814742 <sup>a</sup>	383103 <sup>a</sup>	80.9 <sup>c</sup>	68.7 <sup>c</sup>	-	-	-	-
GM-6	814844 <sup>a</sup>	390879 <sup>a</sup>	87.3 <sup>c</sup>	75.1 <sup>c</sup>	-	-	-	-
GM-7	814852 <sup>a</sup>	390736 <sup>a</sup>	86.5 <sup>c</sup>	71.3 <sup>c</sup>	-	-	-	-
GM-9	813725 <sup>a</sup>	392034 <sup>a</sup>	86.6 <sup>c</sup>	76.2 <sup>c</sup>	-	-	-	-
GM-10	816144 <sup>a</sup>	397881 <sup>a</sup>	99.8 <sup>c</sup>	92.2 <sup>c</sup>	-	-	-	-
N126-4	813414 <sup>d</sup>	392179 <sup>d</sup>	86.3 <sup>e</sup>	71.9 <sup>e</sup>	-	-	-	-
N126-5	813487 <sup>d</sup>	392034 <sup>d</sup>	86.2 <sup>e</sup>	71.6 <sup>e</sup>	63.0 <sup>e</sup>	-	-	-
N126-6	813450 <sup>d</sup>	392103 <sup>d</sup>	86.4 <sup>e</sup>	72.7 <sup>e</sup>	63.0 <sup>e</sup>	-	-	-
S242-10	811329 <sup>d</sup>	389366 <sup>d</sup>	81.5 <sup>f</sup>	67.6 <sup>e</sup>	-	-	-	-
S242-11	811260 <sup>d</sup>	389376 <sup>d</sup>	81.5 <sup>f</sup>	67.2 <sup>e</sup>	-	-	-	-
S242-12	811063 <sup>d</sup>	389500 <sup>d</sup>	81.5 <sup>f</sup>	66.9 <sup>e</sup>	-	-	-	-

Borehole notes: TH-1 to 5 were drilled and logged by the USGS in 1994. N126-4 to 6 were engineering boreholes drilled in 1952 for Building N-126. S242-10 to 11 were drilled in 1983 near Buildings S-242 (10,11) and 1685 (12).

Data Sources:

a E/A&H GPS survey, 1994.

b From Parks (1990); reviewed and in some cases revised by Kingsbury (1994). Latitude/longitude converted to state plane by E/A&H.

c From Geraghty & Miller (G&M), 1985. At G&M wells, E/A&H and G&M elevations differ; G&M data used. Geologic interpretation by E/A&H; reviewed by Kingsbury (1994).

d Estimated from gridded map; x,y error ±50 feet.

e From ERC (1990). Interpretation by E/A&H; reviewed by Kingsbury (1994).

f Rough estimate from USGS topographic maps; formation tops affected by accuracy of estimate.

g Interpreted by E/A&H from geophysical logs and/or geologic logs; reviewed by Kingsbury (1994).

### 3.0 Geophysical Application

#### 3.1 Description of TEM

Transient electromagnetics (TEM), sometimes called time-domain electromagnetics (TDEM) is a geophysical technique which transmits electromagnetic energy into the ground and measures the ground's response. The data are then interpreted for geologic features or for certain contaminants.

Environmental applications often employ a central loop configuration for the measurements. A square wire loop, typically about 20x20 m, is laid out on the ground. The loop acts as the energizing wire and is called the *source loop*. An alternating current transmitted into the source loop creates an electromagnetic field which propagates downward into the ground. If the electromagnetic field encounters a subsurface conductor, such as a clay lens, small secondary fields are generated. These are measured back at the earth's surface by a second, smaller wire, known as the *receiver loop*, which is laid inside the source loop. The elapsed time between the original current pulse and the measurement of a secondary field is related to the depth of the clay lens. Hence, by measuring the secondary field at a wide range of times, one can define the electrical character of the ground as a function of depth. This is known as a *sounding*. By obtaining a series of soundings, one can develop a three-dimensional map of subsurface electrical character. The work is done entirely from the surface without a need for drilling or other invasive activities.

A TEM sounding can be thought of as a "fuzzy" borehole electric log. Whereas a borehole log resolves small-scale features, the TEM sounding sees larger-scale contacts, such as a change in resistivity at a sandstone/clay boundary. The fuzzier TEM image results from the averaging of larger volumes of earth than done in borehole work. The image is sharpest for shallow features because a smaller volume is energized; as the signal gets to deeper features, the image becomes fuzzier and resolution decreases. Finally, at some depth the signals become too weak to measure, limiting the maximum penetration.

TEM is most effective in mapping electrical conductors in the earth, such as water-bearing zones, chlorides, clays, and strata bearing clay and silt fines. Many times these features correspond to formational or facies contacts of interest, as in the present project. TEM is least effective in mapping resistors, especially thin resistors wedged between conductive layers. Typical resistors include dry soil and rock, zones of low porosity, and low-chloride water.

TEM maps electrical structure, not geology. However, with sufficient geologic understanding, these electrical maps can be interpreted for geologic structure and stratigraphy. This report provides an example of how that objective is accomplished.

TEM theory, interpretation, and environmental applications are summarized in Appendix A. Some of this information is useful to understanding specific results reported in Section 4 of this technical memorandum.

### **3.2 Field Application and Logistics**

A small, in-loop TEM array was chosen for its logistical simplicity in crowded industrial sites, its good resolution, and ease of interpretation. The array consisted of a single-turn 20 by 20-m square loop to generate the signal and a 5 by 5-m square loop to detect the magnetic field derivative as an induced voltage. A Zonge Engineering NanoTEM system was used for field work. The system uses a repetitive time-domain pulse at a frequency of 32 Hz. In the configuration used, the transmitter shutoff was approximately 1.5 microsecond ( $\mu\text{s}$ ).

Data were acquired in 31 time windows along the transient decay curve (see Appendix A for a definition of this and other terms in this section). The first window center is at 1.22  $\mu\text{s}$ , and subsequent windows are at integral multiples (2x, 3x, 4x, etc.) of Window 1. The last window is at 3020  $\mu\text{s}$ .

The instrumentation permitted a high degree of data control in the field, including plotting of decay and Bostick-inverted resistivity curves (Bostick, 1977), along with error bars. Data scatter was monitored and displayed during acquisition, allowing the operator to optimize stacking time for the project objectives. Typically about 2,000 decay cycles were stacked and averaged to produce a "stack burst"; at least two complete stack bursts were obtained at every station to quantify the data scatter. Typical acquisition time to produce clean data was a few minutes; it took 10 to 30 minutes to move the system and set up on the next station.

Data were plotted in plan view during field work, and decay curves were noted in a field notebook to provide a readily available record of various types of decay patterns.

Most of the 90 soundings obtained were at semi-random points on the property, although some were obtained in adjacent pairs. All station positions were surveyed with the Navy's global

positioning satellite system to provide plan-view locations and elevations necessary for modeling and plotting.

The field work was done 4 and 6 April and 2-5 May 1994. Weather conditions varied from cool and wet to warm and sunny.

### **3.3 Data Processing**

Following field acquisition, the raw data files were first edited to correct field errors and to separate production data from system tests. Sequential stack bursts were averaged for each station, resulting in a stacked and averaged voltage decay curve for each station.

The data were modeled using an Inman style ridge regression inversion (Inman, 1975). This one-dimensional model assumes a sequence of layers extending infinitely in all directions (the model breaks down for strongly localized conductors). The geophysicist starts the modeling process by looking at the sounding curve and estimating the minimum number of layers needed to reproduce the curve. This estimate is based on experience and, in some cases, is guided by knowledge of the subsurface geology. At NAS Memphis, modeling was independent of geologic assumptions, leaving the integration of the two data sets for the interpretation process.

Between three and six layers were needed to fit the TEM data. A more complex model which adds layers would also have been successful. However, such a model tends to suggest a higher vertical resolution than is possible with TEM, resulting in an overinterpretation of the results. E/A&H favors the simplest model which adequately reproduces the field data, giving a more appropriate solution.

Layer thicknesses and resistivities were estimated and entered as a starting model. Iteration was performed until a stable, high-quality fit to the decay curve was obtained. The result was then examined for uniqueness, superfluous layers, and other problems.

The top three layers were usually well-defined in the models. Past layer 3, and particularly past layer 4, the signal had virtually dissipated, and some of the field curves exhibit unrealistic changes related to the loss of signal. These changes were modeled as if they were real, but then critically examined for artificial effects (see Appendix B). Only data thought to contain reliable geologic information were retained.

### 3.4 QA/QC Summary

Several tests were made of the quality and reliability of the TEM data. These tests fall into the categories of data precision, data aliasing, data biasing, and signal-depletion effects. These are summarized here and detailed in Appendix B.

*Data precision* was tested by acquiring data at station 13 in dry and wet conditions nearly a month apart. The repeatability in modeled depths of the layers was acceptable for purposes of this study. Repeatability in some of the modeled resistivity values was only fair, but this parameter is of secondary importance to this project.

*Data aliasing* or undersampling occurs when the sampling interval is too large to map small-scale features of interest. Several aliasing tests were performed on the data, which had typical separations of 200 to 500 m between soundings. Very small-scale aliasing on the order of 100 m was found to be minor in open, undeveloped areas. Aliasing on the scale of 500 to 1000 m or so was minor to significant, depending on the areas involved. Overall, significant geologic changes appear to have been moderately well sampled, and aliasing is not considered to be a problem in meeting the project objectives.

*Data biasing* comes from non-geologic features which distort the TEM data. The worst offenders are man-made metallic features such as pipelines, underground cables, fences, buildings, and power lines, collectively known as *culture*. Culture can cause the data to be uninterpretable, or worse, wrongly interpreted. A careful study was made of the locations of cultural features with respect to the TEM sounding locations. A four-tiered test was devised to remove soundings suspected of cultural bias. Of the 90 soundings made, 72 were retained for the final interpretation and are believed to be relatively free of cultural bias.

*Signal-depletion effects* arise in the deeper parts of the TEM sounding where the signals become very weak. Care must be exercised to not interpret these artificial effects as deep geologic structure. A test was devised to determine the maximum depth of penetration of each sounding. As described in Appendix B, such a test is critical in picking the top of a deep conductive unit such as the Cook Mountain. The test provides improved confidence in the geologic interpretation.

#### 4.0 Data Interpretation

#### 4.1 Comparison of Surface and Downhole Geophysics

To help translate TEM layers to useful geologic information, TEM data were taken at each of the five USGS test holes, permitting a direct comparison of the two data sets. Downhole logs (long-normal and short-normal resistivity, spontaneous potential, gamma, and sonic velocity) were run by the USGS. The long-normal resistivity data were compared to the TEM modeled resistivity data at each borehole.

The comparisons should be regarded as approximate for several reasons: (1) TEM has poorer vertical resolution than the downhole data; (2) TEM has considerably greater side-looking ability than downhole data; (3) TEM is less effective in seeing resistors wedged between conductive horizons; (4) TEM stations are not always right over the boring, but may be offset up to some 70 m; and (5) downhole data are subject to variable effects of drilling muds, formation penetration, and tool coupling. As a result, one should not expect a precise correlation of the two data sets, but a general one.

Figures 3 through 7 show the surface and downhole geophysics data at the five boreholes. The wiggly line labeled "LN resistivity log" is the long-normal downhole resistivity log. Formation picks from the geological database are shown at the right of the plots.

*Comparison of Absolute Resistivity Values* — Some very large discrepancies in the absolute resistivity numbers between the TEM and downhole data sets are observed in a few of the curves. The worst mismatch is at TH-5 (Figure 7), where the TEM resistivities are up to two orders of magnitude lower than the downhole resistivities. Significant differences are also seen at TH-1 and TH-5. Better matches are found at TH-2 and TH-4, although TEM resistivities are still lower than downhole results. In no case do the two data sets agree to within  $\pm 10$  percent.

The cause of the discrepancy was carefully investigated. No errors from instrumentation or data collection were identified in either data set. Given the hole-to-hole consistency of the downhole resistivities, contrasted with the strong variations in the TEM data, it seems likely that something is affecting the TEM curves to produce the mismatch.

(text continued page 17)

*Technical Memorandum  
Geophysics Study to Characterize Geology  
NAS Memphis  
27 January 1995*

---

**This page intentionally left blank.**

### TH-1 Surface/Downhole Geophysics

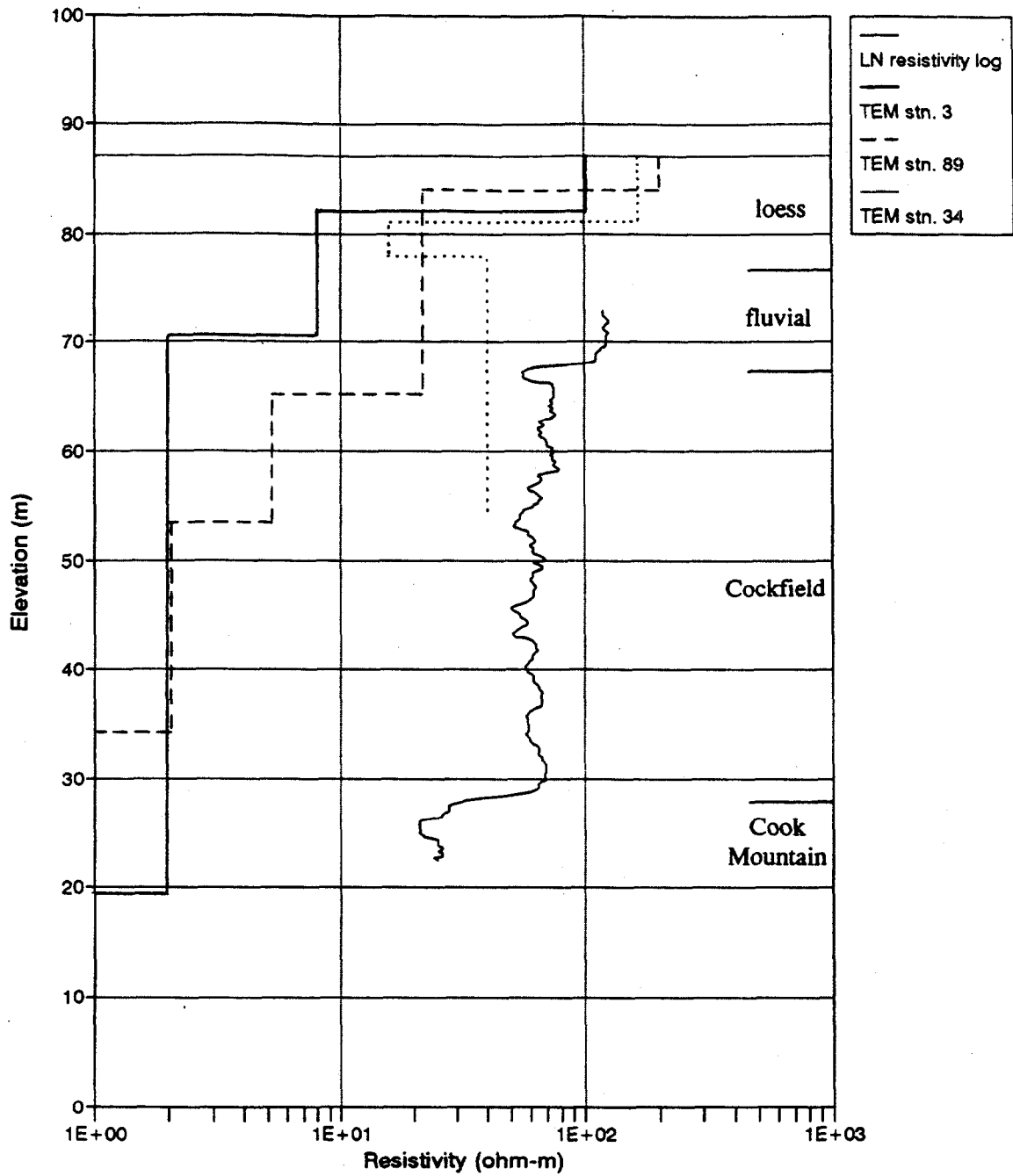


Fig. 3. Comparison of downhole resistivity log and surface TEM model results, test hole No. 1 (V-74).

*Technical Memorandum  
Geophysics Study to Characterize Geology  
NAS Memphis  
27 January 1995*

---

**This page intentionally left blank.**

### TH-2 Surface/Downhole Geophysics

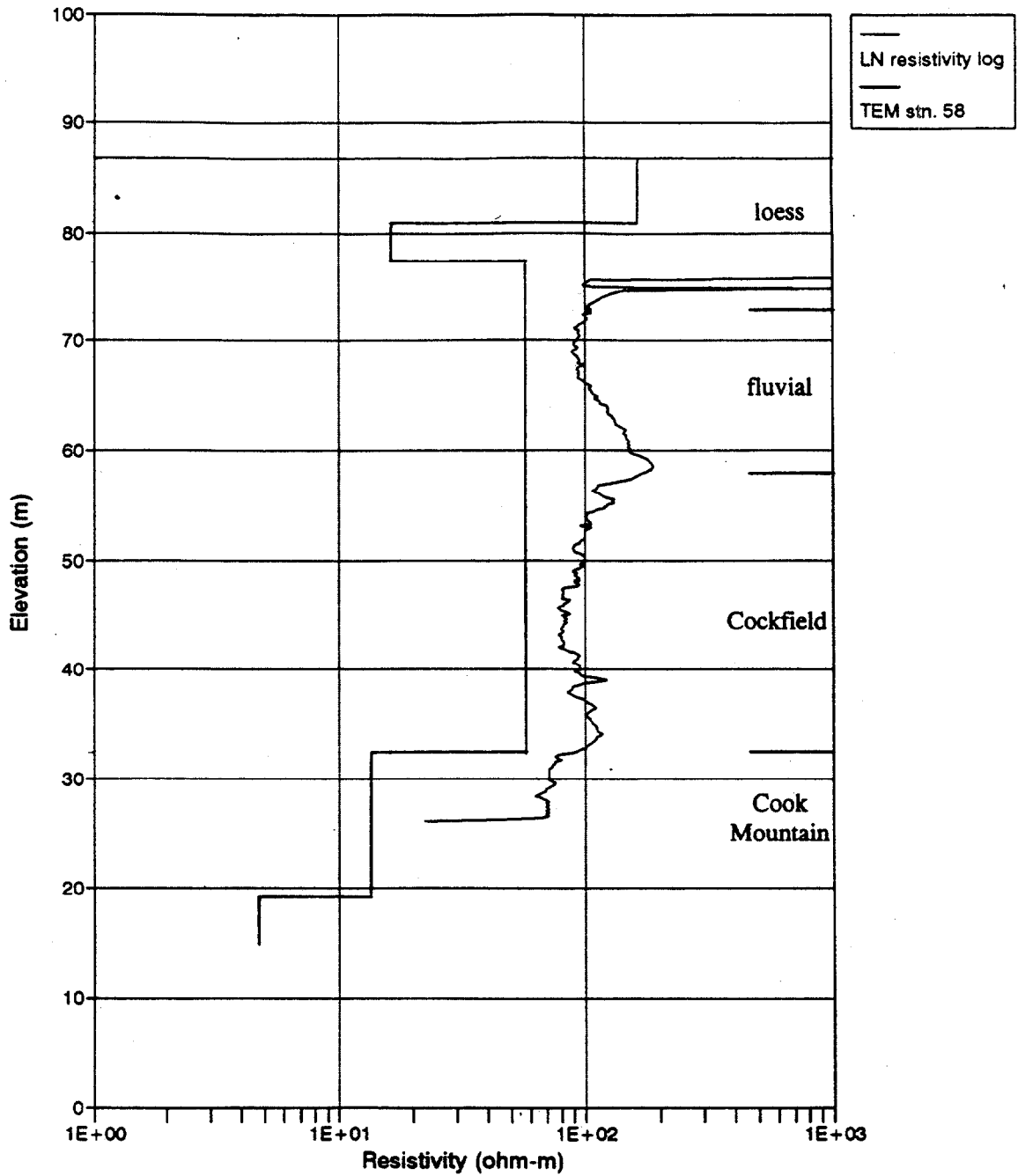


Fig. 4. Comparison of downhole resistivity log and surface TEM model results, test hole No. 2 (U-98).

*Technical Memorandum  
Geophysics Study to Characterize Geology  
NAS Memphis  
27 January 1995*

---

This page intentionally left blank.

### TH-3 Surface/Downhole Geophysics

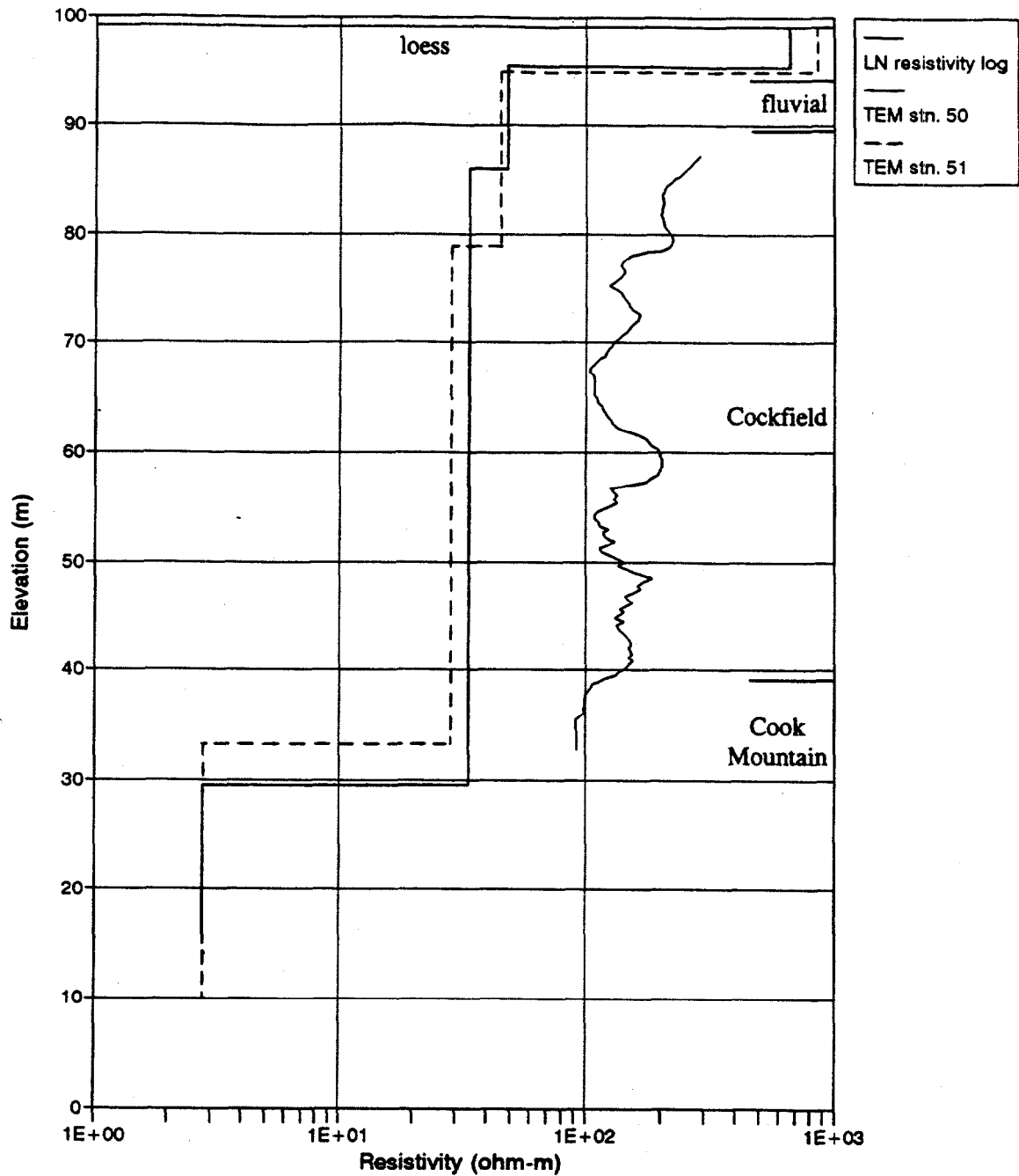


Fig. 5. Comparison of downhole resistivity log and surface TEM model results, test hole No. 3 (V-75).

*Technical Memorandum*  
*Geophysics Study to Characterize Geology*  
*NAS Memphis*  
*27 January 1995*

---

**This page intentionally left blank.**

### TH-4 Surface/Downhole Geophysics

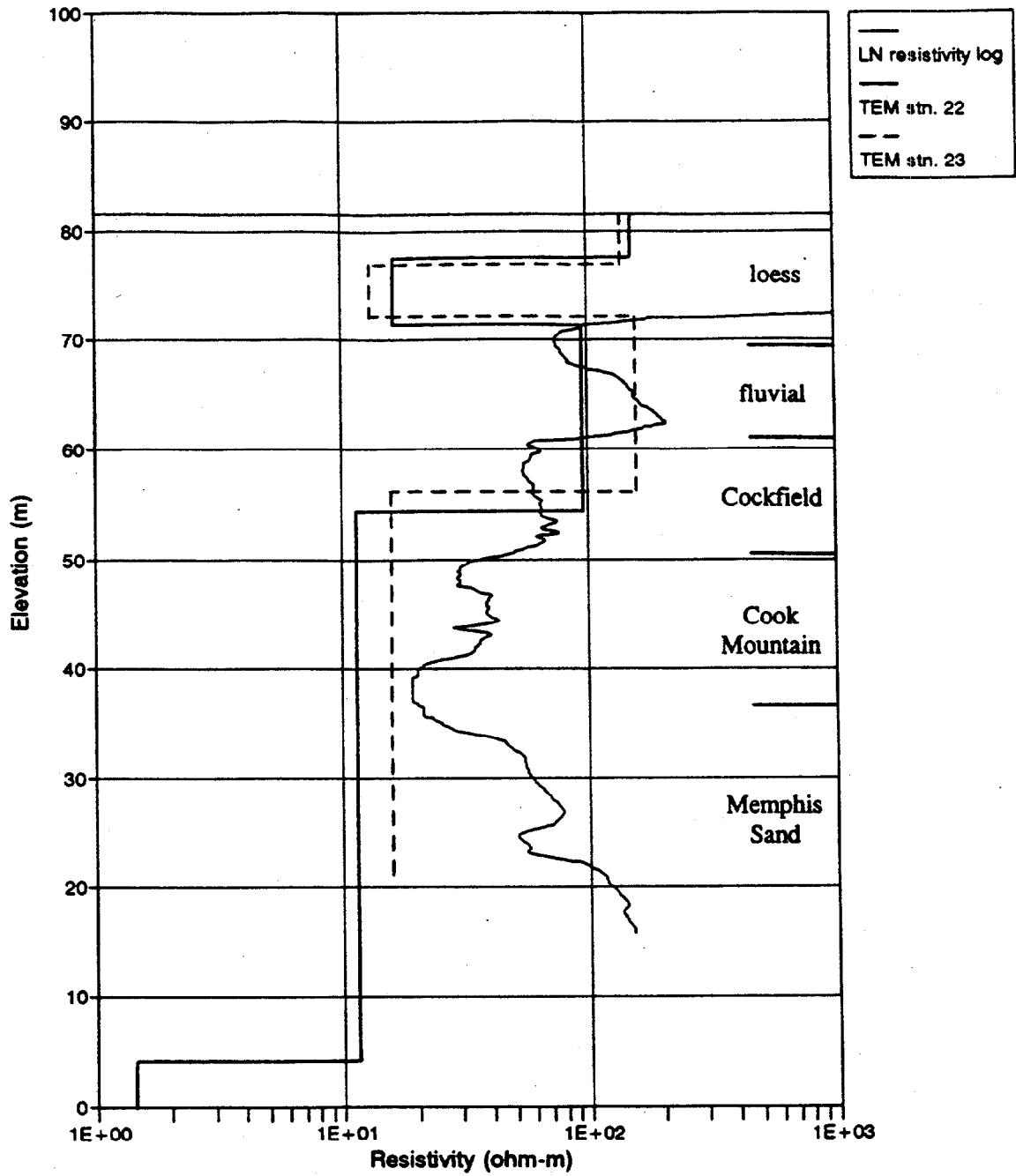


Fig. 6. Comparison of downhole resistivity log and surface TEM model results, test hole No. 4 (U-99).

*Technical Memorandum*  
*Geophysics Study to Characterize Geology*  
*NAS Memphis*  
*27 January 1995*

---

**This page intentionally left blank.**

### TH-5 Surface/Downhole Geophysics

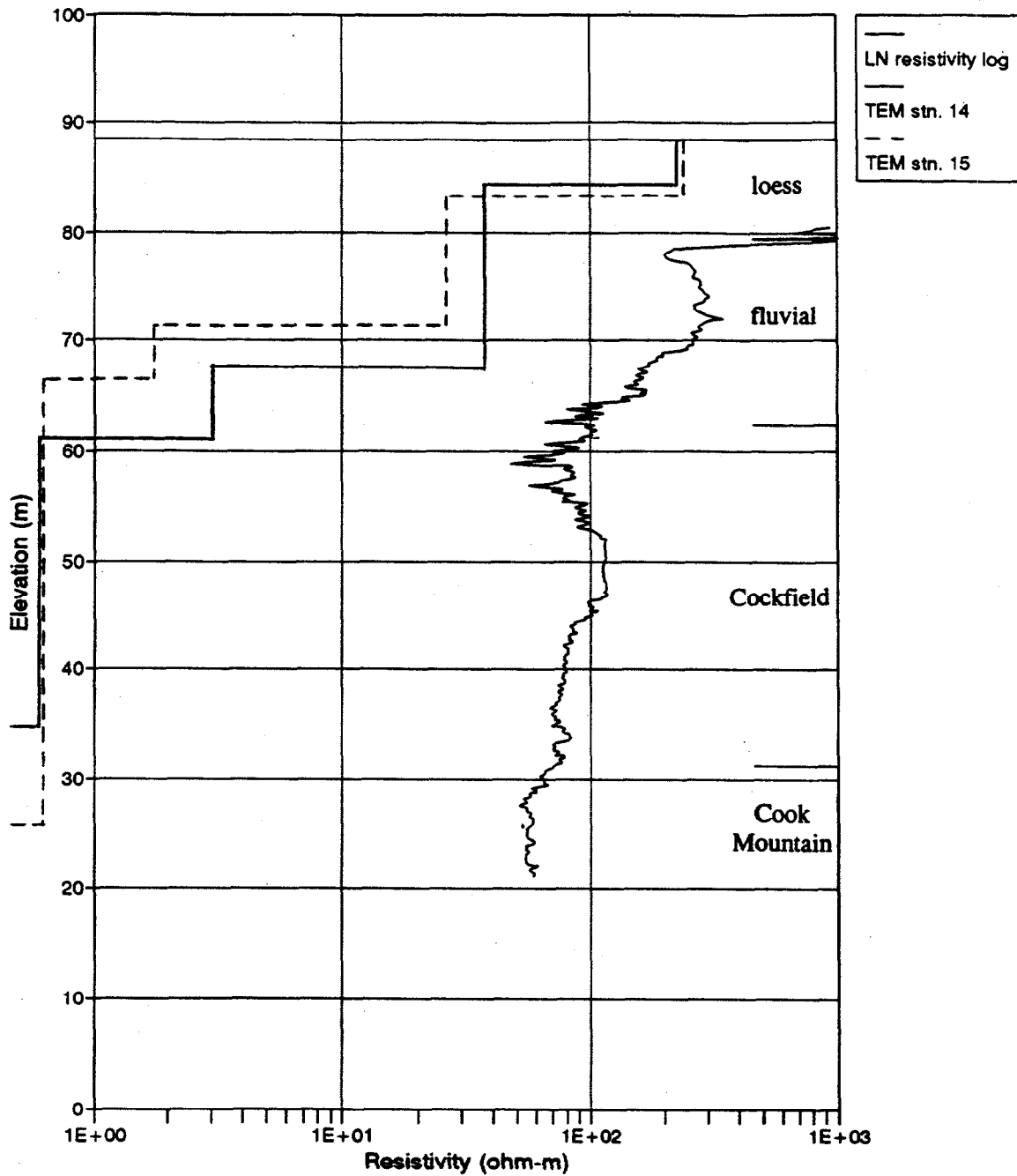


Fig. 7. Comparison of downhole resistivity log and surface TEM model results, test hole No. 5 (V-76).

*Technical Memorandum  
Geophysics Study to Characterize Geology  
NAS Memphis  
27 January 1995*

---

**This page intentionally left blank.**

(text continued from page 11)

The most likely cause of the surface/downhole mismatch is cultural effects in the TEM data. Similar cultural effects have been noted by Fitterman et al. (1990). The worst mismatch, at TH-5, is in an area surrounded by dense culture, and the better matches at TH-2 and TH-4 are in culture-free areas. The data at TH-1 could have been affected by culture along nearby streets or in the golf course area. But TH-3, supposedly in a culture-free area, shows an unexpectedly strong mismatch. Hence, a culture explanation only partly explains the problem.

Three alternative explanations of the mismatch are all unsatisfactory. The first, that three-dimensional effects may be present, is unlikely because it is improbable that so many TEM stations would be so strongly affected, all with the same downward bias in resistivity. Second, the mismatch is clearly not a signal-depletion problem, since it occurs in shallow data where signal is still strong. Third, distortion by a near-surface layer too shallow to be resolved by the TEM cannot explain the mismatch in later-time data. To show this, a seven-layer model was developed for station 3, consisting of five layers derived from the long-normal resistivity log for TH-1, and two shallow layers above them. The depths and resistivities of the five layers were fixed, and the parameters of the two shallow layers were allowed to vary. No combinations of parameters for the shallow layers could even approximate the sounding curve for station 3. Clearly, the mismatch is not the result of unresolved near-surface effects.

To conclude, the mismatch, while most likely culturally induced, is not entirely understood at present.

*Comparison of Depth Picks* — While the absolute resistivities show a mismatch, a better match is observed between the depths of TEM breaks and downhole conductors. It is worthwhile to consider the qualitative results at each borehole separately, then look at a quantitative comparison.

At TH-1 (Figure 3), nearby stations 3 and 89 show a resistivity break corresponding roughly to the top of the Cockfield Formation, which is conductive in the downhole log; station 34 does not show the break. Stations 3 and 89 show a resistivity break roughly at the conductive Cook Mountain top (station 34 did not penetrate deeply enough).

At TH-2 (Figure 4), the top of the Cockfield shows a definite resistivity decrease in the downhole data but not in the TEM. The reason is that the break in the log is only evident

because of the resistive lower fluvial facies; such a thin resistor wedged in a conductive section is not readily discernable with TEM. Hence, TEM fails to see the top of the Cockfield. On the other hand, the agreement between TEM break and downhole break at the Cook Mountain is excellent.

At TH-3 (Figure 5), the log shows that the resistivity drops gradationally at the top of the Cockfield, which is evident in the TEM models. The gradational change prevents a distinct TEM formation pick. The Cook Mountain contact is electrically more distinct, and the breaks in TEM and downhole data are at similar depths. Although the log shows definite resistivity variations within the Cockfield, TEM does not resolve them because it does not recognize the thin resistive facies within the conductive section.

At TH-4 (Figure 6), TEM does not recognize the top of the Cockfield, again because the resistivity break there results from thin resistor amidst conductors. Instead, TEM tends to average the rapid changes evident in the logs. More definite breaks at the top of the Cook Mountain are observed, with fairly good agreement between TEM and downhole depth picks. TEM runs out of signal before reaching the very conductive bottom portion of the Cook Mountain or the resistive Memphis Sand; deeper sounding data with a larger loop would probably resolve both.

At TH-5 (Figure 7), the gradational resistivity drop seen in the log below the lower fluvial causes a TEM break to occur shallower than the top of the Cockfield. The gradational nature of the geology suggests caution in interpreting these TEM stations. A similar gradation is seen at the Cook Mountain, but TEM gives a roughly correct depth.

#### **4.2 TEM Formation Picks at Control Points**

A quantitative comparison of TEM and geologic picks requires a choice of which TEM layer corresponds to which formation. For example, Figures 3 to 7 show the Cook Mountain might correspond to TEM layers 4 or 5, depending on the particular model. The process of making the correct TEM pick is a crucial one because an error can distort the interpreted structure.

The interpretive process was started by carefully comparing the downhole electrical response with the TEM layering at each USGS borehole, bearing in mind the differences in the two data sets. When deemed appropriate, the TEM conductor closest to the Cook Mountain top was designated as the interpreted Cook Mountain. A similar approach was used for the other units,

though with limited success, as will be shown shortly. Note that this process is entirely empirical, as the complex, changing geology does not afford the luxury of a geologic pick at the same TEM layer throughout the area.

Table 2 quantifies the comparisons of the two data sets. Although this compilation is an oversimplification, it helps answer the question: can TEM be used to map geologic units? Results are shown for the tops of the fluvial, Cockfield, and Cook Mountain units. At the bottom of the table are averages for success in picking the unit and percent error in the picks.

**Table 2**  
**Comparison of Drillhole and TEM Depth Picks**

TEM Station	Elevation Picks (m)			Normalized Depth Error in TEM (% of true depth)		
	Top of Fluvial	Top of Cockfield	Top of Cook Mountain	Fluvial Pick	Cockfield Pick	Cook Mountain Pick
<b>TH-1</b>	<b>76.6</b>	<b>67.2</b>	<b>27.9</b>			
Stn. 3	82.2	70.6	19.6	+54%	+17%	-14%
Stn. 34	81.5	failed	- <sup>c</sup>	+47%	failed	- <sup>c</sup>
Stn. 89	84.1	65.4	34.3	+72%	-9%	+11%
<b>TH-2</b>	<b>72.9</b>	<b>72.9</b>	<b>32.3</b>			
Stn. 58	80.9	failed <sup>a</sup>	32.3	+58%	failed <sup>a</sup>	0%
<b>TH-3</b>	<b>94.1</b>	<b>89.4</b>	<b>38.9</b>			
Stn. 50	95.5	85.7	29.6	+26%	-37%	-15%
Stn. 51	95.5	78.8	33.3	+19%	-107%	-9%
<b>TH-4</b>	<b>69.4</b>	<b>60.9</b>	<b>50.5</b>			
Stn. 22	77.5	failed <sup>a</sup>	54.4	+66%	failed <sup>a</sup>	+13%
Stn. 23	77.0	failed <sup>a</sup>	56.0	+62%	failed <sup>a</sup>	+18%
<b>TH-5</b>	<b>79.4</b>	<b>62.3</b>	<b>31.2</b>			
Stn. 14	84.4	61.2 <sup>b</sup>	34.5 <sup>b</sup>	+55%	-4% <sup>b</sup>	+6% <sup>b</sup>
Stn. 15	83.4	66.6 <sup>b</sup>	40.9 <sup>b</sup>	+44%	+16% <sup>b</sup>	+17% <sup>b</sup>
<b>V-4</b>	<b>no data</b>	<b>62.5</b>	<b>25</b>			
Stn. 72	81.5	failed	- <sup>c</sup>	no data	failed	- <sup>c</sup>
<b>Success Rate in Identifying Unit (error &lt;20%)</b>				<b>18%</b>	<b>36%</b>	<b>100%</b>
<b>Average Error</b>				<b>+50%</b>	<b>-21%</b>	<b>+3.0%</b>
<b>± standard deviation</b>				<b>±17%</b>	<b>±47%</b>	<b>±13%</b>

**Notes:**

Entries in bold are borehole data; the rest are geophysics data.

<sup>a</sup> Failed because boundary has poorly defined electrical character for EM.

<sup>b</sup> Result somewhat ambiguous; apparent success should be regarded with caution.

<sup>c</sup> Signal depleted before desired depth achieved.

Success in picking the unit is defined as the percentage of times the pick is better than  $\pm 20$  percent of the true depth, based upon soundings which penetrate deeply enough to see the unit. Percent differences are calculated by obtaining the TEM elevation pick of the break closest to the interface, subtracting the known formation elevation, and dividing by the interface depth. This gives a percent error normalized to depth. For the ideal case of a sharp conductor at depth without overlying conductive layers, TEM can pick the depth to  $\pm 5$  percent. This accuracy degrades in situations that depart from this ideal case.

TEM is unsuccessful in picking the top of the fluvial unit because the logs show there are no distinct resistivity changes there. The best picks are invariably too high in elevation, and in fact correspond to the base of a conductive sub-unit within the lower loess. Thus TEM adds no new information to the database for the top of the fluvial unit. However, note that the picks for the base of the sub-unit are systematically offset from the fluvial contact. This fact will be used later on as a marker bed to characterize the fluvial top where drillhole control is missing.

TEM locates the Cockfield successfully only 36 percent of the time. Note the large percentage error in the picks at TH-3. As noted earlier, this mediocre success rate is due to the variable electrical response at the top of the Cockfield. Where the top is distinctly conductive, TEM makes a good pick. As a result, some Cockfield picks can be made in the TEM data, but generally only near drillhole control. Far from control points, the electrical distinctiveness of the top of the Cockfield cannot be assumed, and picks become more uncertain. Hence, TEM tends to add interpolative, not extrapolative data to the database for the Cockfield. TEM consistently detects a resistivity break at about the right depth for the Cook Mountain. The 100 percent success rate is certainly overstated in this statistically small database, but the rate appears to be quite high. All picks are better than  $\pm 20$  percent, and the average error is not far from zero, lending confidence in the TEM picks of this unit.

It is useful to convert the error data to uncertainties in elevation units, by multiplying the percent errors by the mean formation elevation:

Formation	Detectability	Accuracy in Picking Top (m) <sup>a</sup>
Fluvial	not detected	-
Cockfield	poor to fair	±10 m
Cook Mountain	good	± 7 m
Memphis Sand	not detected	-

<sup>a</sup> Assuming a mean depth of 21 m for the Cockfield and 52 m for the Cook Mountain; the numbers will scale up or down for different depths.

Assuming a mean Cook Mountain depth of 52 m, the error in picking the formation top with any *isolated TEM sounding* is about  $\pm 7$  m. When *several soundings* define a consistent trend, the error decreases in a statistical manner, depending on the number of samples. Since it is not possible to separate statistical from spatial variations in the field data, the statistical error in a spatial plot cannot be quantified. However, the  $\pm 7$  m criterion might be considered the worst case for the Cook Mountain in such a plot, assuming no errors in modeling or in picking the right interface.

#### 4.3 TEM Picks Away From Control Points

The next stage in interpretation was to make formation picks from the TEM data away from the drillhole control. Picks were carefully considered based upon behavior of electric log data from hole to hole. In some cases, the log behavior indicated that a pick would be inappropriate, and none was made. An attempt was made to maintain lateral continuity in drawing correlations from one TEM sounding to the next.

The interpretation started by making TEM picks between the more closely spaced drillholes in an *interpolative* fashion. A number of cross-sections were constructed for quality control; every TEM station appeared on at least one cross-section. The work was then expanded away from the control points in an *extrapolative* fashion. Clearly the largest potential for picking the wrong interfaces is in the soundings farthest from the control points. Distant boring data were used as bounds for these data to reduce the margin of error. The results were then plotted in plan-view and subjected to several QA/QC checks to judge their internal consistency and adherence to the patterns shown by the well data alone.

#### 4.4 Cross-Section Interpretations

Plates 1 to 3 (pages 29 through 31) show three of the cross-sections generated in the interpretation process; Figure 8 shows their locations. TEM data, downhole resistivity curves, and borehole lithologic picks are presented in these sections, which have a 20:1 vertical exaggeration. The maximum penetration of the TEM data and the range of equivalence for each layer are depicted, as keyed in the legend. The scale for the downhole logs is shown at the bottom below each curve ( $\rho$ =resistivity,  $\Omega \cdot m$ =ohm-meters). The interfaces drawn in a thin black line connect TEM interpreted layers; the thick lines incorporate TEM and downhole data and represent the final interpretation. Colors accent the formational picks, with jagged color boundaries indicating areas of exceptionally poor control.

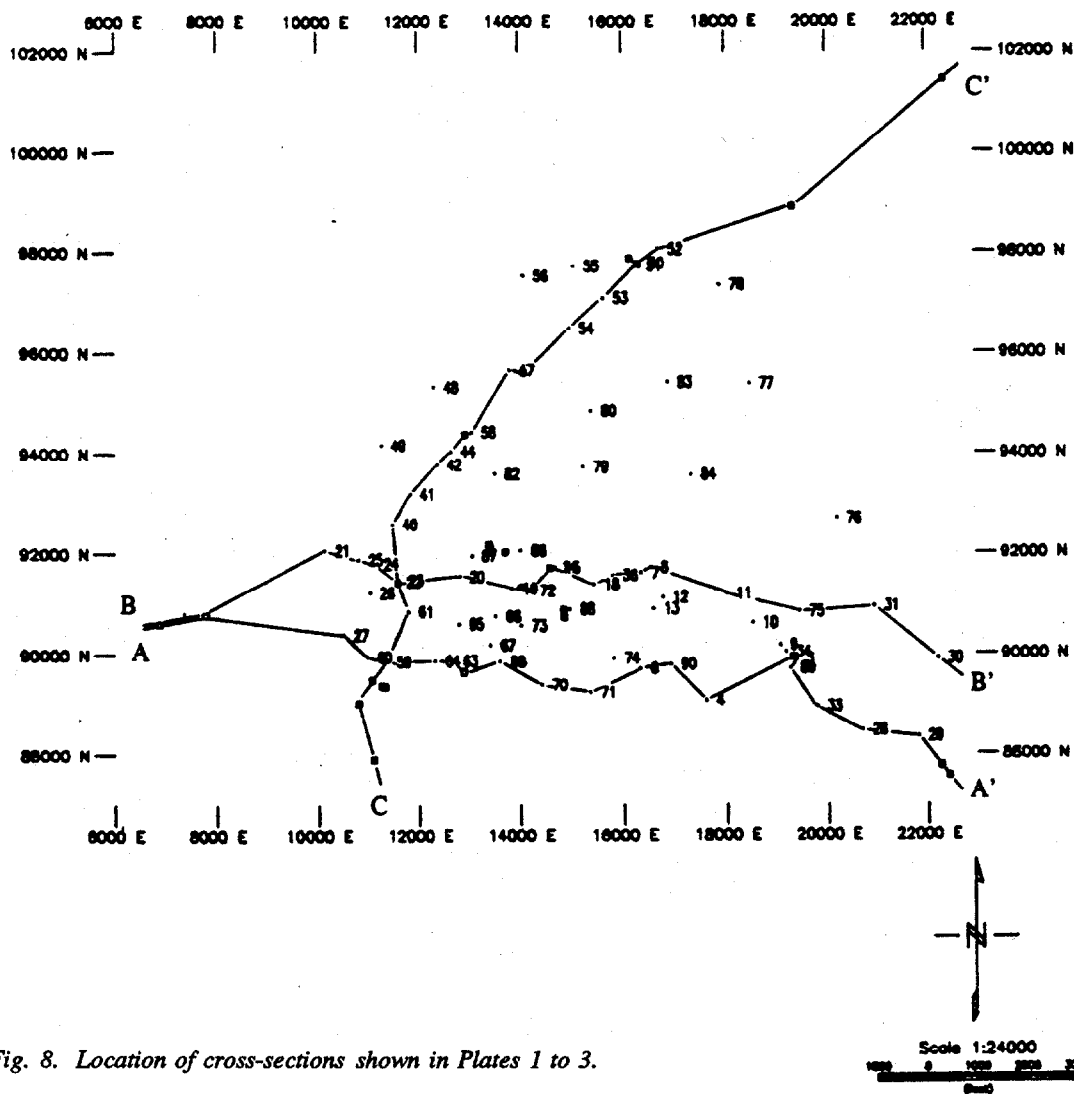
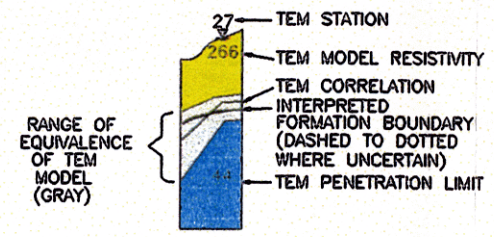
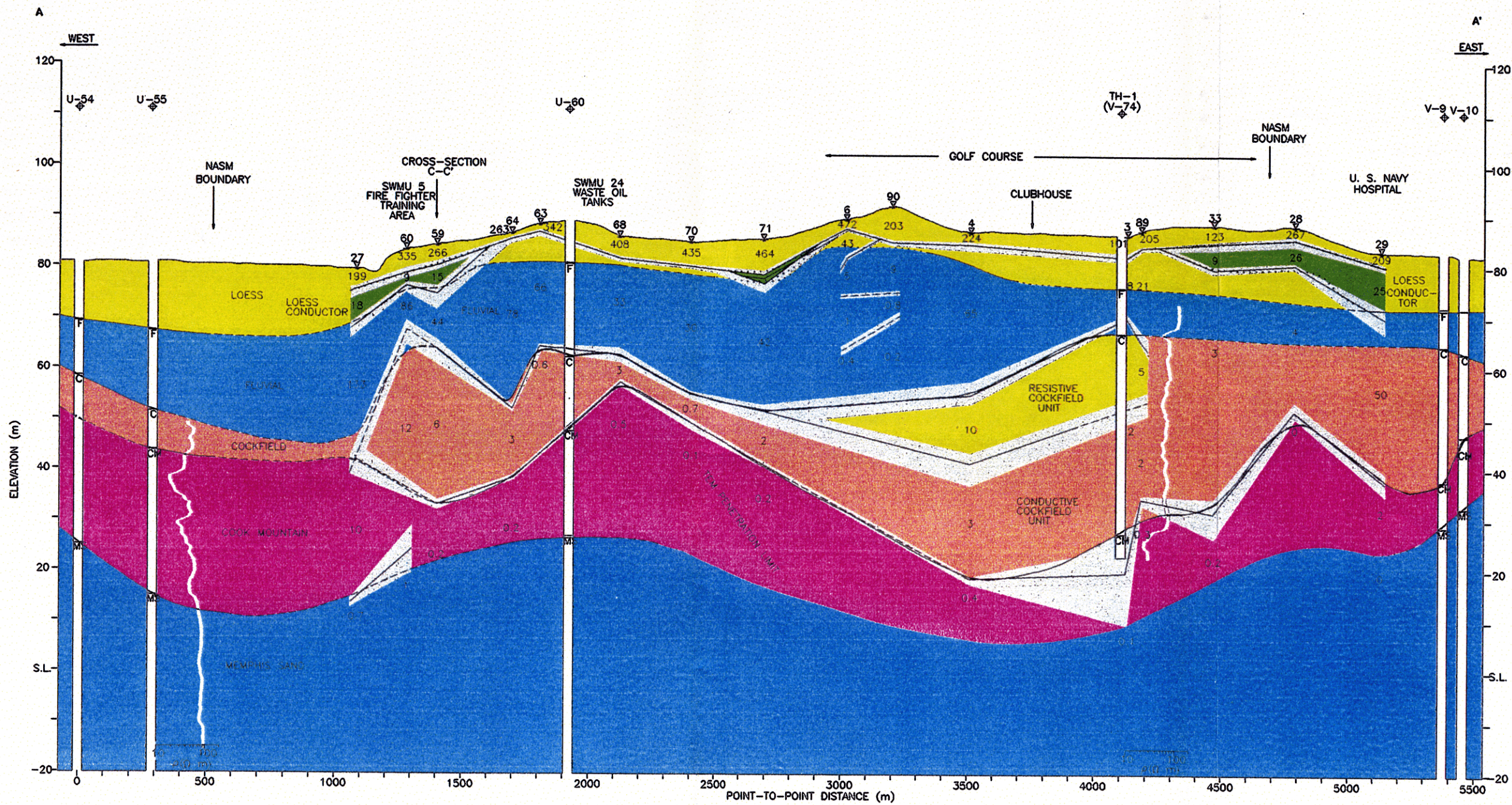


Fig. 8. Location of cross-sections shown in Plates 1 to 3.



DOWNHOLE LOGS ARE LONG-NORMAL, EXCEPT V-55, WHICH IS SHORT-NORMAL  
TEM DATA FROM 1-D INVERSIONS

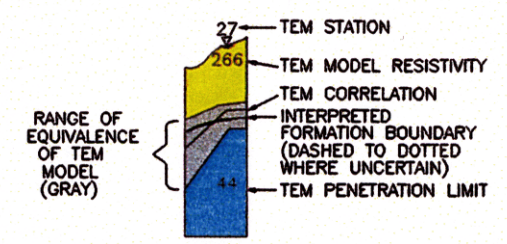
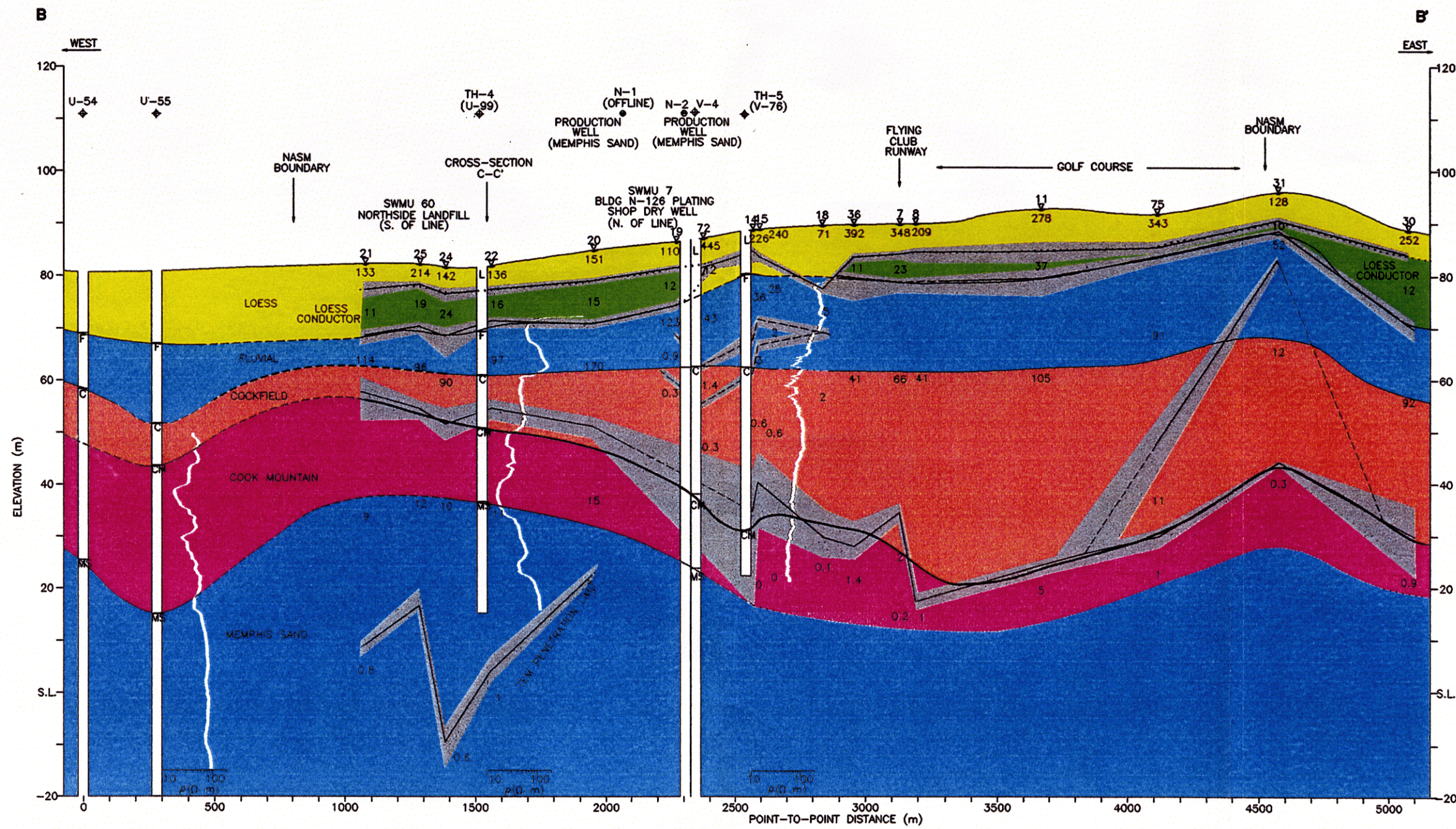


**GEOPHYSICAL INVESTIGATION OF GEOLOGY  
NAS MEMPHIS  
MILLINGTON, TENNESSEE**

**PLATE 1  
JOINT GEOPHYSICS/  
GEOLOGY INTERPRETATION  
TEM CROSS-SECTION  
A-A'  
(VERTICAL EXAGGERATION 20:1)**

DWG DATE: 12/09/94    DWG NAME: 16CSAA

00598CB1Y

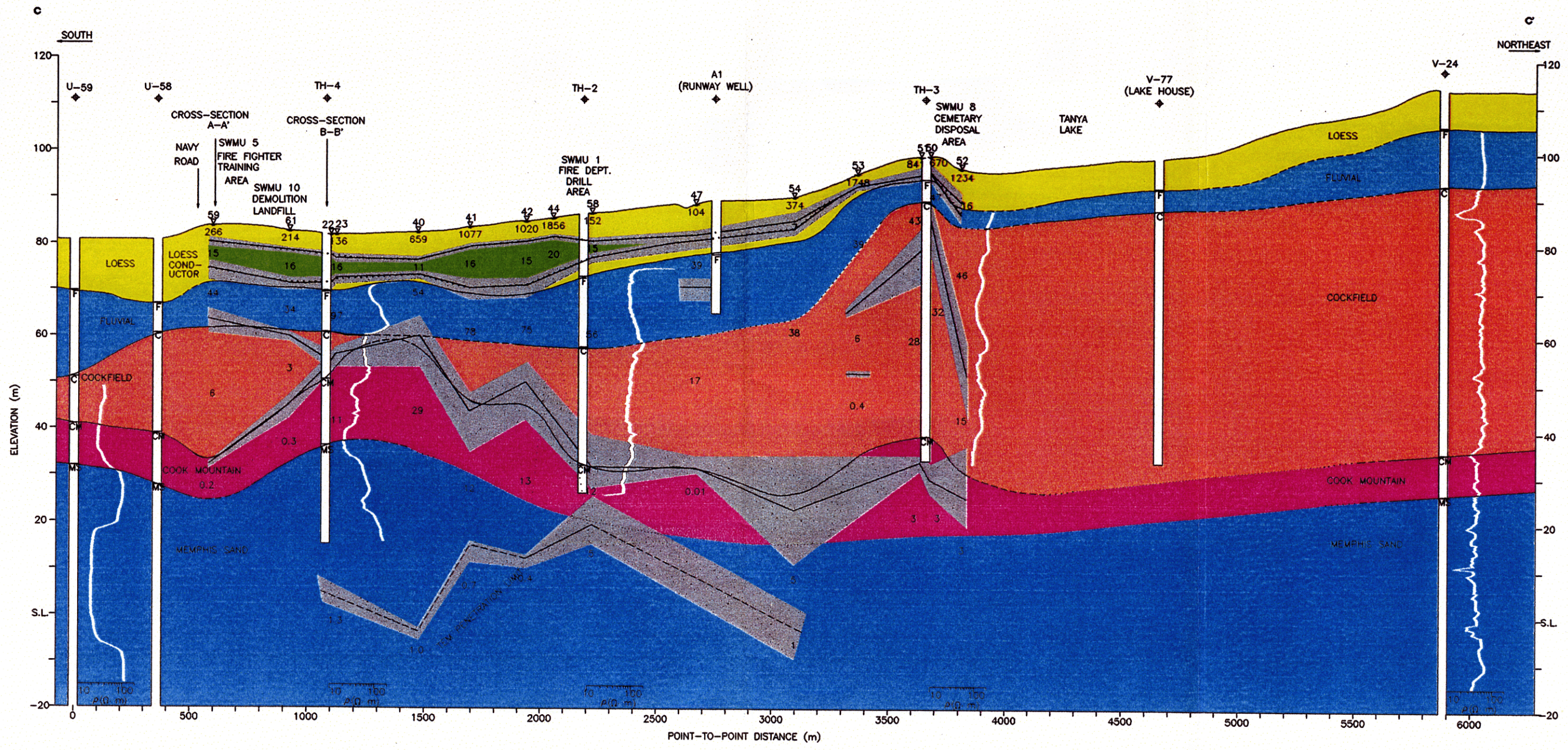


DOWNHOLE LOGS ARE LONG-NORMAL, EXCEPT V-55, WHICH IS SHORT-NORMAL  
TEM DATA FROM 1-D INVERSIONS

GEOPHYSICAL INVESTIGATION OF GEOLOGY  
NAS MEMPHIS  
MILLINGTON, TENNESSEE

PLATE 2  
JOINT GEOPHYSICS/  
GEOLOGY INTERPRETATION  
TEM CROSS-SECTION  
B-B'  
(VERTICAL EXAGGERATION 20:1)

DWG DATE: 12/09/94 DWG NAME: 16CSBB



27 — TEM STATION  
 266 — TEM MODEL RESISTIVITY  
 — TEM CORRELATION  
 — INTERPRETED FORMATION BOUNDARY (DASHED TO DOTTED WHERE UNCERTAIN)  
 — TEM PENETRATION LIMIT  
 RANGE OF EQUIVALENCE OF TEM MODEL (GRAY)

DOWNHOLE LOGS ARE LONG-NORMAL, EXCEPT V-55, WHICH IS SHORT-NORMAL  
 TEM DATA FROM 1-D INVERSIONS


 GEOPHYSICAL INVESTIGATION  
 OF GEOLOGY  
 NAS MEMPHIS  
 MILLINGTON, TENNESSEE

PLATE 3  
 JOINT GEOPHYSICS/  
 GEOLOGY INTERPRETATION  
 TEM CROSS-SECTION  
 C-C'  
 (VERTICAL EXAGGERATION 20:1)

DWG DATE: 12/09/94    DWG NAME: 16CSCC

Plate 1 shows a west to east cross-section just north of Navy Road, extending from Millington to the Navy Hospital. The fluvial correlation is drawn entirely from geologic control, with terrace features inferred from TEM data to the far west. In some areas, a conductive feature is identified near but not directly at the base of the loess. Throughout this report this feature is called the *loess conductor*. The Cockfield appears to be moderately well mapped by the TEM data on this line. An undulating surface is indicated, with particularly strong changes to the west. The most extreme of these slopes corresponds to a local 7 degree dip in the formation. These are smaller-scale details than previously available, so one cannot find direct confirmation in previous drilling; however, Plate 1 is consistent with a general understanding of this erosional boundary. The Cook Mountain top shows large-scale and local undulations, with the steepest slopes corresponding to a 3 degree dip. The geologic picks at boreholes V-9 and V-10, if correct, suggest that the local undulations seen in the TEM picks are not unreasonable. Note that the Cockfield thickness appears to be highly variable, possibly thinning or pinching out to the west; however, a thick section of Cook Mountain appears to underlie the thin area, preserving the integrity of the combined confining unit.

Cross-section B-B' (Plate 2) runs from west to east, sub-parallel to and north of A-A.' The loess conductor is prevalent on this line, and its base is near the loess/fluvial boundary. Several minor terrace features are inferred from the correlations. The Cockfield is not strongly indicated in any of the TEM data because there is no distinct electrical change at its top which can be discerned by TEM (see Section 4.2). The Cook Mountain top appears to be well mapped on this cross-section, although there is more variation in some picks between closely spaced stations than can be attributed to geology. A trough-like feature, later suggested as a paleo-stream channel, is inferred east of the borehole control.

Cross-section C-C' (Plate 3) is a southwest to northeast traverse paralleling the west boundary of NAS Memphis. The loess conductor is found to the southwest but thins or is absent to the northeast. Note that the base of the loess conductor lies above the loess/fluvial contact, but tends to mimic the contact character. For example, the loess conductor thins and rises sharply in elevation wherever fluvial terraces are thought to exist, thus serving as a useful marker to identify terraces. The Cockfield is not indicated in the TEM data except perhaps to the southwest, so its surface is poorly mapped. The Cook Mountain, on the other hand, is well mapped on this cross-section. Most notable is the apparent ridge near TH-4, where slopes of up to 4 degrees are indicated. The ridge is even more interesting because it implies a local thinning or pinchout of the Cockfield Formation. However, TEM appears to not distinguish the

Cockfield and Cook Mountain at this spot, so a pinchout cannot be confirmed. There is no reason to suspect a similar thinning of the Cook Mountain below this zone.

#### 4.5 Plan-View Interpretations

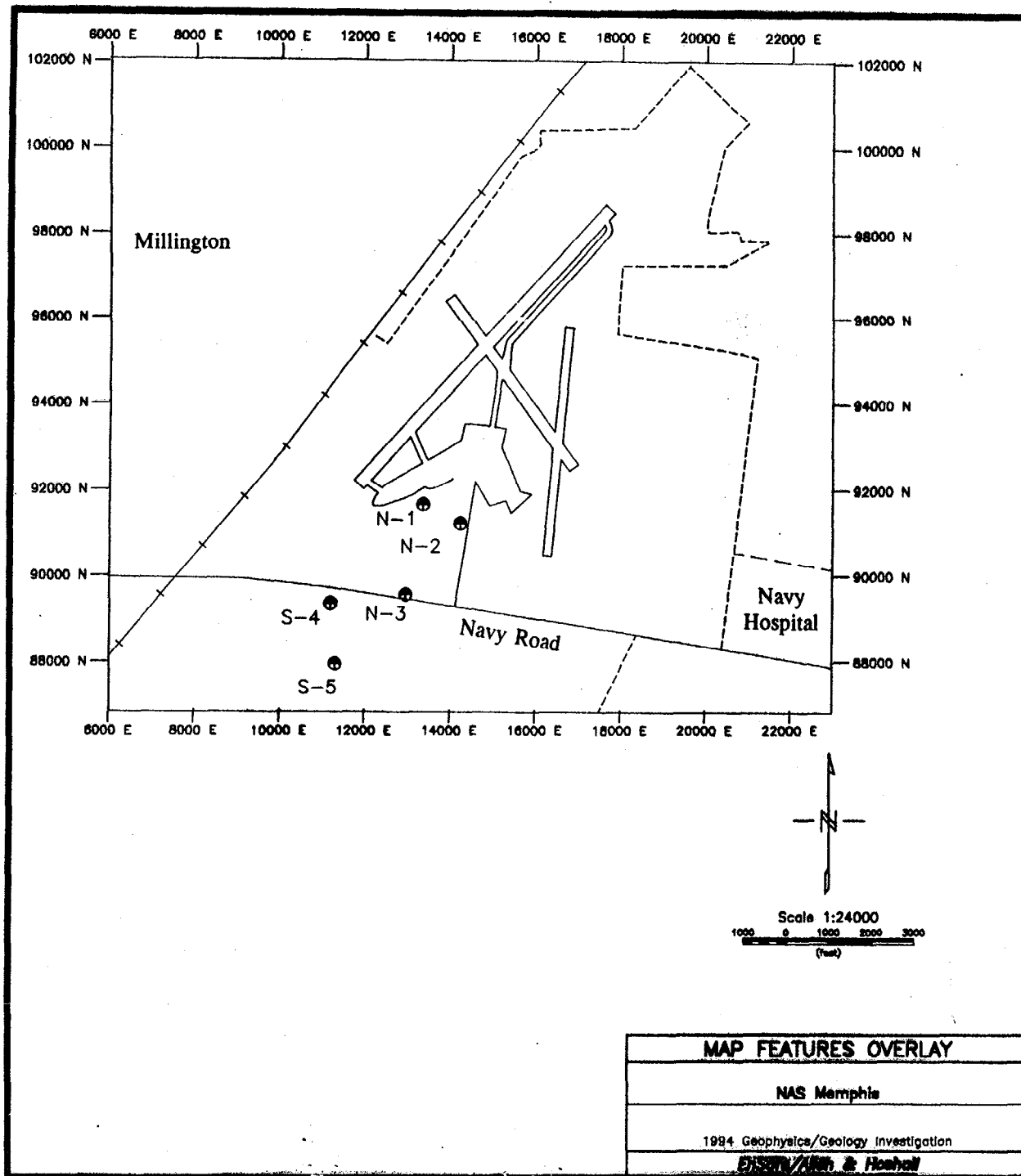
Plates 5 through 16 present aspects of the interpreted geology features, in ascending order. The data come from the geologic database (Table 1) and/or the TEM interpretations, depending on the particular plot. Each plot shows the data control points, differentiating the geologic and geophysical control. Note that the grid coordinates are abbreviated on all plots by dropping the first digit of northings and eastings. For example, 388000N becomes 88000N in the plot, and 819000E becomes 19000E.

The data are presented in color, with warmer colors (orange through magenta) representing higher data values (e.g., higher elevation or thickness), and cooler colors (green through blue) representing lower data values. Color scales have been shifted between some plots to permit adequate resolution of the features. Areas of poor data control have been masked off, producing the sometimes odd shaped color boundaries. A clear overlay shows the main topographic features and boring locations and is useful for following the interpretation. A detailed map (Plate 4) is also with the overlay.

Plate 5 shows the surface topography, based upon global positioning system (GPS) elevations obtained on borings, wells, monuments, and TEM stations during the summer of 1994. The elevation increases to the northeast.

*The Memphis Sand* — Plate 6 shows the top of the Memphis Sand unit. The plot is incomplete because only a few borings have penetrated this unit and have been described well enough to make a formation pick. The available data suggest a reasonably flat surface. The strongest relief indicated in the database (Table 1) is 12.7 m over a horizontal distance of 746 m, corresponding to a 1 degree slope. Memphis Sand elevations reported by Kingsbury and Parks (1993) show local slopes less than 1 degree in all cases.

*The Cook Mountain Formation* — Plate 7 shows the top of the Cook Mountain Formation, based on drillhole and geophysical data. A zone of low paleotopography cuts roughly north-south. It is about 1.5 km wide and shows a typical vertical relief of 25 m with respect to surrounding highlands. The boundary is fairly well defined and has an average slope of about 4 degrees to the west, where a ridge-like structure is interpreted, and a gentler 2 degrees to the east.



<b>MAP FEATURES OVERLAY</b>
NAS Memphis
1984 Geophysics/Geology Investigation
<b>EDS&amp;I/Wh. &amp; Hoehel</b>

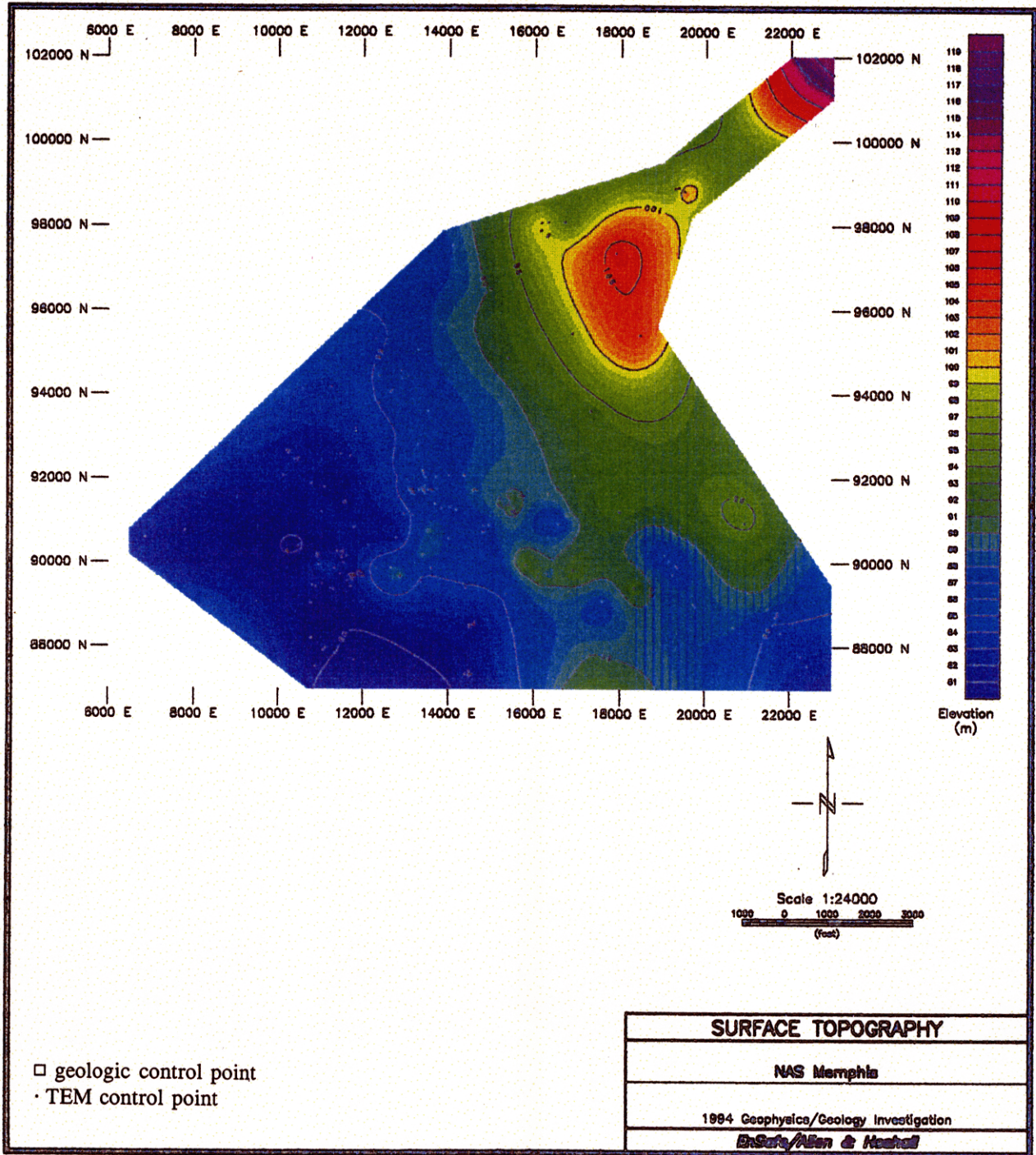


Plate 5. Surface topography, NAS Memphis.

00598CB2Y

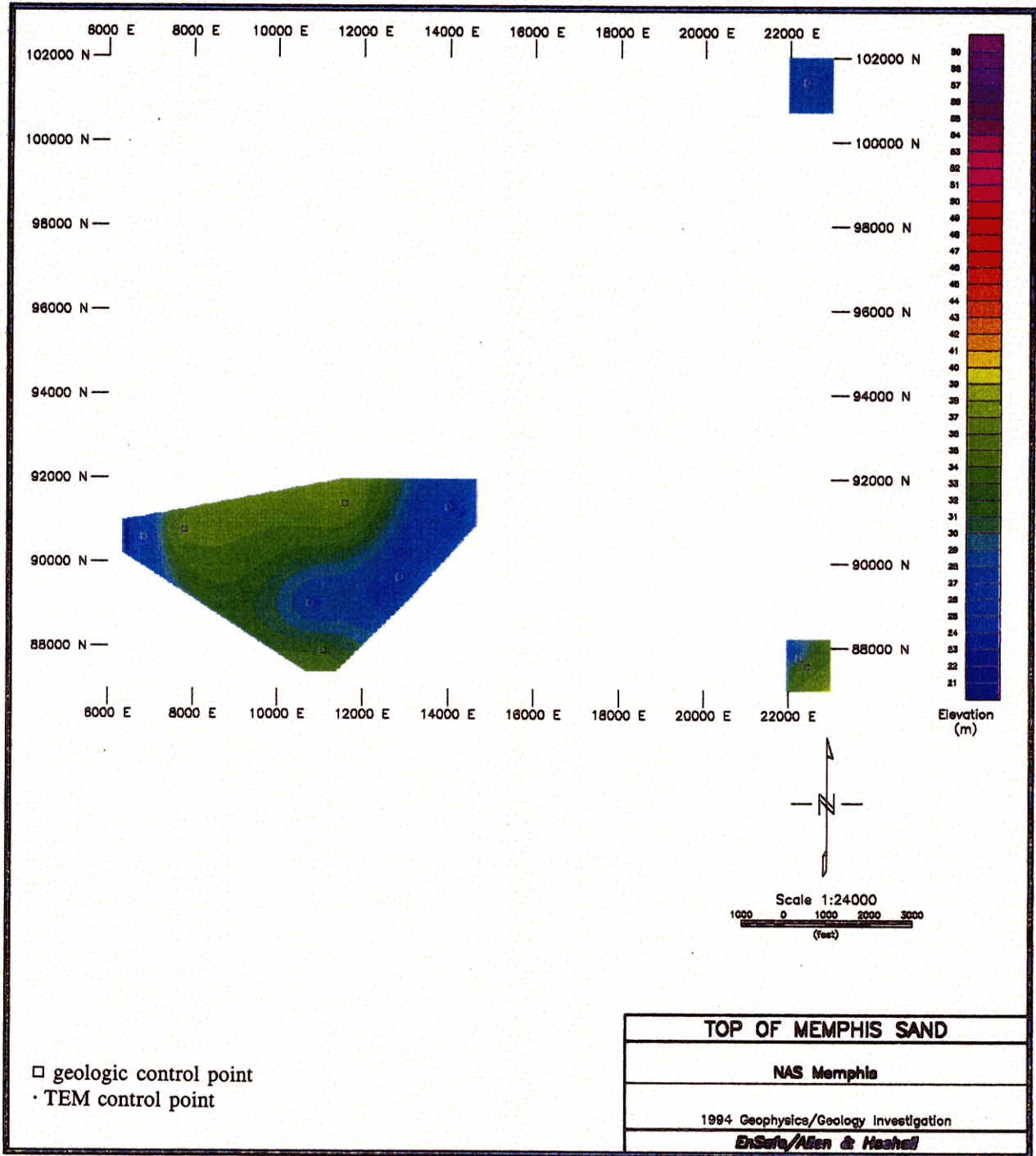


Plate 6. Top of Memphis Sand. Control is limited to drillholes which have penetrated the unit, since the TEM survey did not detect it. The steepest local slopes are one degree or less.

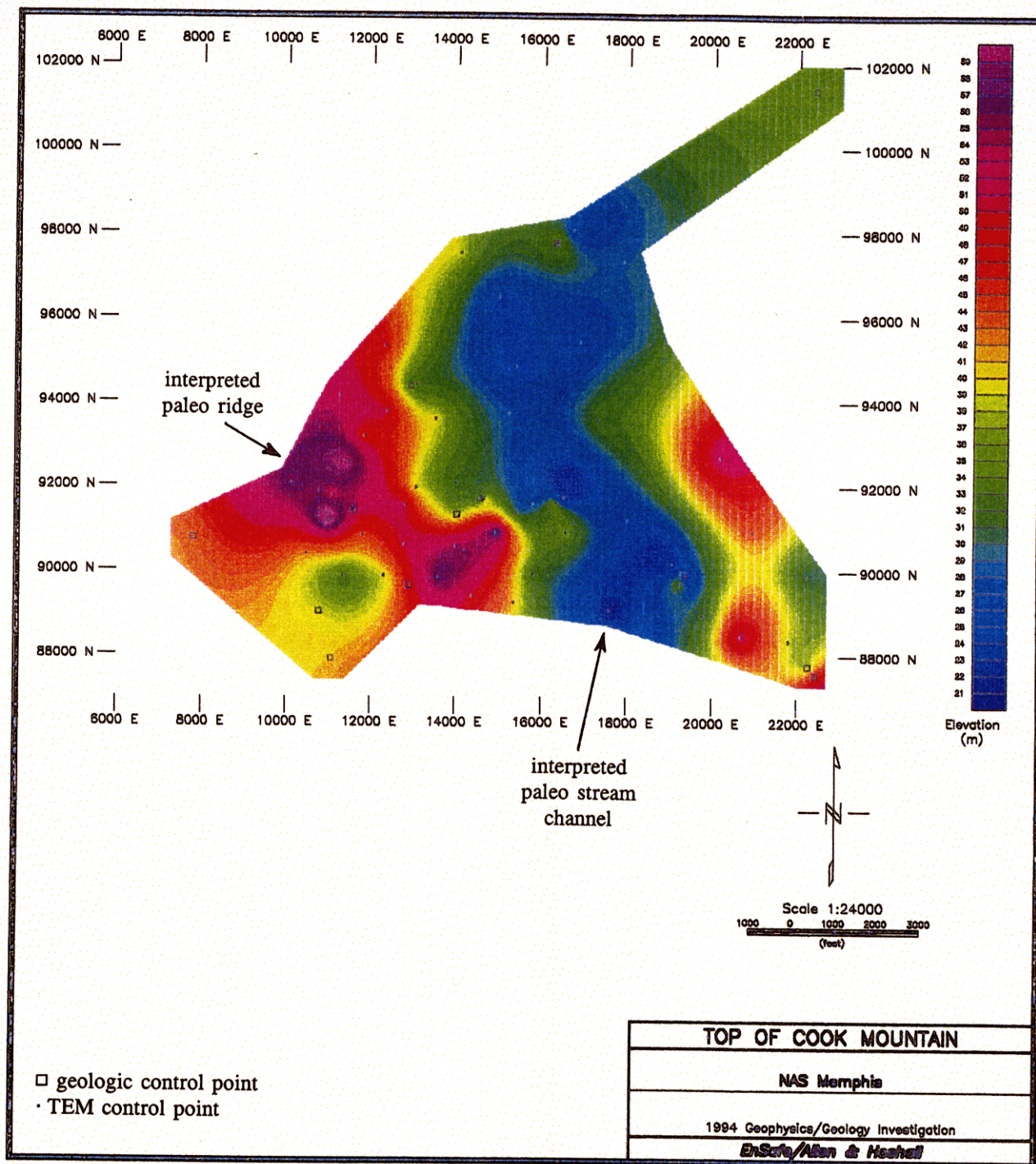


Plate 7. Top of Cook Mountain. The meandering north-south trough (blue colors) is interpreted to be a paleo-river channel, possibly with a southward flow direction. The steepest slopes are 4 degrees, though gentler slopes are more typical. A ridge-like structure is interpreted west of the river channel.

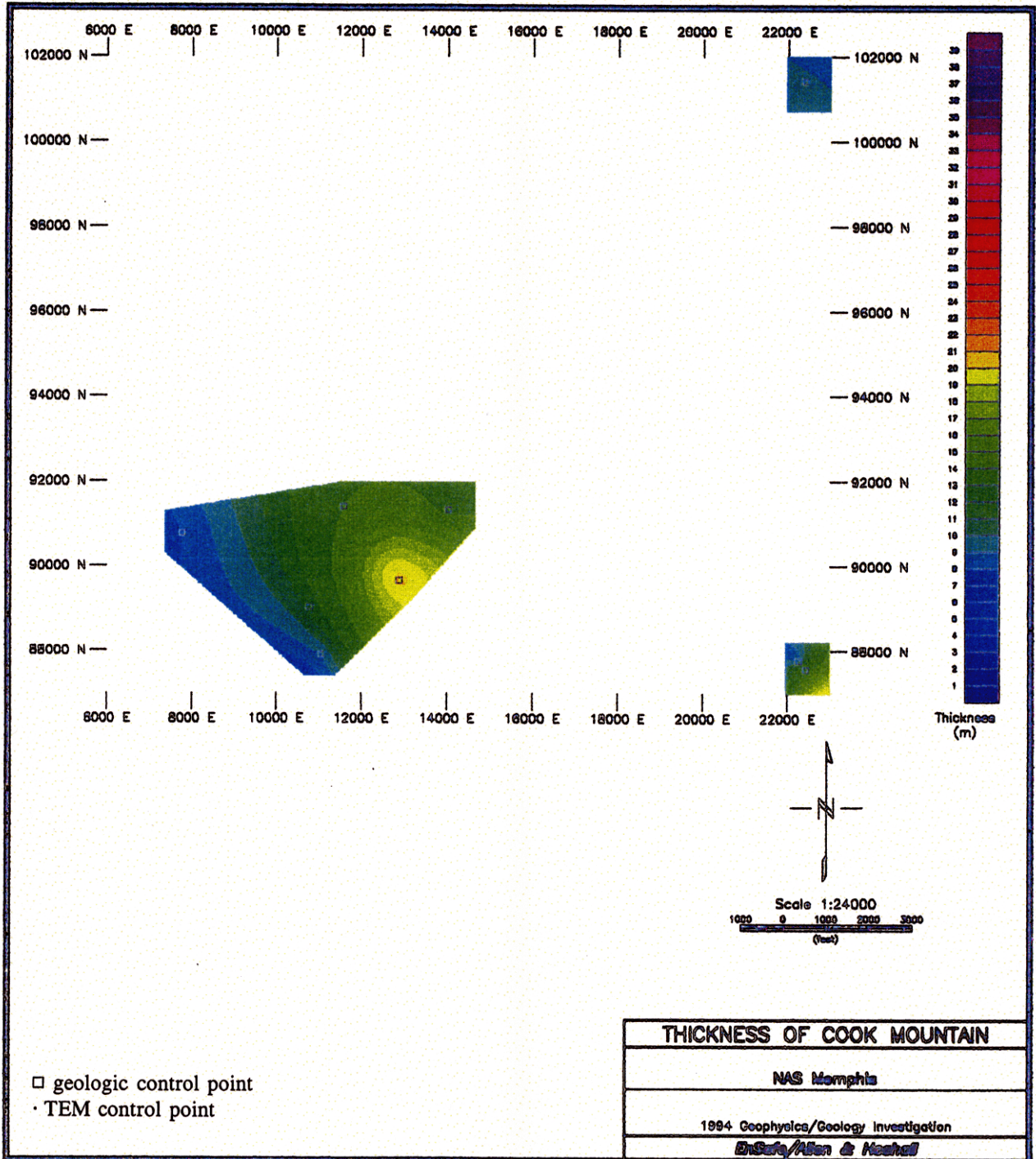


Plate 8. Thickness of Cook Mountain. Control is limited to drillholes which penetrated the top of the Memphis Sand. Drillholes in the areas of no control (blank areas), including the areas of low relief such as the river channel, have intersected a minimum of 5 m of Cook Mountain before termination. Thus the unit seems to be contiguously present across the study area.

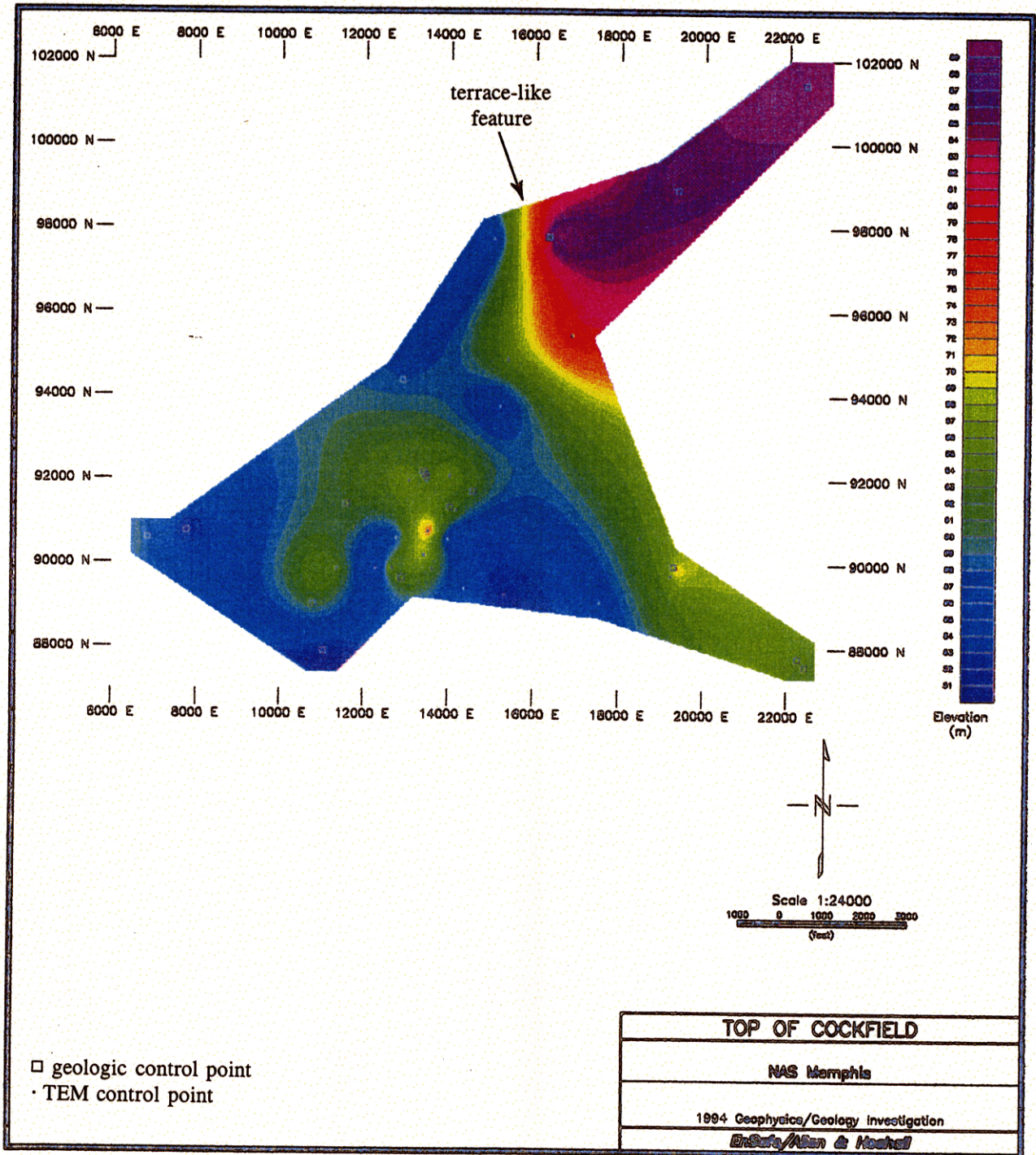


Plate 9. Top of Cockfield. The sharp rise in elevation to the northeast is along a bench-like feature resembling a terrace deposit. The bench could be either depositional or erosional, although an erosional explanation is preferred. Note the localized high and low zones southwest of the bench.

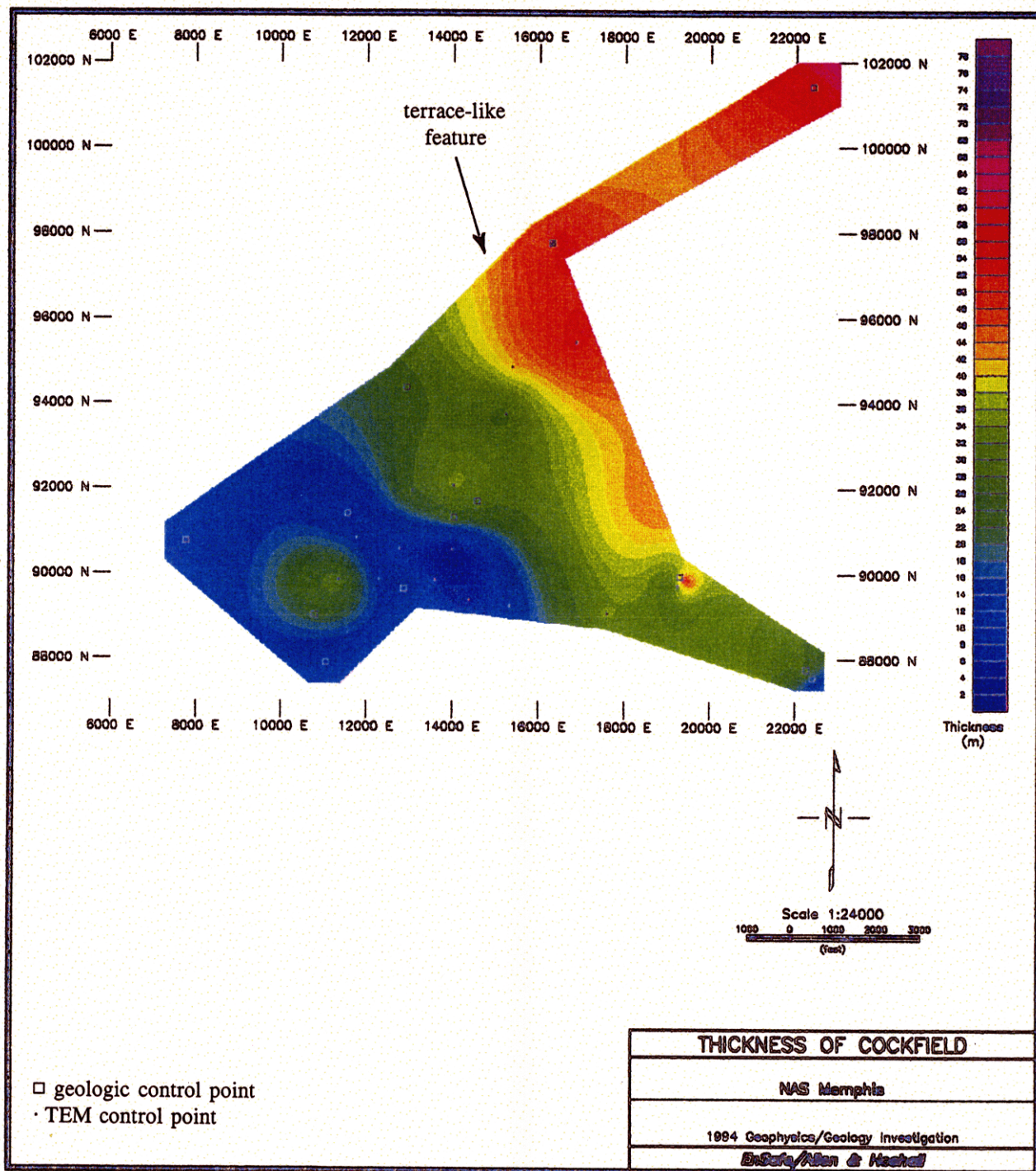


Plate 10. Thickness of Cockfield. Note the formation thinnings (blue zones), which might indicate thinnings or windows in the Cockfield; however, note that Plate 8 indicates a competent Cook Mountain sequence below these interpreted thinnings, preserving the confining layer's integrity. Local highs and lows correspond to undulations of the top and/or bottom of the Cockfield (Plates 9 and 11, respectively).

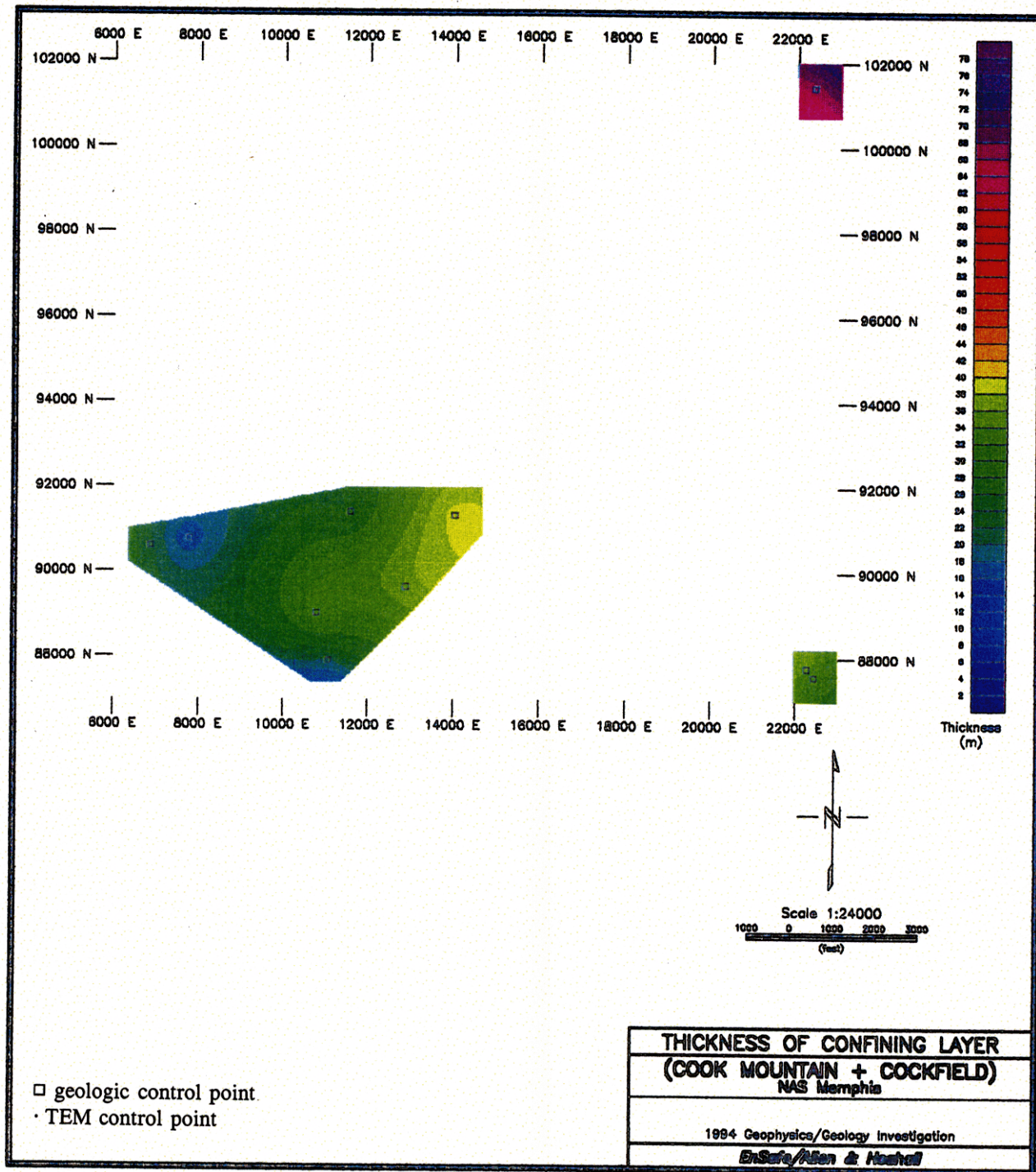


Plate 11. Thickness of confining layer, defined as the Cockfield and Cook Mountain formations. The thinnest confining layer yet intercepted by a borehole is 16 m, and every borehole drilled to its depth has encountered the unit. Thus there is good evidence that the confining sequence has no pinchouts or windows in the study area.

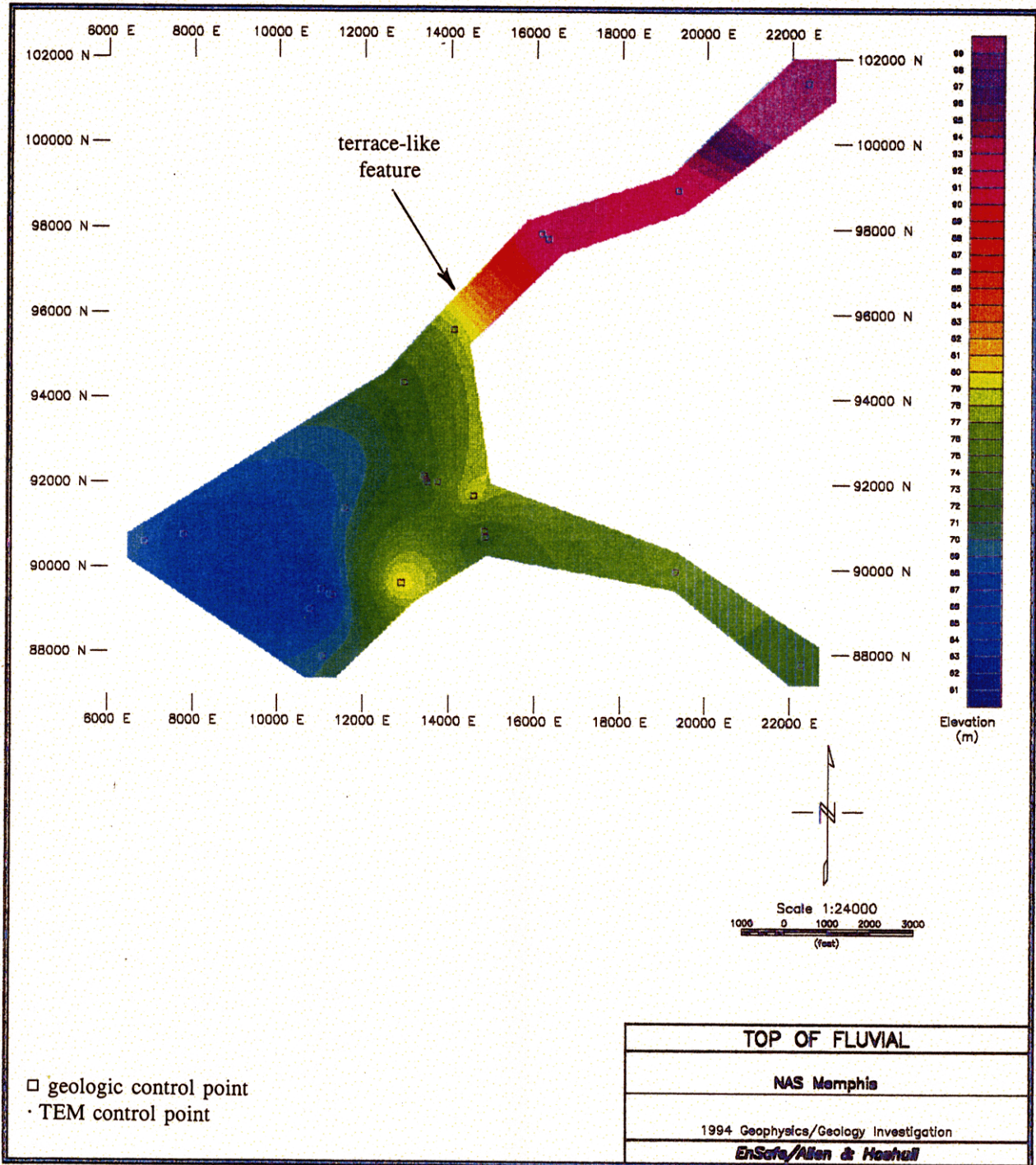


Plate 12. Top of Fluvial Unit. The elevation rise to the northeast may be a terrace deposit. Note that the feature roughly corresponds to a similar rise in the top of the Cockfield (Plate 9).

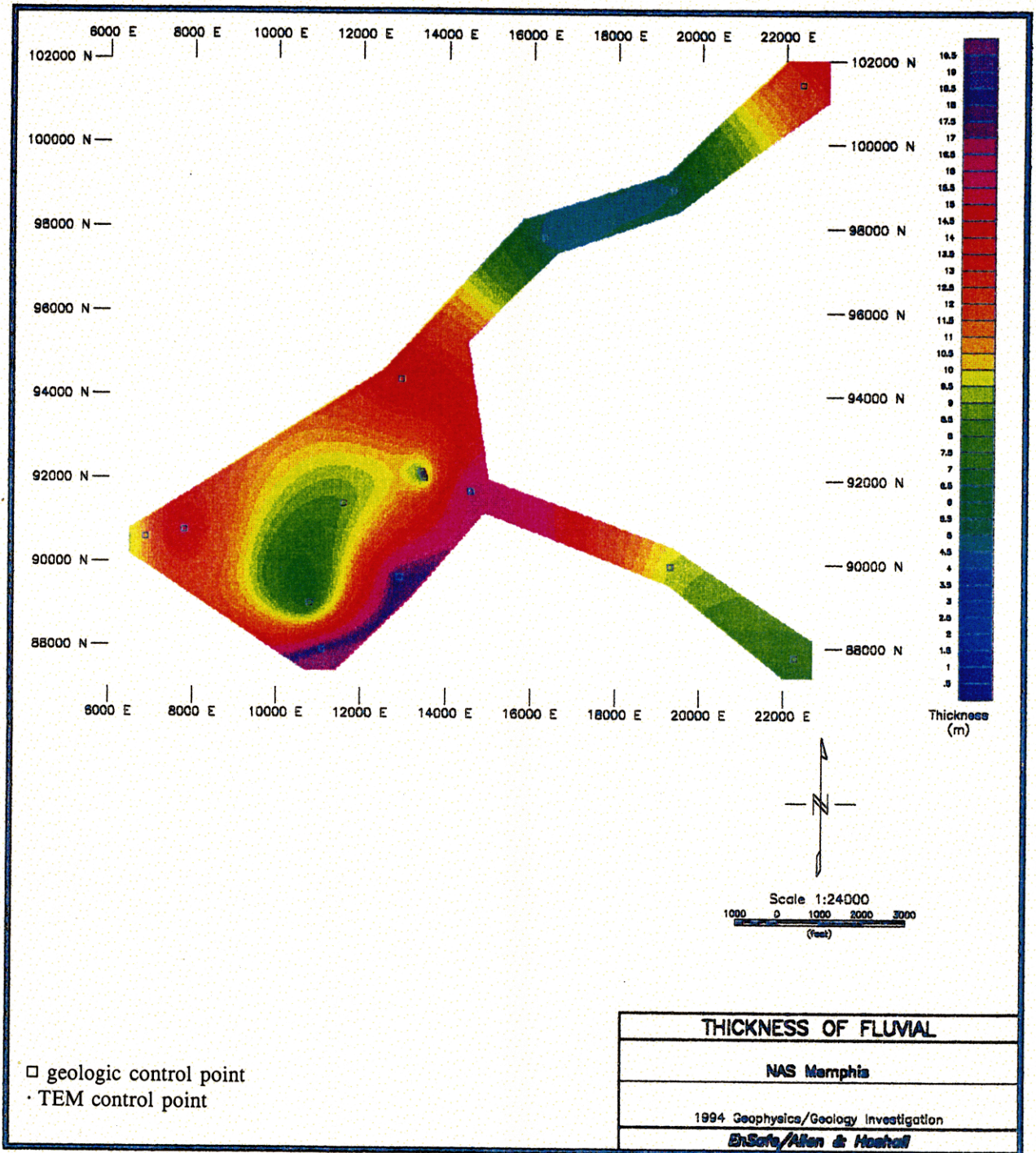


Plate 13. Thickness of Fluvial Unit. Thin areas may correspond to depositional draping over highs in the Cockfield, or may be related to terrace deposition.

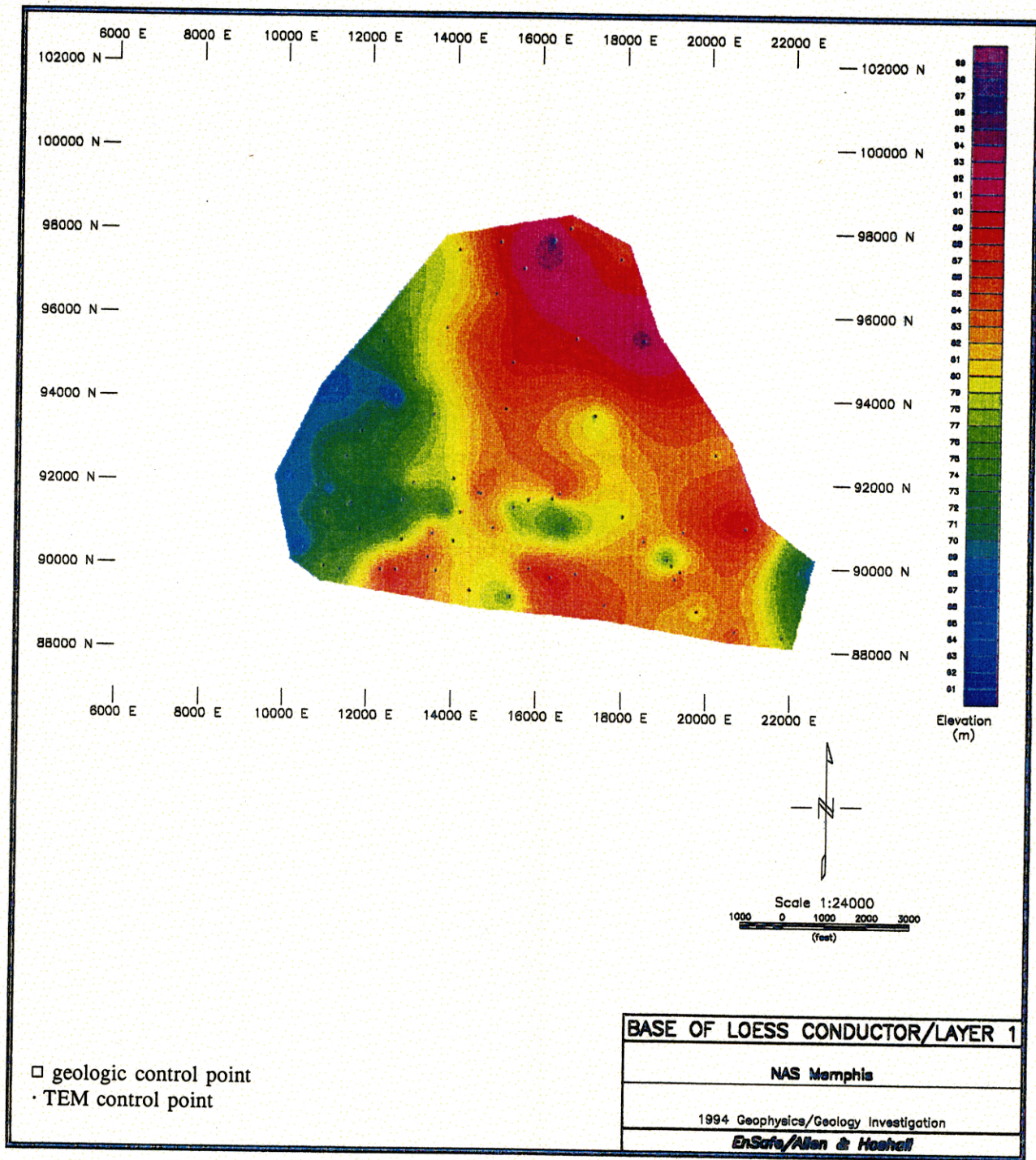


Plate 14. Base of Loess Conductor. This feature is electrically conductive, and appears to be a semi-continuous stratigraphic layer within the lower to middle loess. Where the conductor is absent, the base of TEM layer 1 is used for the plot.

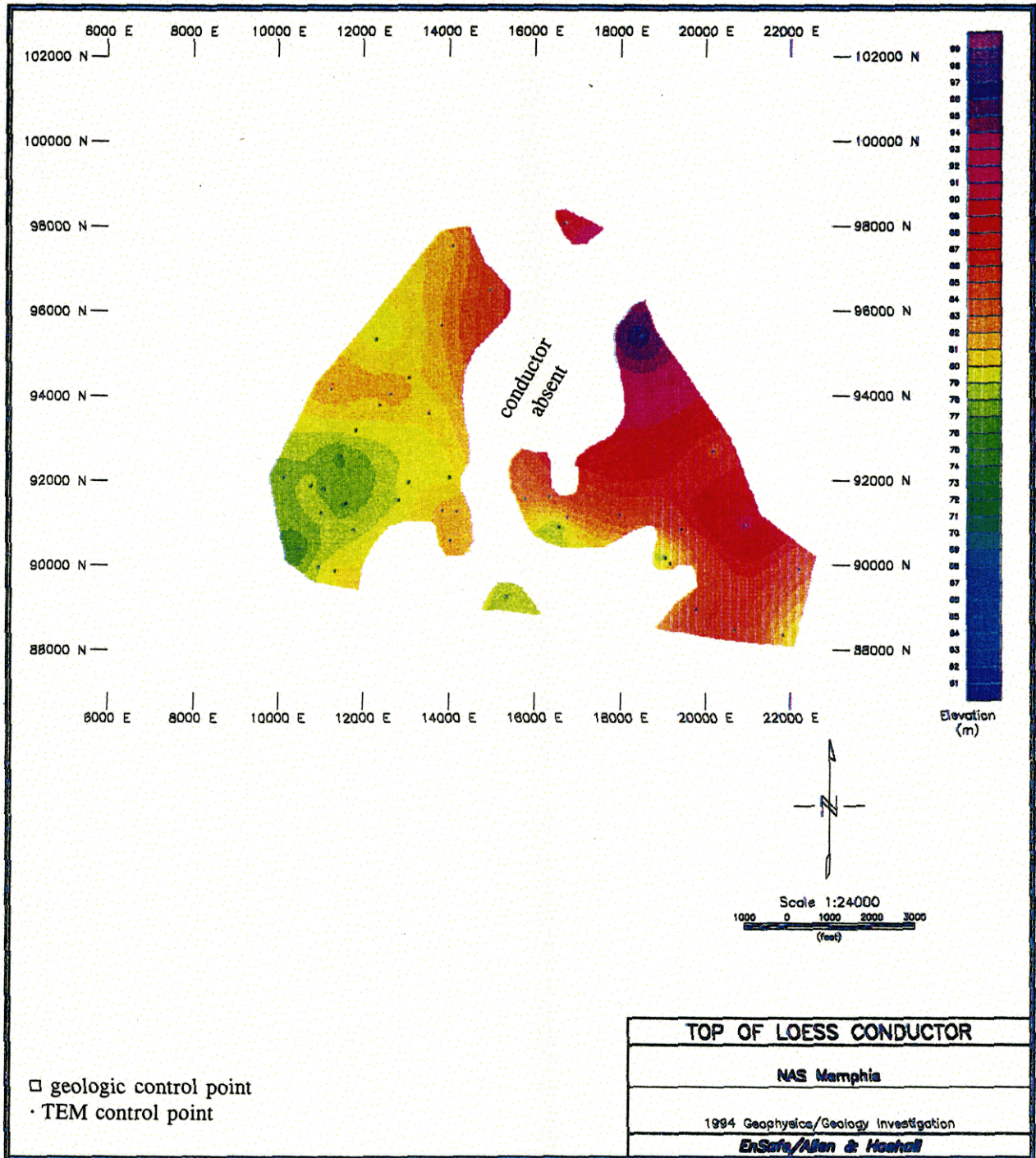


Plate 15. Top of Loess Conductor. The meandering blank area in the center of the plot shows where the conductor is absent.

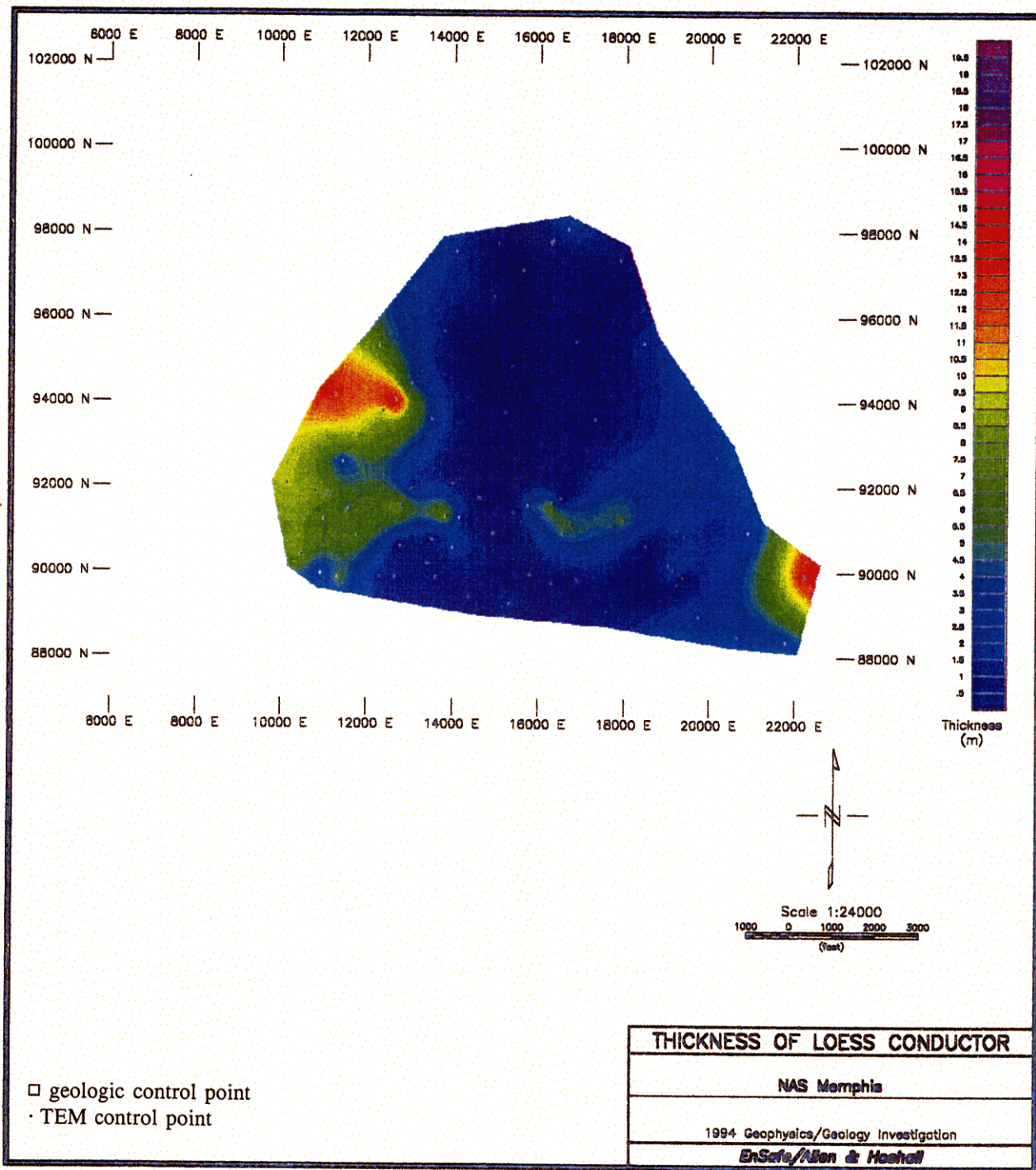


Plate 16. Thickness of Loess Conductor. The unit is thickest over low fluvial paleotopography, suggesting that it is depositional in origin.

The meandering shape of the low zone is reminiscent of an erosional river channel. The steeper slope to the west and the arcuate turn in the meander near the bottom-center of the color plot are suggestive of bank erosion from a wide, south-flowing river. Undulations in the topography within the channel are reminiscent of those one might expect in such a scenario. However, flow direction at this point is highly speculative and would require data over a considerably larger area.

Plate 8 shows the thickness of the Cook Mountain, which is known to vary from 9 to 22 m in the available drillhole results. Since the geophysics did not detect the contact with the Memphis Sand, the data in this plot are from drillhole data only, and a large no-data zone exists. Is it possible that the Cook Mountain might pinch out locally in the no-data zone? To find out, consider that a pinchout would most likely occur over a Memphis Sand high or a Cook Mountain top low. As it turns out, a Memphis Sand high, if it exists, would likely occur in the center of the no-data zone — the same area in which the paleo-channel depression occurs in the Cook Mountain top, and hence the most probable area for a pinchout. However, two test holes in the channel (TH-1 and TH-3) show at least 5 m of Cook Mountain (the borings were terminated before reaching the formation base). Thus, in the areas most likely to show pinchouts, a pinchout does not occur. It seems reasonable to conclude that the Cook Mountain, which is the most effective aquitard to the Memphis Sand aquifer, is present throughout the study area.

*The Cockfield* — Plate 9 shows the top of the Cockfield Formation, based on drillhole and geophysical data. The dominant feature is a sharp rise in elevation to the northeast. The rise is along a well-defined bench which has a northwest-trending strike. The linear geometry and 15 m relief of the bench suggest a fault, but the behavior of underlying Cook Mountain contradicts this. Instead, the bench appears to be an erosional remnant, characteristic of the Cockfield. The bench is located approximately above the Cook Mountain paleo-channel, which may have had some controlling influence on its formation.

Local highs and lows are evident at the top of the Cockfield. Some of these have a local dip of up to 5 degrees, although typical dips are much gentler. The undulations are probably the result of heavy erosion. Since this is the first time that such high spatial sampling density has been obtained in the Memphis area, it is not possible to say if such small-scale erosional features are common or unusual.

Plate 10 shows the Cockfield thickness. Since this parameter is controlled by tops of the Cook Mountain and Cockfield, undulations of both surfaces are reflected in the figure. Of special

importance are the blue-colored areas to the southwest, which represent interpreted thinning of the Cockfield to less than 10 m. One area around TEM station 73 is interpreted as a potential Cockfield pinch-out.

Plate 11 shows the total thickness of the upper Claiborne confining layer (Cockfield and Cook Mountain). It is unfortunate that the Cook Mountain thickness is only determined in a few drillholes, since the result is a plot with poor control. Note that the interpreted thinning of the Cockfield to the southwest is not accompanied by a similar thinning of the Cook Mountain, but rather a thickening. To the northeast, the Cockfield thickens dramatically. Further, as concluded earlier, the Cook Mountain is believed to exist without pinchouts or severe thinnings in this area. For these reasons, the confining layer is believed to be reasonably thick throughout the study area. The thinnest upper Claiborne encountered to date by a borehole is 16 m, and typical thickness is about 20 to 35 m.

*The Fluvial* — Plate 12 shows the top of the fluvial unit. Since no TEM picks were made at this electrically indistinct contact, the database consists only of drillhole picks, which are sparsely located. The data show a topographic low to the southwest and a sudden rise of about 20 m toward the northeast. This trend mimics the underlying Cockfield topography, although the match is imperfect to the southeast, where fluvial material does not form a high bench like the Cockfield.

Plate 13 shows the thickness of the fluvial unit. A thinning is seen to the northeast, with a thickening in the downslope direction to the southwest. Local thinnings are seen over highs in the underlying Cockfield erosional top. These observations are expected results of fluvial deposition over the Cockfield paleotopography of Plate 9. Depositional draping or terrace deposits may account for the fluvial paleotopography.

*The loess conductor* — A thin conductive unit lying toward the middle of the loess was required to fit the data at many soundings. Plate 14 shows the base of the loess conductor, or, where it is absent, the base of the resistive TEM layer 1 in which the conductor is always found. The surface shown in this plot can be thought of as an electrical "marker bed" within the middle to lower loess, although it sometimes lies near the base of the formation. Strong local variations are seen in these data.

Plate 15 shows the top of the conductor; the masked-out area is where the loess conductor is absent. It is higher to the northeast, following underlying trends, and lower to the southwest. It is interesting to note how these plots correspond to the present surface topography.

Plate 16 shows the thickness of the loess conductor. Note that it is absent over areas where Plate 14 shows local highs in the underlying topography. The conductor thickens to the west and east in areas of low underlying topography. This is entirely consistent with the patterns of eolian deposition, with low spots collecting the most material.

The loess conductor could arise either from groundwater distribution or depositional/erosional facies. A large number of shallow loess wells have been installed across the property, and these are invariably water-bearing, even in the areas where the loess conductor is absent. Hence the mere absence or presence of groundwater cannot explain the conductor. Instead, a facies explanation seems more likely. Erosion would have been concentrated at paleo-topographic highs, with smaller particles, including silts and clays, being transported the farthest into low-lying areas. Comparison of Plates 12 and 16 shows that the loess conductor is thickest in a low zone atop the Cockfield, lending credence to the explanation of depositional control.

#### **4.6 Implications For the RFI**

Several findings from this study may have important implications for the current RFI field work at NAS Memphis. Of particular attention are potential pathways for downward contaminant transport (faults, windows in the confining layer) and the patterns of shallow water-bearing zones which could be affected by contaminants.

*Contaminant transport paths via faults* — Normal faults with up to 20 m of throw are thought to occur in the Memphis Sand and deeper units, but it is uncertain whether they cut more recent deposits. Lack of spatial data density and the difficulty of distinguishing fault offsets from depositional/erosional patterns have contributed to the uncertainty. This study provides the first data set of sufficient data density to help resolve this issue at NAS Memphis.

The data show significant relief in the tops of all formational units except the Memphis Sand, for which few data are available. However, there are no linear features with vertical offset evident in the interpreted top of Cook Mountain (Plate 7). Instead, the patterns in this plot have every indication of being depositional/erosional in character. Therefore, the evidence is fairly strong that faults with significant vertical offset are not present within the study area.

*Contaminant transport via confining layer windows* — The most effective aquitard of the Upper Claiborne confining unit is the Cook Mountain Formation, whose pervasive clays result in a vertical hydraulic conductivity of  $10^{-8}$  to  $10^{-9}$  cm/s (Inberg-Miller Engineers, written communication, 1994). Therefore the only opportunity for downward migration through it is a stratigraphic window. A window has not been observed in wells drilled within 10 km of NAS Memphis, including 13 wells drilled on or adjacent to the property. Very small-scale windows are not likely, based upon the relatively flat nature of the Cook Mountain/Memphis Sand contact. Indeed, borings placed into depressions of the Cook Mountain top — places where it should be thinnest — show a minimum thickness of 5 m. Further, the minimum confirmed thickness of the Cook Mountain at NAS Memphis is 8 m. Thus it is very unlikely that the Cook Mountain has stratigraphic windows or sufficient thinnings to permit vertical migration of contaminants.

Overlying the Cook Mountain is the Cockfield, which, because of its fine-grained nature and inclusion of thick clay beds is also considered an aquitard in the NAS Memphis area. Within this unit, however, there is a possibility of migration pathways through a network of interfingering sandy lenses. The unit is thinnest to the southwest part of the study area, where a window might exist locally; however, a 21-m thick section of Cook Mountain lies below it. The Cockfield thickens in areas of no control on Cook Mountain thickness.

The Upper Claiborne confining sequence is present at every location where data were taken, and appears to be contiguous across the site without stratigraphic windows or extreme thinnings. This fact, coupled with the apparent absence of faults, is strong evidence that the Memphis Sand aquifer is protected from near-surface contaminants within the immediate study area.

*Shallow aquifers* — Water-bearing zones were not mapped directly in this project. Near-surface stratigraphy which may control near-surface waters has been mapped with fair success, and the results may become useful as the RFI progresses.

## **5.0 Conclusions**

The project is a good example of the value of integrated interpretation of geology and geophysics. The sparse well control in the area provides firm geologic control at specific points and hints of large-scale changes, but it lacks the spatial detail needed to construct an adequate geologic conceptual model. The TEM data set gives a fair amount of spatial detail, but alone is not interpretable for formation boundaries. A joint interpretation combines the strengths of each technique and results in a conceptual model which has real geologic boundaries and good spatial resolution at the same time.

The study shows no evidence of paths for downward contaminant migration via faults, pinchouts, or windows in the Upper Claiborne confining unit. Thus the main potable aquifer in the Memphis Sand should be reasonably well sealed against near surface contaminants found at NAS Memphis, at least within the confines of the study area. Left open is the question of possible southward migration of contaminants in the fluvial aquifer and potential communication to the Memphis Sand via a yet-unknown fault or window outside the study area. The RFI should provide sufficient data to determine if this possibility needs to be pursued.

The present data set is sufficient to propose a geologic conceptual model for the RFI. At this point, no additional work on the model is recommended. Additional work, either geophysical or deep drilling, might be an option later on, depending on the results of the RFI work.

## **6.0 References**

- Bostick, F.X. (1977). A simple almost exact method of MT analysis: Workshop on electrical methods in geothermal exploration, Snowbird, UT: U.S. Geological Survey Contract 14-08-001-6-359.
- ERC (1990). Preliminary Review Document for RCRA/CERCLA Activities, NAS Memphis, Millington, Tennessee. ERC Environmental and Energy Services Co.
- Fitterman, D.V., Frischknecht, F.C., Mazella, A.T., and Anderson, W.L. (1990). Example of transient electromagnetic soundings in the presence of oil-field pipes: in Ward, S.H., Ed., *Geotechnical and Environmental Geophysics*, vol. 2, 79-88.
- Geraghty & Miller (G&M) (1985). NACIP Program Confirmation Study, Verification Phase, NAS-Memphis.
- Graham, D.D., and Parks, W.S. (1986) Potential for Leakage Among Principal Aquifers in the Memphis Area, Tennessee. U.S. Geological Survey Water-Resources Investigations Report 85-4295.
- Inman, J.R. (1975). Resistivity inversion with ridge regression: *Geophysics*, 40, 798-817.
- Kingsbury, J.A. (1994). Written and verbal communications to E/A&H (not formally reviewed or approved by the USGS).
- Kingsbury, J.A., and Parks, W.S. (1993): Hydrogeology of the Principal Aquifers and Relation of Faults to Interaquifer Leakage in the Memphis Area, Tennessee. U.S. Geological Survey, Water-Resources Investigations Report 93-4075, 1-18.
- Kingsbury, J.A. (1994). Written communication to EnSafe/Allen & Hoshall; not reviewed or approved by the USGS.
- Mirecki, J.E., and Parks, W.S. (1994): Leachate Geochemistry at a Municipal Landfill, Memphis, Tennessee. *Ground Water*, 32, 390-398.
- Parks, W.S. (1990): Hydrogeology and Preliminary Assessment of the Potential for Contamination of the Memphis Aquifer in the Memphis Area, Tennessee. U.S. Geological Survey Water-Resources Investigations Report 90-4092, 1-39.
- (1992): Four Levels of Terrace Deposits and Remnants of High-Level Fluvial Deposits in the Hatchie River Valley, Hebron Area, Hardeman County, Tennessee. *Mississippi Geology*, 13, 63-70.

Parks, W.S., and Carmichael, J.K. (1990): Geology and Groundwater Resources of the Cockfield Formation in Western Tennessee. U.S. Geological Survey Water-Resources Investigations Report 88-4181, 1-17.

Parks, W.S., and Lounsbury, R.W. (1975): Environmental Geology of Memphis, Tennessee: *in* Field Trips in West Tennessee. Tennessee Division of Geology Report Inv. 36, 35-63.

Path: NAUSERSLJH016016TEM.RPT

**APPENDIX A**

---

**Description of the TEM Technique**

---

**Contents**

1.0	Applications . . . . .	A-3
2.0	How the Signal is Generated and Measured . . . . .	A-4
3.0	Depth Penetration . . . . .	A-7
4.0	Vertical and Lateral Resolution . . . . .	A-8
5.0	Types of Data Generated . . . . .	A-8
6.0	Sources of TEM Anomalies . . . . .	A-10
7.0	References . . . . .	A-13

*Technical Memorandum  
Geophysics Study to Characterize Geology  
NAS Memphis - Appendix A  
27 January 1995*

---

This page intentionally left blank.

## **The TEM Technique**

Transient electromagnetics (TEM), sometimes called time-domain electromagnetics (TDEM), inputs an electromagnetic signal to the ground and measures the earth's response to it. The technique senses vertical and horizontal changes in ground resistivity, allowing it to map three-dimensional subsurface variations. These variations can then be related to stratigraphy, geologic structure, and certain types of contaminants.

### **1.0 Applications**

Although it was originally developed for deep investigations for mining, TEM is becoming an important tool for shallow environmental investigations. Typical published applications include mapping groundwater (Taylor et al., 1992), identifying naturally occurring degradation of groundwater quality (McNeill, 1990 summarizing Fitterman, 1986; Hoekstra et al., 1992b; Stewart and Gay, 1981; Fitterman and Hoekstra, 1982; Mills et al., 1988), and mapping increased groundwater salinity due to contaminant sources (Buselli et al., 1986, 1990; Sinha, 1993; Hoekstra and Blohm, 1990; James and Borns, 1993; Hoekstra et al., 1992; Fitterman et al., 1990; Hanson et al., 1993). TEM also has been used to map conductive stratigraphy (Hoekstra et al., 1992). In addition to its environmental applications, TEM is commonly used to map lithology and structures for mining and petroleum exploration (see Spies and Frischknecht, 1991, and Nabighian and MacNae, 1991, for a review and bibliography).

TEM's chief advantages for environmental work are its vertical discrimination of conductive targets, usefulness at shallow and intermediate depths, and ease of use in crowded industrial settings. The data can be converted to three-dimensional subsurface maps, which can be of considerable assistance in mapping certain contaminants or stratigraphy and structure.

TEM is a key component of an environmental geophysics program. It provides significantly better vertical resolution than frequency-domain electromagnetics (FDEM) profiling techniques, and better lateral resolution and speed than galvanic resistivity (e.g., Schlumberger array soundings). A chief disadvantage, especially compared to DC resistivity, is that TEM is fair to poor at resolving resistive features and is very poor at mapping resistivity variations within a resistor; when such features need to be delineated, another technique must be selected. Compared to FDEM, TEM is much slower (acquiring perhaps 2 percent of the data points

per day), and it requires considerably more involved data processing and interpretation procedures. It is also more strongly affected by culture (e.g., fences, buried cables and pipes, etc.). Thus it may be a poor choice in high-culture areas. To summarize, TEM is best used when a conductive target is being mapped and vertical discrimination is required. Thus it can be regarded as a specialized tool for solving certain types of problems, such as mapping conductive contaminant plumes, conductive stratigraphic units, faults, etc.

## 2.0 How the Signal is Generated and Measured

TEM puts an electromagnetic signal into the ground and measures the response at the surface due to buried conductors. The signal is often generated by transmitting an alternating current into a square-shaped wire loop laid flat on the ground. The current waveform usually consists of a repetitive sequence of positive current, off, negative current, off, positive current, etc. Each time the current is switched on or off, an electromagnetic pulse is generated. The pulse produces an electromagnetic (EM) field which encircles the wire loop. Since an EM field flows preferentially through a conductor, it couples inductively into the conductive earth as a downward-traveling EM wave. The signal can be visualized as an electromagnetic "smoke ring" blown into the earth by the source loop (Nabighian, 1979), illustrated in Figure A-1.

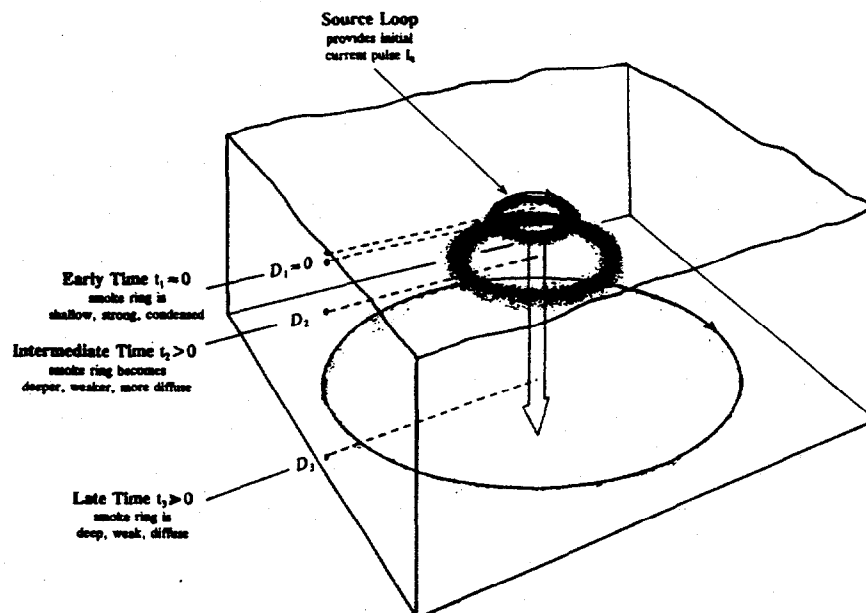


Fig. A-1. The TEM signal propagates like a "smoke ring" blown into the earth. As time increases, the smoke ring gets deeper, larger, and more diffuse.

Three snapshots of the downward-traveling smoke ring are shown in the smoke ring illustration of Figure A-1. Within a small fraction of a second after a current pulse (time  $t_0=0$ ), the smoke ring lies just beneath the wire loop and it has a strong, doughnut-shaped magnetic field. After an elapsed time  $t_1$  of several microseconds after current shutoff, the smoke ring has traveled downward some distance  $D_1$  into the earth. It is now larger in diameter and more diffuse, and it has a much lower magnetic field strength. After an even larger elapsed time  $t_2$ , the smoke ring has penetrated deeper and is significantly larger, more diffuse, and weaker. Eventually the signal is too weak to measure.

To visualize how a return signal is measured, consider that the downward-traveling smoke ring has associated with it a time-dependent voltage field. The voltage field extends outward from the smoke ring in all directions, and hence can be sensed from the surface even when the smoke ring is deep in the earth. If the earth is of uniform resistivity, the voltage measured everywhere on the surface will be the same. On the other hand, if the smoke ring encounters a conductive layer at depth, it is channeled preferentially into the conductor, and the voltage at the earth's surface is distorted. It is this distortion which is interpreted for earth structures.

Environmental TEM often makes use of an in-loop array, which uses a larger loop to transmit the signal and a smaller loop, inside the larger one and concentric with it, to make the measurement. One can measure either the vertical magnetic field  $h_z$  in a magnetic antenna or the voltage  $V=\partial h_z/\partial t$  ( $t$ =time) in the inner loop. The latter is often chosen for environmental work because of simplicity of layout and interpretation. The general equation for the voltage at the surface is somewhat complex, but can be simplified in the two cases of *early-time* (small  $t$ ) and *late-time* (large  $t$ ) measurements. For early time, the expression is

$$\frac{\partial h_z}{\partial t} = \frac{-3I\rho}{\mu_0 A^3}, \quad (\text{A-1})$$

and for late times, the expression is

$$\frac{\partial h_z}{\partial t} = \frac{-IA^2\mu_0^{3/2}}{20\pi^{1/2}t^{5/2}\rho^{3/2}}, \quad (\text{A-2})$$

where: voltage is the partial differential of the magnetic field  $h_z$  with respect to time  $t$  in seconds,  $I$  = the current flowing in the loop (amperes),  $A$  = the area of the loop,  $\mu_0$  is the free-space magnetic permeability, and  $\rho$  = the resistivity of the ground in ohm-meters ( $\Omega \cdot \text{m}$ ).

Resistivity is a measurement of the resistance of a volume of material to electrical energy flow, and is the inverse of conductivity  $\sigma$ .

The field measurements consist of voltage in the receiving loop as a function of time, forming a *decay curve* (Figure A-2). The curve is sampled in discrete time intervals called *windows*. In the earliest windows, the early-time response of equation A-1 prevails, and the decay curve is flat (not proportional to time  $t$ ). The flat response indicates the return signal is still dominated by the original current pulse. At later times the smoke ring has moved downward and become more diffuse. The decay curve dips downward and the voltage becomes inversely proportional to time and resistivity. In effect, the late-time response is free from source current effects and is due to induced eddy currents in the subsurface which decay very rapidly. Eventually the signal becomes so weak that it cannot be measured.

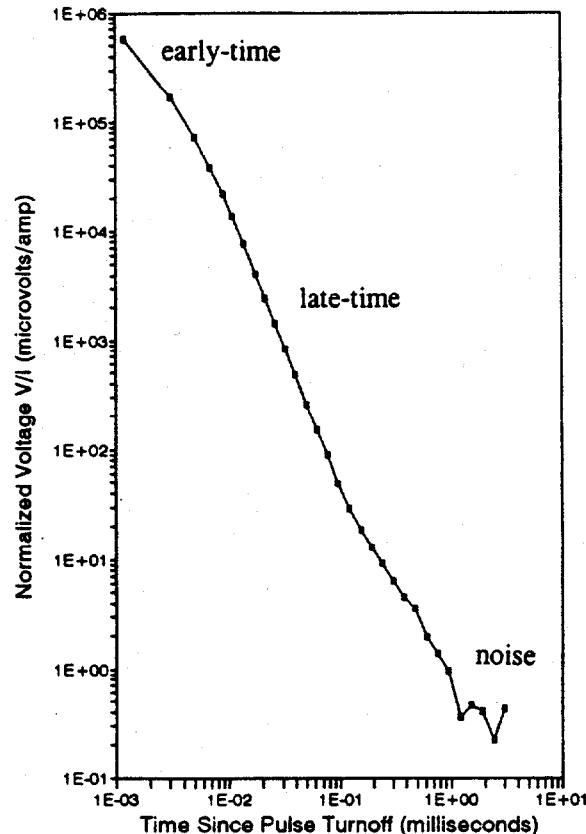


Fig. A-2. The TEM decay curve, showing how received signal voltage decays exponentially with time. Each point on the curve represents the center of a measurement window, as described in the text.

The shape of the decay curve is determined by the resistivity structure of the ground. When the smoke ring encounters a conductive body at depth, current is focused preferentially into the conductor, and the transient response dies out more slowly. The net effect is that the decay curve becomes shallower. Because of the physics of EM transients, however, a resistor has much less of an effect on the decay curve. Hence TEM is far better at resolving a conductive feature than a resistive one. A resistive basement is more easily resolved than a small resistive body, but the interface depth estimate is subject to greater error than it would otherwise be for a conductor. Further, TEM is very poor in resolving resistivity variations within a resistive feature.

### 3.0 Depth Penetration

It can be seen in equation A-1 that vertical penetration increases with elapsed time  $t$ . The effective penetration depth  $D$  (in meters) is given by

$$D = 0.89\sqrt{\rho t_{\mu s}}, \quad (\text{A-3})$$

where, for convenience,  $t_{\mu s}$  is in units of microseconds. While this would suggest an unlimited range of vertical resolution, in actuality both the shallow and deep limits of the curve are set by instrumentation and field noise considerations.

The shallowest limit is determined by how fast the source signal can be turned off. This is essentially a function of self-inductance of the loop and, to a degree, the capacitive effects in the instrumentation. Modern systems achieve turnoff times of about 1-10  $\mu s$ , which typically places the first window at several meters deep.

The latest times at which a signal can be measured are determined by the signal-to-noise ratio of the measurement system. This is a complex issue involving the degree of randomness in the noise, amplitude of the noise, loop geometry, dynamic range and electronic design factors of the instrumentation, noise-rejection architecture, and numerous other factors. On the average, modern 16-bit digital instruments can measure a dynamic range of about four to five orders of magnitude, which corresponds roughly to about three orders of magnitude range in time. Typical penetration on environmental projects is 20 to 100 meters. To achieve deeper penetration, much larger arrays or dynamic gain-ranging techniques must be used, but this is rarely necessary. The issue of maximum penetration depth is an important one in evaluating any data set.

#### 4.0 Vertical and Lateral Resolution

TEM produces a vertical sounding which can be thought of as a "fuzzy" electric log. The data identify the larger, more conductive features in the subsurface, sometimes averaging the responses of several thin horizons together. The fuzziness increases with depth as the smoke ring becomes more diffuse. As a result, TEM's ability to pick depths depends, in part, on the depth of the interface. Typically the top of a conductive layer can be located to within  $\pm 10$  percent of its depth of burial; the error in picking the top of a resistor is often larger. In some cases the error increases to  $\pm 20$  percent of the depth of burial, which may still provide useful information for large-scale geologic mapping. The latter can be thought of as the largest acceptable error for most practical purposes.

Lateral resolution is also a function of the smoke ring's diffusive nature. Near the surface, resolution is roughly proportional to the loop size. As the smoke ring travels downward, it expands, and its ability to resolve lateral features is degraded. Hence, the lateral resolution of features such as a fault or edge of a plume tends to be best at the surface and gets worse at depth.

#### 5.0 Types of Data Generated

The voltage decay curve is normally converted to resistivity values for various depths, which can be related to subsurface structure. There are three types of resistivity representations: apparent resistivity, imaged resistivity, and inverted resistivity. Figure A-3 illustrates these three parameters.

*Apparent resistivity* can be plotted as a function of time window or against depths estimated from the skin-depth equation A-3. The term *apparent* resistivity is used because any individual data point on the sounding curve does not correspond to a discrete resistivity value for material at its calculated depth, but rather is a complex response to the entire section of material overlying it. In effect, it is a first guess of the resistivity structure of the subsurface.

*Imaging* is the attempt to convert apparent resistivity to a truer representation of the resistivity values associated with specific depths. This is accomplished by assuming a number of thin layers and iteratively varying their resistivities to reproduce the decay curve. The resistivity transitions from one thin layer to the next are constrained to be smoothly varying, giving rise to the term *smooth modeling*. The result is a gradational, "fuzzy" image of resistivity structure,

without sudden, distinct electrical breaks. This type of image is entirely appropriate for an electromagnetic sounding, which, because of the diffusing signal, has a certain fuzziness to its resolution.

Smooth-modeled data are less than satisfying to many geologists because the models yield no firm depth to various contacts. If such information is required, *layered inversions* are carried out. The inversion process finds a one-dimensional set of layers which reproduce the measured decay curve (two- and three-dimensional TEM algorithms are not yet available in practical application). The layer parameters are not required to be smoothly varying. The model output consists of resistivity and thickness of each layer, accompanied by a range of equivalence data, which provide a way to assess confidence in the numerical values.

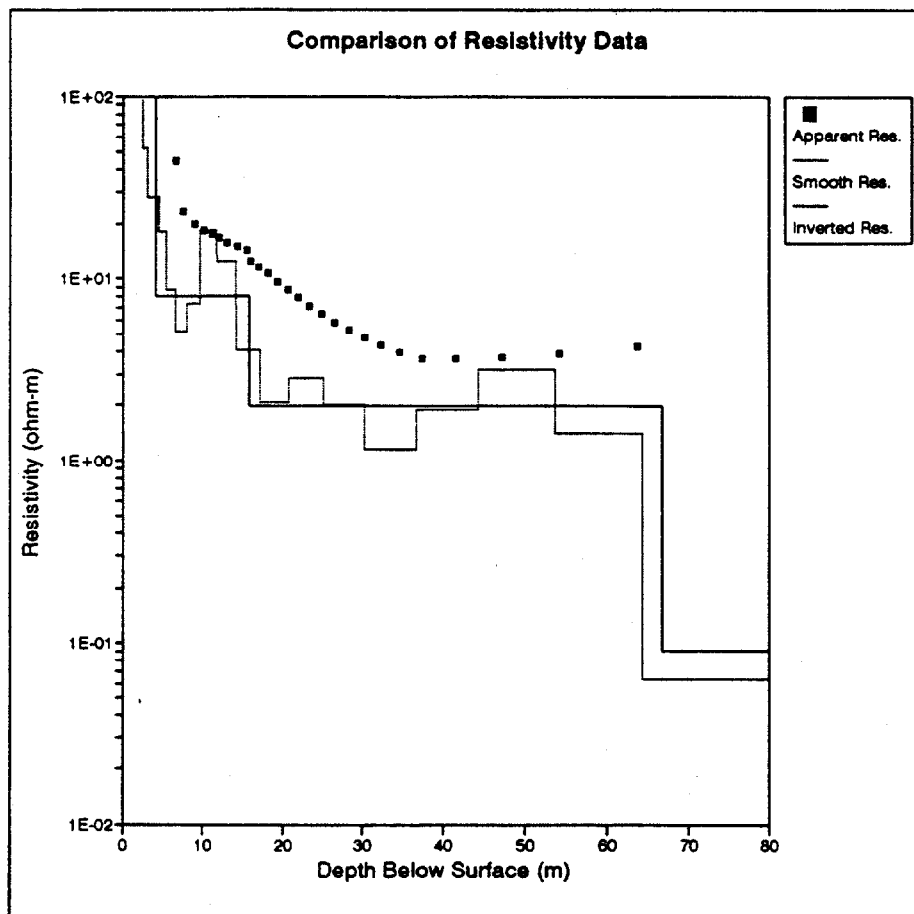


Fig. A-3. Comparison of apparent resistivity to one-dimensional imaged and inverted model resistivities. Imaging best simulates the resolution ability of TEM, while inverted resistivities give a result most useful for structure mapping.

The final step of the process is to interpret the modeled electrical structure for geologic structure. In many cases the model and actual structure are quite different. For example, TEM will map a conductive feature which may or may not correspond to a mapped geologic unit. By comparing the TEM results to available geologic data, the two data sets can be interpreted jointly. Frequently the geologic data provide reliable geologic information at a few locations; the geophysics data, when properly correlated, yield somewhat less reliable geologic data but at a much greater data density. Combined, the two data sets provide a better picture of the subsurface than would be possible with either data set alone.

At the present time, two- and three-dimensional modeling is not well suited for production geophysics. Accordingly, it may be difficult to fit data with such effects with one-dimensional models. In such cases it is necessary to increase the spatial data density to help resolve the structures. The problem is particularly important in evaluating data in late time, where three-dimensional effects are often observed (Goldman et al., 1994; Newman et al., 1987; E/A&H, unpublished work). Many of these effects may be related less to three-dimensional influences and more to signal-depletion problems in late-time data. Appendix B describes this issue in more detail.

## 6.0 Sources of TEM Anomalies

Electrical conduction in the earth is primarily controlled by the availability of exchangeable cations in a liquid. Thus it is not unexpected that dry earth materials tend to be resistive, while those containing water are more conductive. However, several factors control the conductivity of materials containing water. *Porosity* is an important control, since it determines the amount of fluid the material can contain, and thus the ability to exchange available cations. *Permeability* is also of some importance in certain instances. The degree of pore saturation is clearly an important factor as well. Some materials are only partly saturated due to low permeability or other factors. For example, vadose-zone soils may be slightly moist due to downward percolation or capillary effects from deeper groundwater. *Cation availability* is of critical importance. The soil or rock matrix is the chief contributor to available cations. For example, a vuggy basalt has few cations to exchange, and hence is resistive. On the other hand, weathered clays, by virtue of their chemistry as well as their extensive pore path network, contribute a large number of cations to pore fluids, making them conductive. The type of clay, its degree of weathering, and the particular geometry of its pore spaces will also influence the

conductivity. Cation availability is also affected by sources outside the soil/rock matrix, such as introduced chlorides or acids from contaminated sites, incursion of coastal brines into an aquifer, etc. In rare cases, such as porphyry copper deposits, the presence of *conducting metals* may also influence ground conductivity. Other controls, such as temperature, inclusion of organic matter, and biologic activity may also have secondary controls.

Each of these controlling factors produces a broad range of conductivity values for different rock and soil types, making it impossible to generalize the characteristic response of any particular type of material. Controlling factors may also vary within a site due to facies, the presence of fractures and faults, structure, introduction of contaminants, etc. However, one can summarize the response of certain earth materials as follows:

<b>Geologic Origin of Conductors and Resistors</b>	
<b>Conductors</b>	<b>Resistors</b>
<b>PRIMARY CONTROLS</b>	
wet soils/rock	dry soils/rock
saline water	fresh water
clays	unweathered soil/rock
high porosity	low porosity
<b>SECONDARY CONTROLS</b>	
high temperature	low temperature
high pressure	low pressure

In near-surface environmental investigations, the earth's electrical response is often dominated by the presence of saturated zones (or depth to water in simple cases) and the presence of saturated clays. These factors provide valuable marker horizons in characterizing shallow hydrology and geology.

In addition to geologic anomalies, TEM is influenced by the presence of culture, which includes underground pipes and cables and above-ground fences, powerlines, buildings, and other conductive features. The influence of culture on TEM has been inadequately described in the literature, with a single exception. Fitterman et al. (1990) describe and model the effects of a

pipeline, concluding that the strongest effects are in mid-time, causing a depression of the resistivity curves even for stations many tens of meters from the pipeline. E/A&H, in unpublished work, has found that while culture is sometimes detectable by early-time data scatter, usually there is no obvious clue that there is a problem unless a spatially dense data set is obtained. Hence, in the typical case of a spatially aliased data set, cultural influences might go undetected, instead being falsely interpreted as conductive structure. Until culture-detection techniques are better developed, the best way to solve the problem is to obtain soundings far from culture whenever possible.

## 7.0 References

- Buselli, G., Barber, C., and Williamson, D.R. (1986). The mapping of groundwater contamination and soil salinity by electromagnetic methods: Hydrology and Water Resources Symposium, Griffith University, Brisbane, 317-322.
- Buselli, G., Barber, C., Davis, G.B., and Salama, R.B. (1990). Detection of groundwater contamination near waste disposal sites with transient electromagnetic and electrical methods: in Ward, S.H., Ed., *Geotechnical and Environmental Geophysics*, vol. 2, 27-39.
- Fitterman, D.V. (1986). Transient electromagnetic sounding in the Michigan Basin for groundwater evaluation: in Proc. of the National Water Well Assn. Subsurface and Borehole Geophysical Methods and Ground Water Instrumentation Conf., Denver, 334-353.
- Fitterman, D.V., Frischknecht, F.C., Mazella, A.T., and Anderson, W.L. (1990). Example of transient electromagnetic soundings in the presence of oil-field pipes: in Ward, S.H., Ed., *Geotechnical and Environmental Geophysics*, vol. 2, 79-88.
- Fitterman, D.V., and Hoekstra, P. (1982). Mapping of salt water intrusion with transient electromagnetic methods: Proc. NWWA EPA Conf., Surface and Borehole Geophysical Methods in Ground Water Investigations, Las Vegas, NV.
- Fitterman, D.V., and Stewart, M.T. (1986). Transient electromagnetic sounding for groundwater: *Geophysics*, 51, 995-1005.
- Goldman, M., Tabarovsky, L., and Rabinovich, M. (1994). On the influence of 3-D structures in the interpretation of transient electromagnetic sounding data. *Geophysics* 59, 889-901.
- Hanson, J.C., Tweeton, D.R., and Friedel, M.J. (1993). A geophysical field experiment for detecting and monitoring conductive fluids: *The Leading Edge*, 930-937.
- Hoekstra, P., and Blohm, M.W. (1990). Case histories of time-domain electromagnetic soundings in environmental geophysics: in Ward, S.H., Ed., *Geotechnical and Environmental Geophysics*, vol. 2, 1-15.
- Hoekstra, P., Lahti, R., Hild, J., Bates, C.R., and Phillips, D. (1992). Case histories of shallow time domain electromagnetics in environmental site assessment: *Ground Water Monitoring Review*, Fall 1992, 110-117.

- Hoekstra, P., Hild, J., and Toth, D. (1992b). Time domain electromagnetic measurements to determine water quality in the Floridan Aquifer: Proc. of the Symposium on the Application of Geophysics to Engineering and Environmental Problems, v.1, 111-127.
- James, B.A., and Borns, D.J. (1993). Two-dimensional subsurface imaging with transient EM for mapping of a buried dissolution structure near the Waste Isolation Pilot Plant: Proc. of the Symposium on the Application of Geophysics to Engineering and Environmental Problems, v.2, 633-656.
- McNeill, J.D. (1990). Use of electromagnetic methods for groundwater studies: in Ward, S.H., Ed., *Geotechnical and Environmental Geophysics*, vol. 1, 191-218.
- Mills, T., Hoekstra, P., Blohm, M., and Evans, L. (1988). Time domain electromagnetic soundings for mapping sea water intrusion in Monterey County, CA: *Ground Water*, 26, 771-782.
- Nabighian, M.N. (1979). Quasi-static transient response of a conducting half-space: an approximate representation: *Geophysics*, 44, 1700-1705.
- Nabighian, M.N., and MacNae, J.C. (1991). Time domain electromagnetic prospecting methods, in Nabighian, M.N., Ed., *Electromagnetic Methods in Applied Geophysics*, v.2A: Society of Exploration Geophysicists, 427-520.
- Newman, G.A., Anderson, W.L., and Hohmann, G.W. (1987). Interpretation of transient electromagnetic soundings over three-dimensional structures for the central loop configuration: *Geophysical Journal of the Royal Astronomical Society (Geophysical Journal International)*, 89, 889-914.
- Sinha, A.K. (1993). Application of two ground electromagnetic systems in environmental investigations (abs.): Proc. of the Symposium on the Application of Geophysics to Engineering and Environmental Problems, v.1, 163-165.
- Spies, B.R., and Frischknecht, F.C. (1991). Electromagnetic sounding: in Nabighian, M.N., Ed., *Electromagnetic Methods in Applied Geophysics*, v.2A: Society of Exploration Geophysicists, 285-425.
- Stewart, M.T., and Gay, M. (1981). Evaluation of transient electromagnetics for deep detection of conductive fluids: *Ground Water*, 24, 351.
- Taylor, K., Widmer, M., and Chesley, M. (1992). Use of transient electromagnetics to define local hydrogeology in an arid alluvial environment: *Geophysics*, 57, 343-352.

**APPENDIX B**

---

**Quality Assurance/Quality Control**

---

**Contents**

1.0	Data Accuracy . . . . .	B-3
2.0	Data Precision . . . . .	B-3
3.0	Spatial Aliasing . . . . .	B-6
4.0	Cultural Bias . . . . .	B-10
5.0	Maximum Depth of Soundings . . . . .	B-17
6.0	References . . . . .	B-23

*Technical Memorandum  
Geophysics Study to Characterize Geology  
NAS Memphis - Appendix B  
27 January 1995*

---

**This page intentionally left blank.**

## **QA/QC Procedures**

A number of quality assurance/quality control tests were performed during the TEM investigation at NAS Memphis. This Appendix describes the procedures used. A summary is provided in the report text.

### **1.0 Data Accuracy**

Since most geophysical work looks at relative changes more than absolute numerical values, data accuracy (conformance to an exact quantitative standard) is not usually of paramount importance. However, care was taken to achieve maximum accuracy. The field instrument calibrated itself prior to every data collection event, compensating for drift in analog components. Setup parameters were systematically checked at each sounding, and data were plotted in the field to ensure that the voltage and resistivity measurements conformed to the expected range of numbers at the site. Sufficient checks were made that the large disparity between the modeled resistivities near USGS test holes and the downhole geophysics logs, discussed in Section 4 of the report, is not believed to be an accuracy problem originating with the instrument or field procedure.

### **2.0 Data Precision**

Data precision (repeatability) is of great concern on any geophysics project. Instrument problems, field noise, slight setup changes (loop configuration, etc.), and operator error are potential sources of poor precision.

Short-term precision was monitored by comparing the scatter in data from one stack burst to the next. Scatter is plotted as error bars in the final averaged field curves. Long-term precision is best measured by repeating data at a station over the course of a survey.

Station 13 was measured twice as a check on long-term precision, and the resulting decay curves are shown in Figure B-1. The first curve (filled boxes) was obtained in cool, wet conditions in April; the second curve (open boxes) was obtained in warmer weather in May after several weeks of drying conditions. The two curves show a consistent level shift in early and mid times, where noise is minimal, and more irregular differences in the noisy late-time data. The

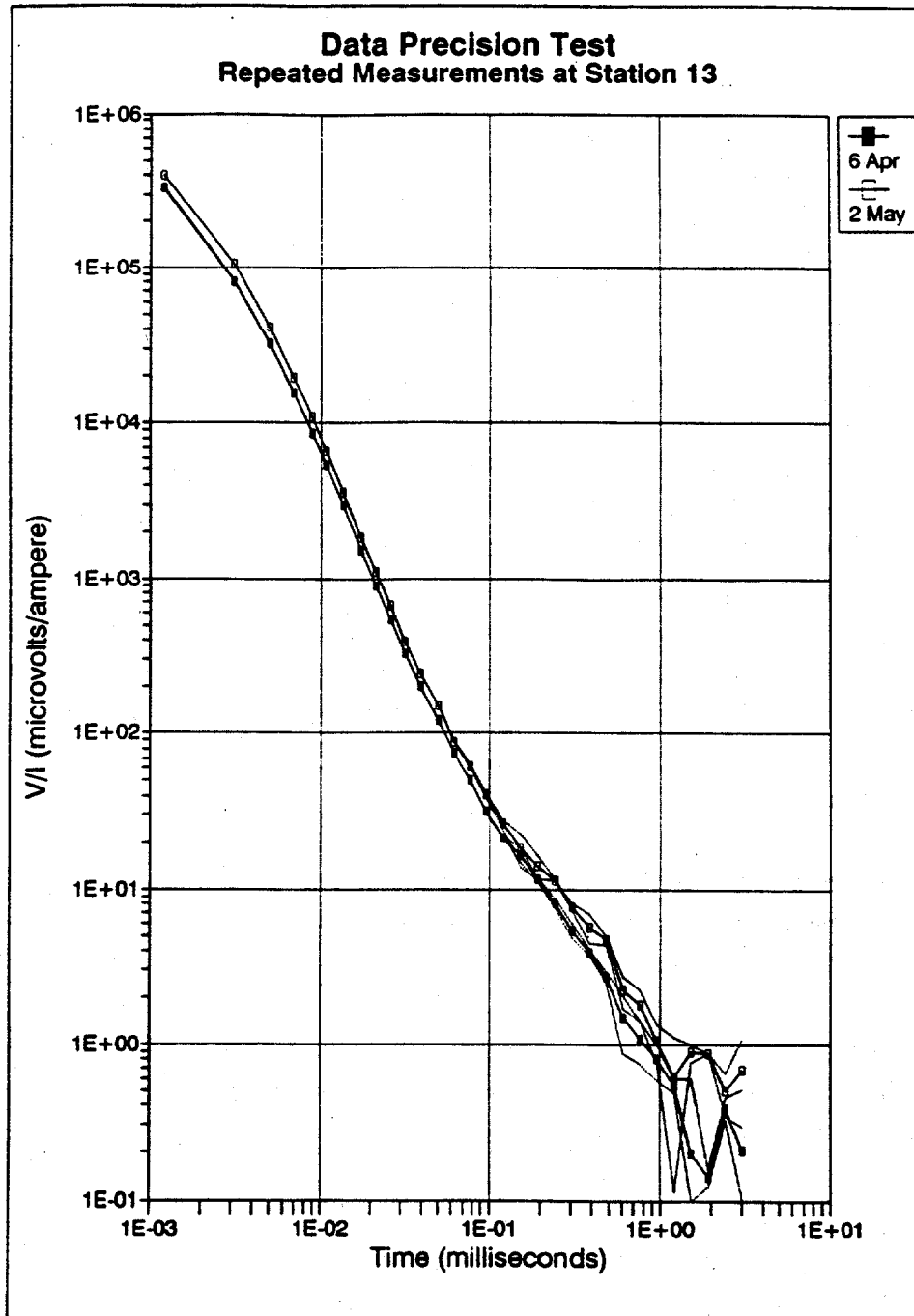


Fig. B-1. Repeat at station 13 over a period of nearly a month. Note the upward shift in the decay curve with time. Dotted lines connect the high and low error bars for each window, forming error envelopes.

sign of the shift is opposite that expected from drying surface conditions, since more conductive ground is indicated in the second data set. Additionally, changing surface conditions should show an early-time shift but achieve close agreement in mid and late times, a character which is not seen in these data. Therefore it is unlikely that the shift is a result of weather-related changes in the ground. Since loop positioning and other factors were the same for the two measurements, the curve shift is a mystery.

Failing to explain the cause of the shift, one must next question how important it is to the project interpretation. The two sets of data were modeled separately, and the results are compared in Table B-1. Resistivities and depth picks for the top three layers show a consistent shift which is less than the range of equivalences of the models. More significant changes which exceed the ranges of equivalence are seen in layers 4 and 5, particularly in the resistivity solutions. Depth picks are shifted but the relative change normalized to layer depth is still under the  $\pm 20$  percent criterion used to define useful TEM data. Most importantly, the ability to pick the Cook Mountain, which is tied to layer 4 at station 13, would be shifted by +4 m between the two data

Table B-1  
**TEM Repeatability at Station 13 (Modeling Results)**

Parameter	— 6 Apr Data —		— 2 May Data —		Percent Change <sup>a</sup>
	Solution	Range of Equivalence	Solution	Range of Equivalence	
<b>LAYER RESISTIVITIES <math>\rho_n</math> (ohm-meters)</b>					
$\rho_1$	240	169-387	210	141-390	-13
$\rho_2$	28	21-34	23	17-29	-18
$\rho_3$	96	85-111	88	74-110	-8
$\rho_4$	<b>7.5</b>	5.6-9.9	<b>4.1</b>	2.9-5.5	-45
$\rho_5$	1.1	.85-2.0	<b>.31</b>	.23-.55	-72
( $\rho_0$ )	(.1)	(.032-.20)	(.1)	(.029-.23)	(+11)
<b>LAYER ELEVATIONS <math>E_n</math> (meters)</b>					
$E_2$	77.8	76.8-78.7	78.2	77.2-79.2	+6
$E_3$	73.0	72.0-74.3	73.6	72.5-74.9	+5
$E_4$	<b>37.2</b>	35.1-41.0	<b>42.9</b>	41.2-45.9	+12
$E_5$	<b>19.0</b>	17.0-23.9	<b>29.1</b>	26.8-33.5	+15
( $E_0$ )	(-1.9)	(-6.2-+9.8)	<b>18.3</b>	14.6-25.4	(+23)

Notes:

bold numbers show exceedances of range of equivalence in matching data set

<sup>a</sup> Percent difference in elevations are normalized to depth.

(data) in parentheses are deeper than the maximum depth of resolution.

sets. This is less than the  $\pm 7$  m error in picking this formation (see Section 4 of the report). Hence, with the main emphasis of this study on picking formational units and not absolute resistivities, the problems in repeatability are not serious.

### 3.0 Spatial Aliasing

Spatial aliasing occurs when the spacing between sampling points is larger than the spatial variations present. For example, acquisition of two or three soil samples on a large site with isolated spots of contamination would result in heavily aliased data. Instead, one would have to choose between a dense sampling grid scheme or a statistically-based sampling scheme to adequately characterize the soil contamination. The sampling design is usually a compromise between the desire to obtain minimally aliased data and the budget constraints of the project.

Geophysics faces similar challenges. Although the lower cost of geophysics allows a higher sample density to be obtained than with direct media sampling approaches, the costs of obtaining a truly unaliased data set are almost always prohibitive. Therefore geophysics data sets are aliased to some degree, and it is important to examine the practical effects of aliasing on the interpretation.

Aliasing checks were built into the survey design by establishing six areas where two adjacent soundings would be made. Source loops were placed end-to-end in a *butterfly* pattern. Two butterflies were run in non-cultured areas to check spatial aliasing due to geology alone; four were located near culture and are presented in the next section.

Figures B-2 and B-3 show the decay curves from butterflies at stations 22/23 and 50/51, respectively. Both locations are in areas believed to be free from culture, and thus illustrate the true degree of geologic aliasing in closely spaced data. Solid lines in the figures show the averaged data, and dotted lines show the noise envelopes ( $\pm 1$  standard deviation) for the data. The agreement is excellent in the two wings of each butterfly at early and mid-times. Even at late times, divergence of the curves is well within the noise envelopes. This result suggests that, in uncultured areas, *small-scale* spatial aliasing is minor.

A larger-scale aliasing check can be made by comparing the results along a 1,570-m traverse in an uncultured area on the northwest part of the study area, as shown in Figure B-4. The

(text continued page B-10)

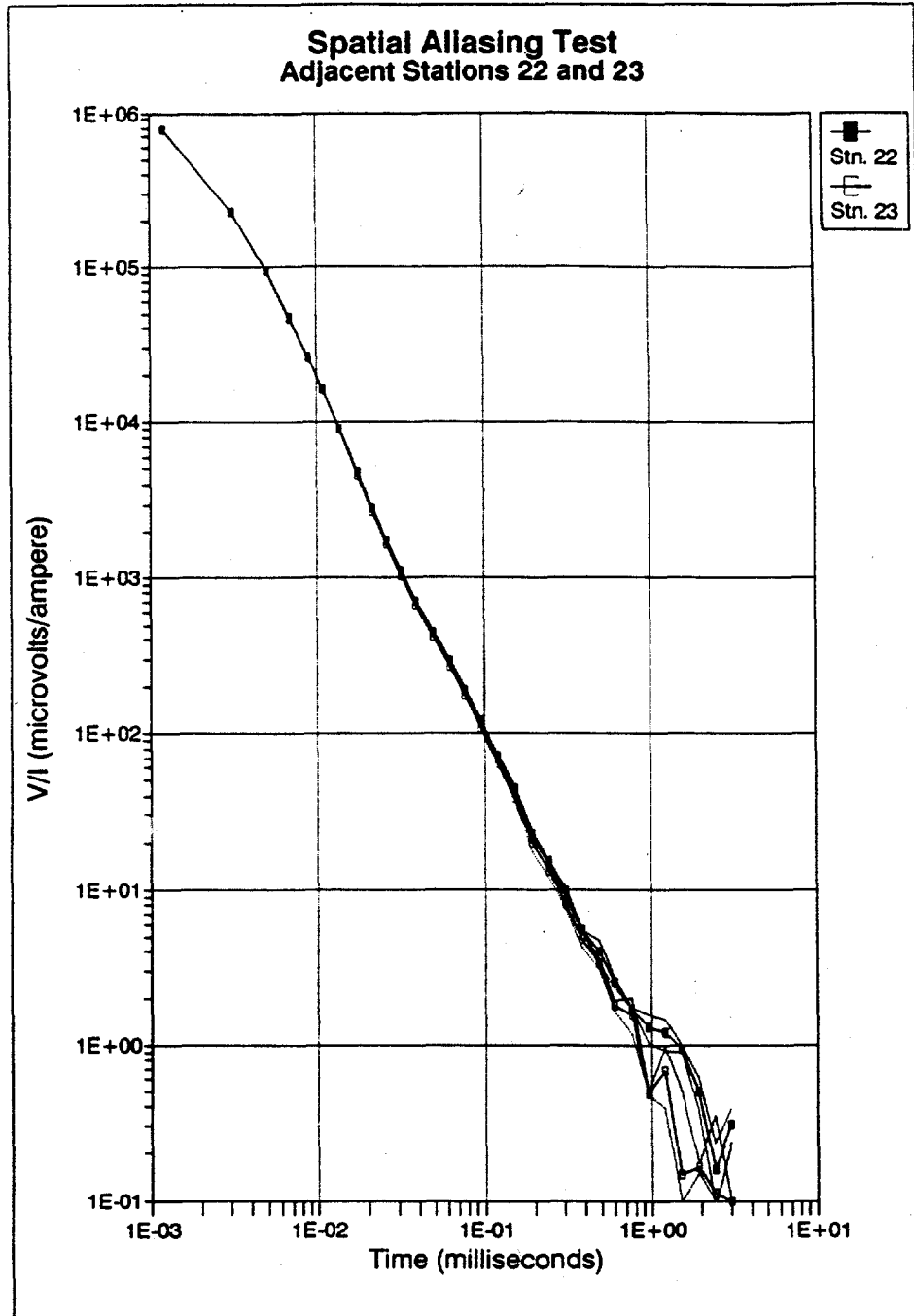


Fig. B-2. Spatial aliasing between adjacent stations 22 and 23.

*Technical Memorandum  
Geophysics Study to Characterize Geology  
NAS Memphis - Appendix B  
27 January 1995*

---

**This page intentionally left blank.**

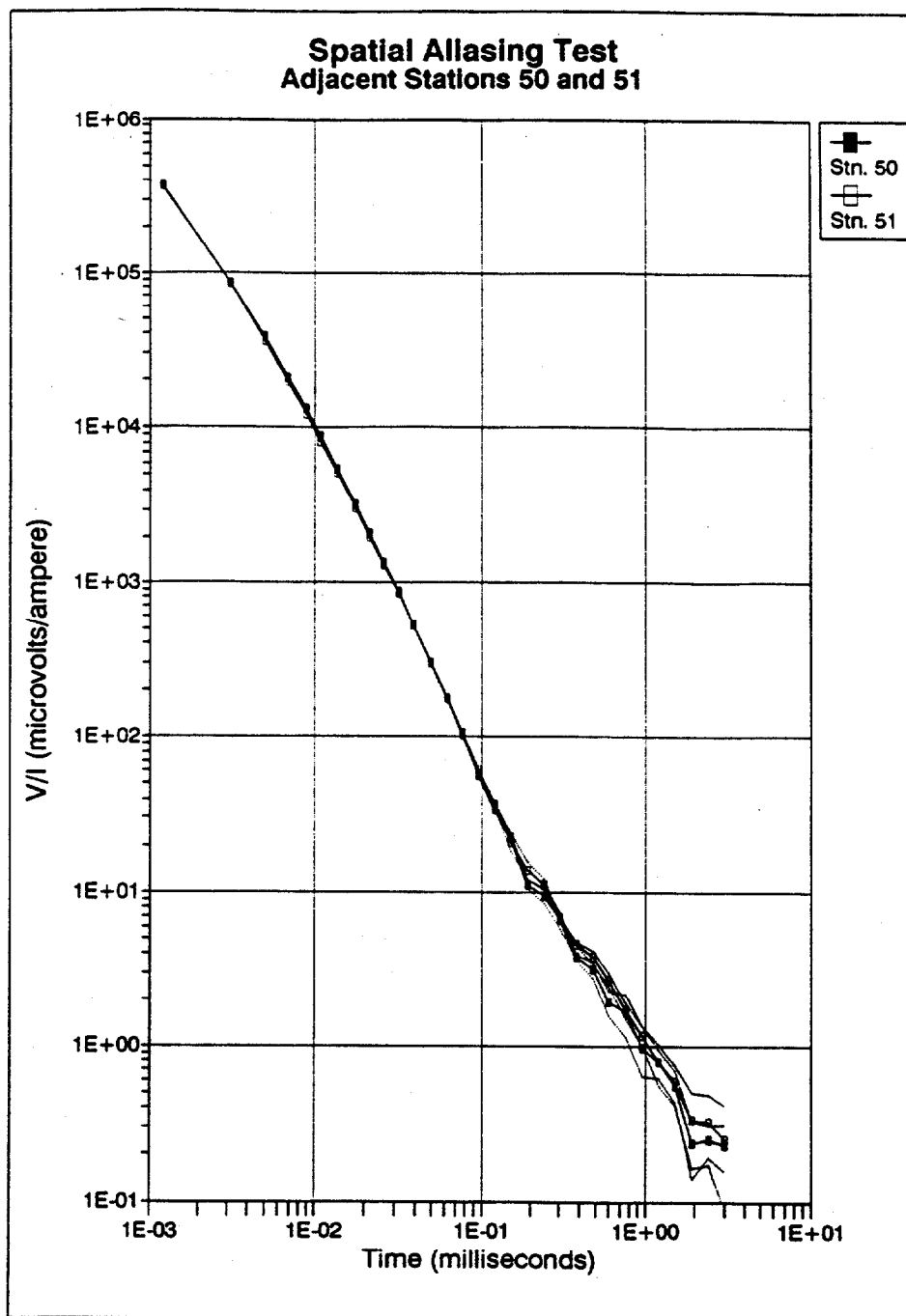


Fig. B-3. Spatial aliasing between adjacent stations 50 and 51.

*Technical Memorandum  
Geophysics Study to Characterize Geology  
NAS Memphis - Appendix B  
27 January 1995*

---

**This page intentionally left blank.**

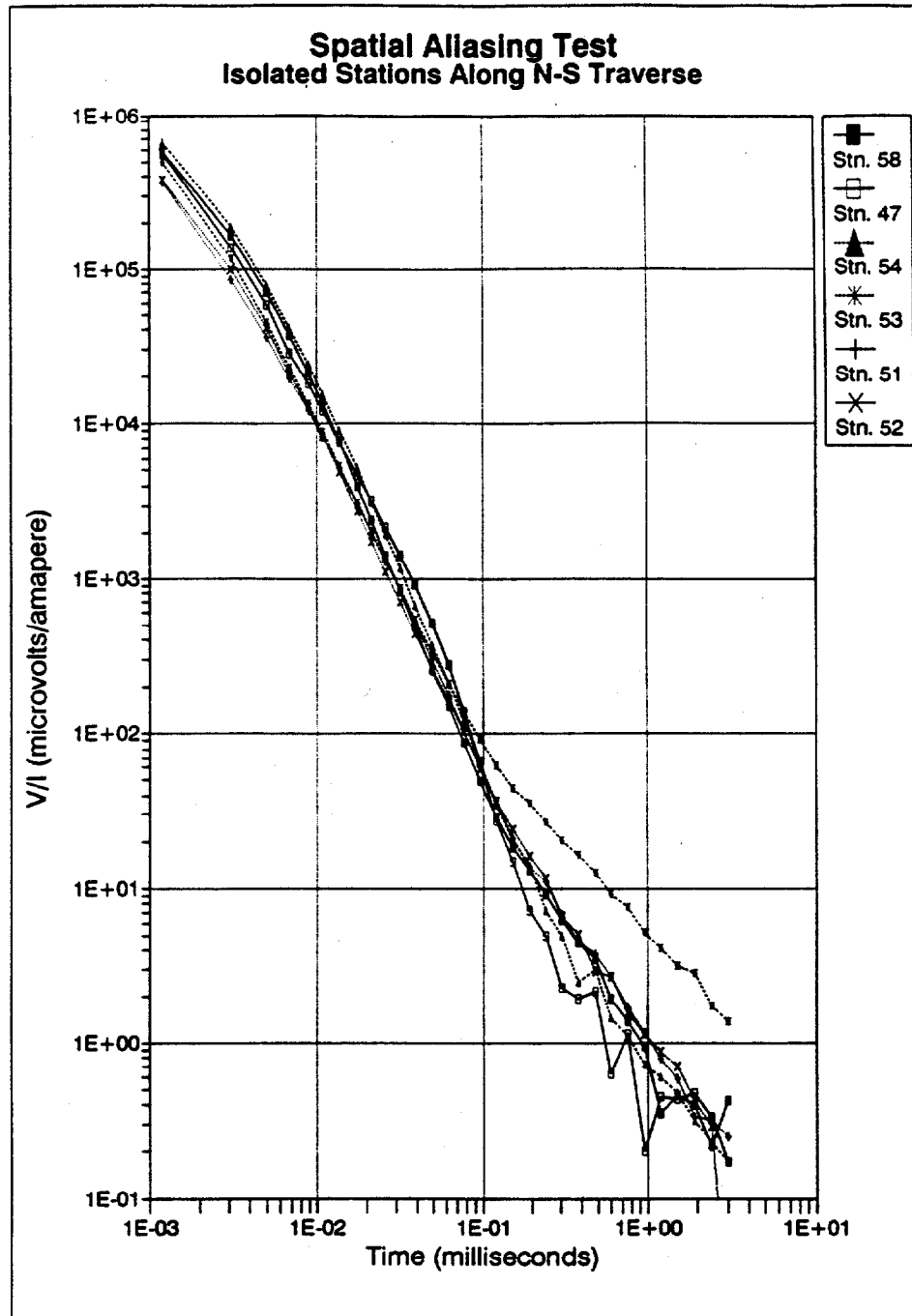


Fig. B-4. Spatial aliasing along a north-south traverse in which stations are spaced some 100 to 300 m apart. The data are a test of larger-scale aliasing.

**This page intentionally left blank.**

(text continued from page B-6)

noise envelopes have been omitted for reasons of clarity. This plot shows the aliasing expected for the typical case of 100 to 300 m separations between soundings. Moving from south to north (stations 58 to 52), one can see a small but quite definite change in the decay curves. The changes are not smoothly progressive from south to north, but jump around — a typical aliasing phenomenon. One station (53) shows a change in the late-time data suggestive of a strong conductor at depth. Clearly there is significant *large-scale* aliasing in the data set.

The critical question is: how significant is the impact of aliasing on the practical interpretation? To answer this, one must define a minimum target size. The objective is to map larger-scale geology to provide a conceptual model for evaluating the transport of potential contaminants. While smaller structures are of some interest, the primary objective is to map larger, aurally contiguous features, with dimensions of several hundred meters. From Figure B-4 it can be seen that some degree of aliasing is expected at this scale. A simple check can be performed by examining plan-view plots for a pattern of disconnected one-point anomalies without any spatial coherency, perhaps superposed on coherent large-scale patterns. An examination of Figures 13 to 23 shows few such signs of aliasing. Instead, the plots show mostly coherent patterns which are sampled by several soundings or more. The conclusion is that aliasing is certainly present in the data set but does not harm the overall interpretation of large-scale structure, such as downdropped fault blocks, thinnings of layers, and erosional formation surfaces; however, aliasing is a problem in characterizing small-scale structures such as local clay lenses. In any case, one-point anomalies should be interpreted with more caution than multiple-point anomalies.

#### 4.0 Cultural Bias

TEM can be strongly affected by *culture* — artificial conductors or harmonic noise sources at or below the surface. Cultural effects on TEM data can be divided into two categories: data scatter and data biasing.

*Data scatter* is produced by powerlines and other signal sources which produce or carry electromagnetic signals in the spectral range at which measurements are obtained. Examples include high-order harmonics of the 60 Hz powerline frequency, communication signals, and cathodic corrosion protection on some underground steel pipes. The frequencies of most of these signals are regulated only to within a few percent and amplitudes can vary significantly, resulting in data scatter. If the noise is random, it is overcome by increased stacking and averaging; if it is periodic, the scatter problem becomes a bias problem, as discussed below.

By carefully monitoring data scatter in the real-time data, stack length was optimized to produce minimal data scatter at most stations.

*Data bias* is by far the most difficult problem caused by culture. Bias is caused when the electromagnetic signal couples into metal culture, producing a spurious, usually conductive response. If the operator is unaware of the presence of the culture, the data might be erroneously interpreted as an anomalously conductive subsurface. This could, for example, cause a conductive horizon to be interpreted at an erroneously high elevation.

Although culture is an important problem in TEM interpretation, it has been virtually ignored in the literature. There are no standard techniques for identifying or dealing with cultural influences. EnSafe has collected some 330 soundings in the last year, some of which were used to evaluate culture. These limited studies have shown that grounded metals, both above and below ground level, may have a noticeable effect on TEM data even when located 15 m or more away from the outer loop. While some soundings show severe disruption in the normally smooth sounding curves, others show no such obvious effects but instead have a slower decay, resulting in an erroneously low resistivity. The strongest effect is not in early time, as one might intuitively expect, but in mid-time. Based upon several field studies, layering information appears to be retained in such cases, but resistivity values for the layers, and to a lesser degree the depths to the layers, would be in error for one-dimensional models. If these preliminary findings are correct, even culturally affected data may still yield useful geologic information.

Sounding positions at NASM were designed to avoid culture, but the density of underground lines, coupled with the large area of diffusion of the expanding smoke ring, made it impossible to completely avoid cultural influences in some areas, particularly in the industrialized center of the study area. Some stations show obvious culture, with "bumpy" data in the mid-time part of the curves. Excessively disrupted (but repeatable) data were encountered in a well-defined zone on the west part of the study area, in open plowed fields where no culture is indicated on the facility maps. Interviews with maintenance officers of the nearby communications network, which roughly encloses the problem area, indicated that the network utilizes megaHertz-range frequencies — far above the TEM frequency range. It might be speculated that some sort of beat frequency between two signals with slightly different frequencies might have caused the trouble, but at present the noise source is unexplained. Strongly affected stations have been removed from the database used for interpretation.

Figures B-5 through B-8 show four spatial aliasing tests at known or suspected culture sites. Figure B-5 shows data from a triple-winged butterfly traversing the edge of a thick concrete taxiway for jet aircraft. The concrete is reinforced and has numerous imbedded tie-down loops. Station 36 is in grass away from the taxiway; station 37 is half on grass and half on the taxiway; station 38 is entirely on the taxiway. As the TEM array moves onto the taxiway, the decay curve shifts upward, mostly in mid and late times. One might erroneously interpret a more conductive ground beneath the taxiway. Clearly the data are responding to the metal rebar grid in the concrete, which acts as a semi-infinite conducting sheet. Note that the absence of disruptive bumps in the decay curve would make it hard to identify the culture problem here without the aid of dense spatial data provided by the triple butterfly.

Figure B-6 compares TEM soundings 14 and 15, located in an industrialized part of NASM south of the runway control tower. Both show a small bump around 0.01 msec, indicating a slight cultural influence, and then diverge smoothly in later times. Since these soundings are in a butterfly pattern, it is hard to maintain that this strong divergence is geologic in origin. Instead, the downward- and outward-expanding TEM smoke ring seems to be energizing more and more off-line culture with increasing time.

Figure B-7 shows a butterfly at stations 32 and 33, in a golf course west of the Navy Hospital. Station 32 was inadvertently located over a water line, believed to be metal, and shows a characteristic bumpiness. Station 33 is off the water line and is smoother in response. Note the longer transient (upward shift) of station 32, which translates into an erroneously low resistivity for that station. The station was eliminated from the database because of clear culture problems.

A final example is six soundings made near USGS test hole 1 (Figure B-8). Stations 1 and 3 are a butterfly, and station 2 is halfway between them; stations 9, 34, and 89 are located in the general vicinity. Although one would expect relatively similar geology beneath all these soundings, the curves show a great deal of variation. Station 1 shows a classic culture bump which disappears toward station 3; it also shows a shift in the decay curve. The other stations show no strong bumps but decay at different rates. Though these stations are more widely spaced, such variability raises a question of how much the mid and late time data are affected by culture.

*(text continued page B-10)*

**This page intentionally left blank.**

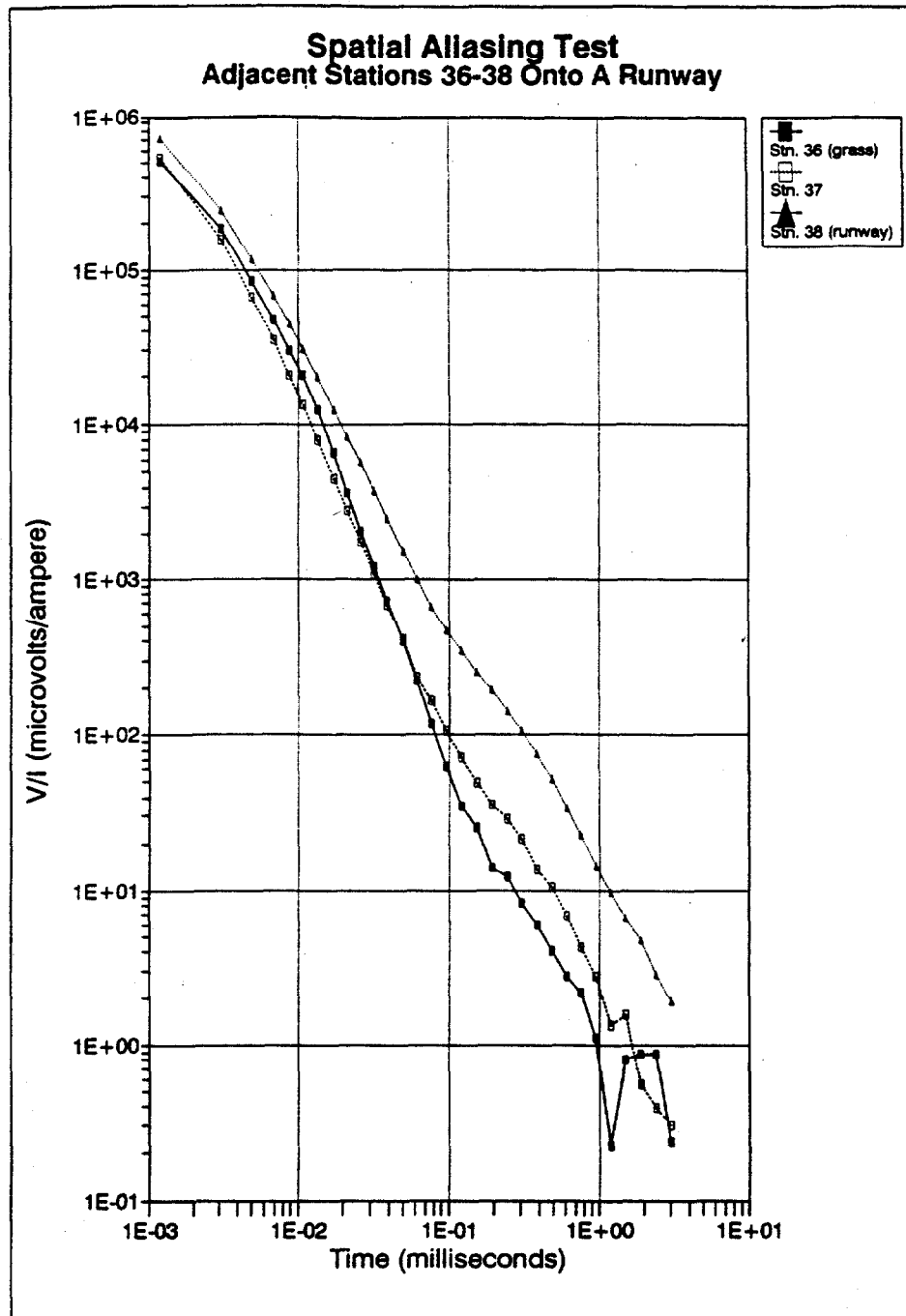


Fig. B-5. Culture test: data taken over a jet taxiway. The station on the taxiway shows a strong transient (upward shift in the decay curve). It is possible to erroneously interpret a conductive layer beneath this sounding. When the culture is not obvious, as with a buried pipeline, the potential for misinterpretation increases.

*Technical Memorandum  
Geophysics Study to Characterize Geology  
NAS Memphis - Appendix B  
27 January 1995*

---

**This page intentionally left blank.**

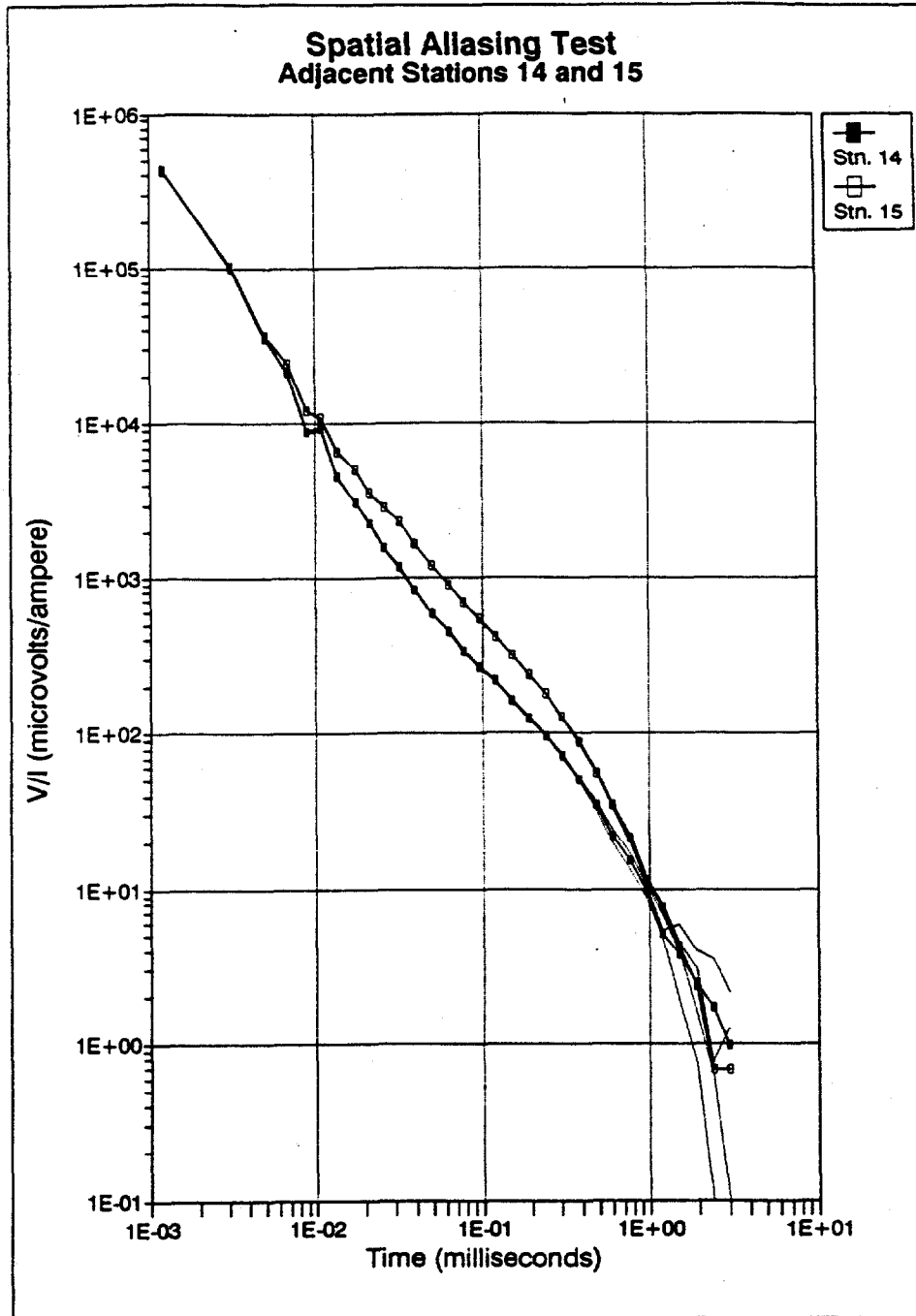


Fig. B-6. Spatial aliasing at stations 14 and 15. Aliasing is probably caused by nearby culture.

**This page intentionally left blank.**

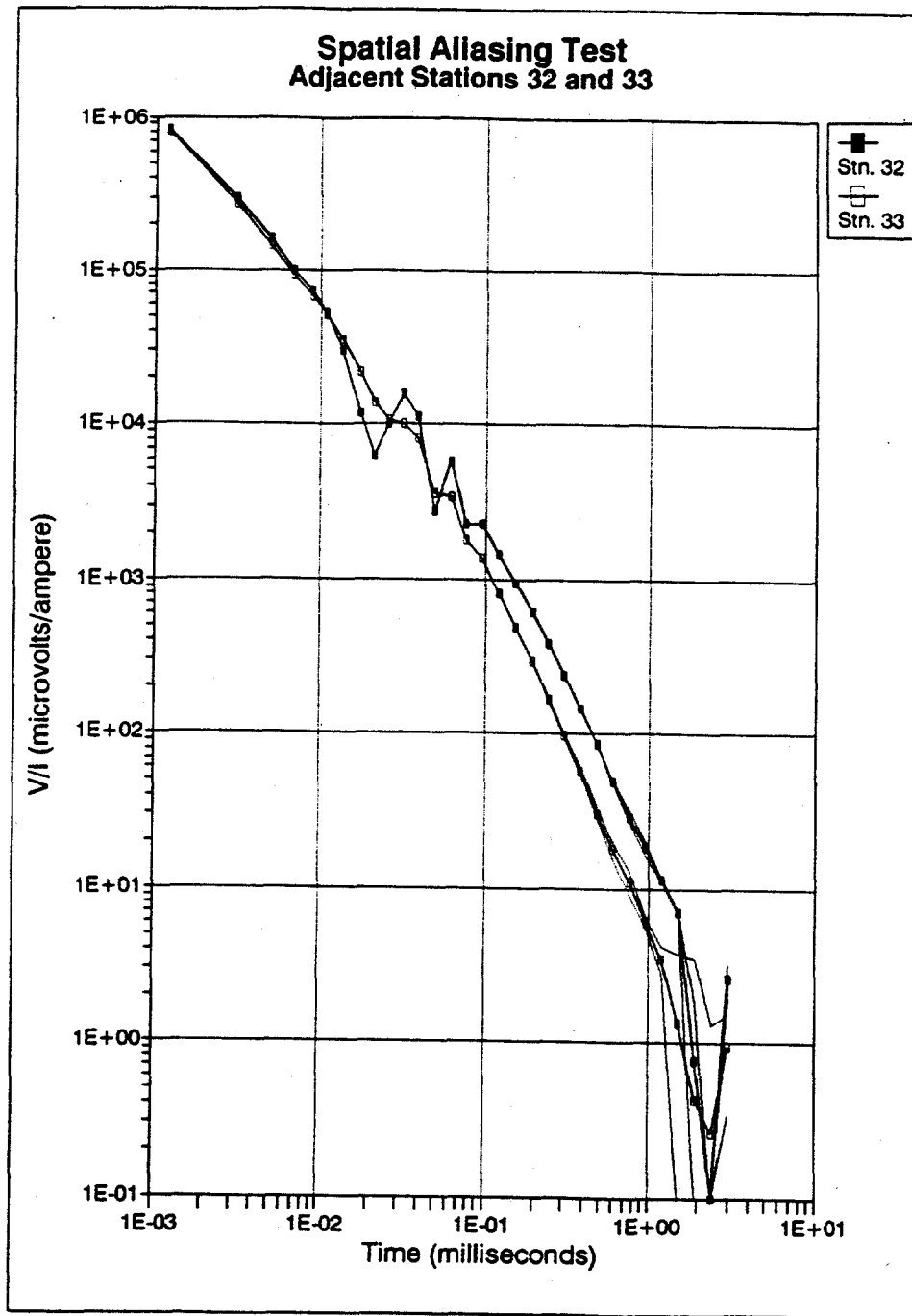


Fig. B-7. Apparent cultural influence at stations 32 and 33. Station 32 shows a characteristic disruption in mid time, followed by a prolonged decay transient (upward shift) in late time.

*Technical Memorandum  
Geophysics Study to Characterize Geology  
NAS Memphis - Appendix B  
27 January 1995*

---

**This page intentionally left blank.**

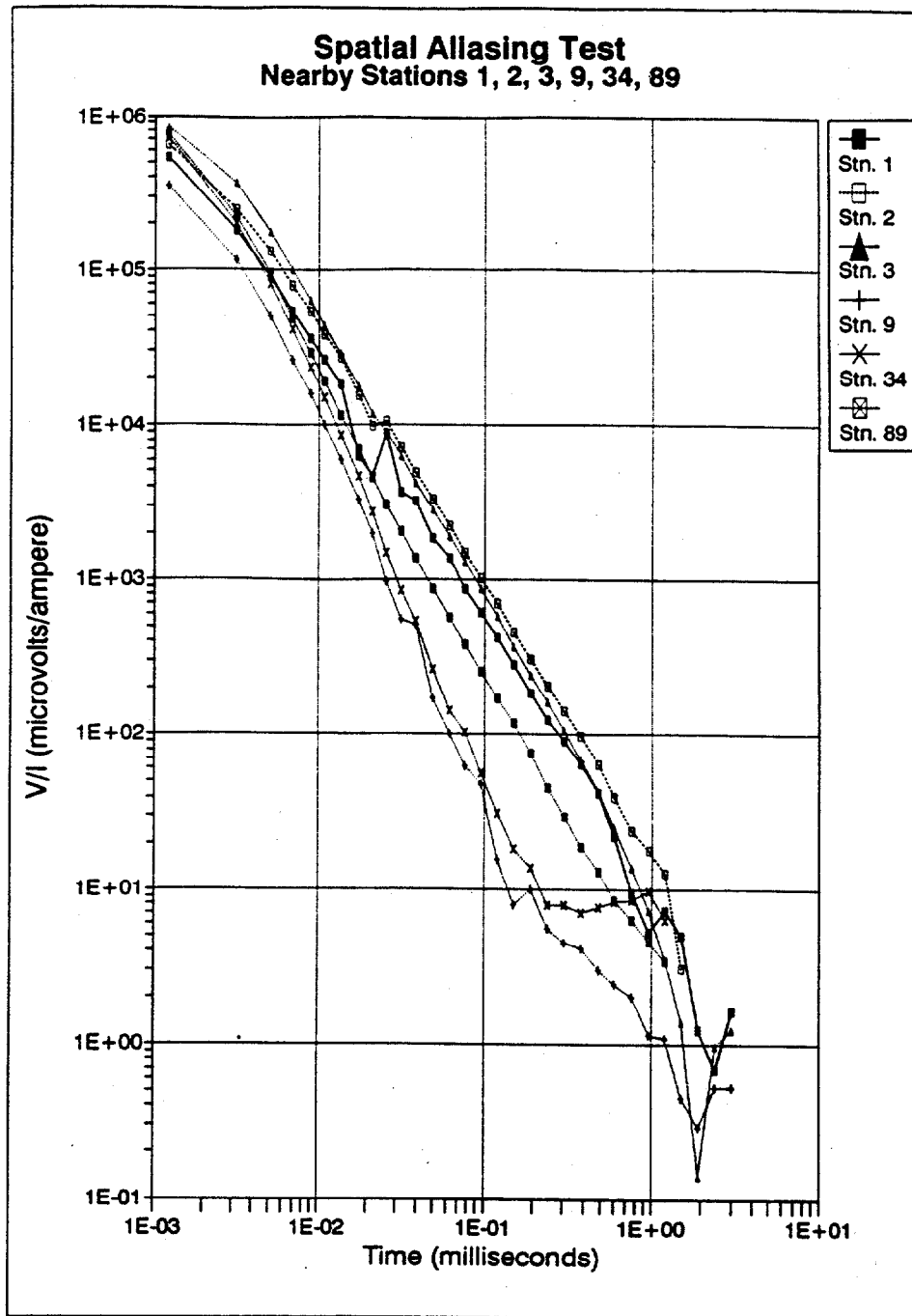


Fig. B-8. Apparent cultural influences at data taken in the vicinity of test hole TH-1. Such large changes in the transient curves is not expected as a pure aliasing effect, but instead is thought to be partly culture. While the disruption at station 1 is clearly culturally induced, the signs are not so obvious at the other stations.

**This page intentionally left blank**

A careful study was made of the influence of culture on the data. TEM soundings were located on Navy maps showing sewer, storm drain, electric, and water lines. Each sounding was reviewed on the basis of three criteria: (1) evident bias or bumpiness in the data; (2) radical departures of curve character from that of curves from nearby stations, with particular attention to anomalously long transients; (3) proximity to potentially biasing culture, especially buried metal lines. In general, curves which failed one of the three tests were rejected from the data base. The model results from the remaining data were then plotted in plan view and the results were subjected to test (4): examination of plots for unusual bullseyes, patterns, and gradients. Suspect areas were then re-examined for culture. In the end, 72 data points of the original 90 were retained as a final data set. Although soundings with evident cultural bias have been rejected, it is likely that subtler effects are present in some of the retained data.

### 5.0 Maximum Depth of Soundings

While equation A-3 might suggest that depth penetration can be controlled to a virtually unlimited degree by varying the measurement time, there is a practical limit to the latest times at which significant information can be obtained. That limit is controlled by competition between signal strength (response of geology to the downward-travelling smoke ring) and noise (interference from spurious electromagnetic signals, instrument noise, etc.). A useful measurement of this competition is the *signal-to-noise ratio*. As the smoke ring gets deeper, it decays in strength, and the signal-to-noise ratio gets smaller. This determines the maximum sounding depth. Measurements at later times would consist entirely of noise, which could be misinterpreted as a real earth response at depth. Clearly, it is important to establish the maximum depth of each sounding to determine if deeper units are detected or not.

Spies and Frischknecht (1991) give an approximation to the maximum penetration  $D_{\max}$ :

$$D_{\max} \approx 0.5 \left( \frac{IA\rho}{\eta_v} \right)^{1/5}, \quad (\text{B-1})$$

where  $I$  is the current,  $A$  the loop size,  $\rho$  is the ground resistivity, and  $\eta_v$  is the threshold noise of the instrument system, which Spies notes is often around  $5 \times 10^{-10}$  V/m<sup>2</sup> for modern digital instruments. The actual noise threshold will vary according to the type and degree of ambient field noise, instrument filtering and digitization schemes, and digital dynamic range.

A system's dynamic range is of paramount importance to determining the maximum depth penetration. Dynamic range is the difference between the smallest and largest signal the instrument can measure. In modern instruments, an analog signal is measured electronically by digitizing it, which is converting the signal to binary signals that can be read by a computer. The signal is digitized by factors of  $2^n$ , where  $n$  is the number of bits of accuracy. For example, an instrument with 16 bit capability can divide a signal of some amplitude  $V_0$  into  $2^{15}=32,768$  parts (the first bit is used for sign). In this case, the digitization error is  $1/32,768$ , and the amplitude is extremely well resolved. However, late-time TEM measurements run into trouble when the signal decays such that resolution drops below one bit of accuracy.

To determine the true dynamic range of the data, consider first an ideal, noise-free decay curve. The Zonge receiver obtains an analog signal of some amplitude  $V_0$  in the first time window, and adjusts the digital gain until  $V_0$  is strongly resolved with 15 bit ( $2^{15}$ ) resolution or accuracy. As the signal decays, the digital resolution of the rapidly diminishing signal decreases because it is measured by the fixed gain, which is referenced to the original voltage (automatic gain-ranging cannot be used for microsecond-range acquisition due to capacitive distortion of electronic components). For example, when the signal has decayed by a factor of 128, say from 1 volt to 7.8 millivolts, the digital resolution has decreased by  $128=2^7$ , or 7 bits, giving a net resolution of  $15-7=8$  bits. Once the signal has decayed by  $2^{15}$  (15 bits, or a factor of about  $10^{4.5} = 4.5$  decades), the digital resolution is zero bits and the noise-free signal is not detected.

Now consider the case where both signal and noise are present, illustrated schematically in Figure B-9. Suppose that an instantaneous, unstacked transient is measured. At any given time  $t$ , the measured voltage  $V$  is the sum of the transient decay signal  $V_s$  and the unstacked noise  $V_{n(u)}$ . In the early windows,  $V_s \gg V_{n(u)}$  and the sum is a noise-free decay curve. After 4 to 5 decades of voltage decay,  $V_s \approx V_{n(u)}$  and noise becomes an important factor. At some point the transient  $V_s$  drops below 1 bit of resolution. By itself, it would be undetectable, but the addition of positive noise spikes raises the total signal back over 1 bit and the signal is still partly resolved. This effect is known as signal *whitening*, which in effect extends the dynamic range of the instrument. Since  $V_s$  is positive, and  $V_{n(u)}$  has both positive and negative peaks, their sum has a slight positive *bias*, and the total decay curve takes on a more shallow slope. This is the "first slope break" noted in Figure B-9a. Finally, when  $V_s \ll V_{n(u)}$ , only noise remains, and the measured signal consists of rapidly varying positive and negative peaks centered about  $V=0$ . This is the "second slope break" noted in Figure B-9a. Only the strongest peaks reach the 1 bit digitization limit, so the resulting voltage jumps rapidly and erratically between positive and negative pulses, making an extremely noisy, flat voltage response.

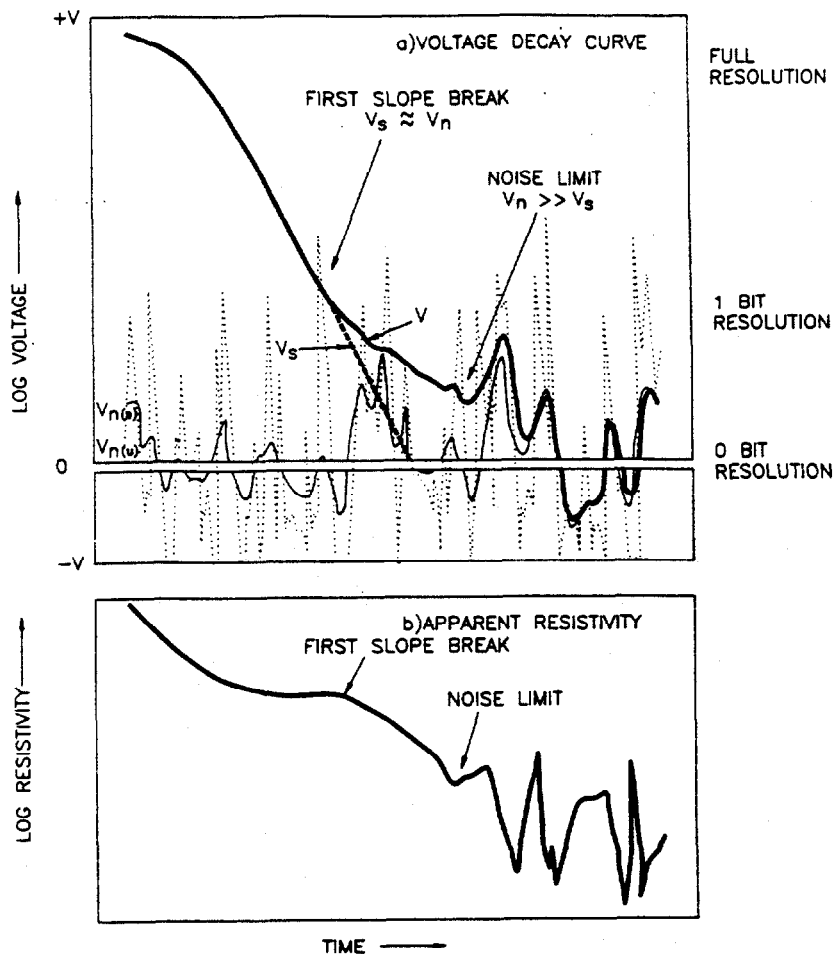


Fig. B-9. Schematic illustration of signal-depletion effects in late-time. Loss of analog and digital resolution causes an artificial slope break, giving an erroneous deep conductor. Later in time, only noise is measured.

Now consider what happens to the measurement when the data are stacked and averaged, assuming that noise is primarily random and high in frequency. Down to the first slope break, the noise is removed nicely by stacking. Near the second slope break, sub-1 bit peaks are not resolved, and the signal is aliased. Aliased random data can still be smoothed by extended stacking, but the field time required to do so would be prohibitive. Further, there is always a certain component of non-random noise which cannot be removed by stacking. Such noise begins to dominate the stacked signal somewhere between the first and second slope breaks. The

result of all this is a rather sudden and severe onset of noise in the stacked data around the second slope break.

Figure B-9b shows the corresponding behavior of the calculated apparent resistivity curve. Note that each slope break is accompanied by an artificial drop in resistivity which unrelated to the geology. Many times a one-dimensional model will yield unrealistically low resistivities at these depths, and there is a very real danger of misinterpretation.

The signal-depletion problem may be more widespread than is presently recognized. Although Spies and Frischknecht (1991) and others have discussed some aspects of the problem, late-time peculiarities are routinely attributed to three-dimensional conductors located away from the loop. As an example, Goldman et al. (1994) and Newman et al. (1987) have noted a steep resistivity increase and, in some cases, a sharp decrease in late-time TEM data, which cannot be reproduced with one-dimensional models but are explainable by three-dimensional conductive bodies at depth. This is certainly a valid observation, but nearly every TEM data set one might encounter, regardless of geographic location, shows a late-time drop in resistivity. Hence one cannot conclude that all such effects observed in the field are from deep conductors. Instead, signal depletion seems to be the culprit.

Figure B-10 shows signal depletion effects at station 58. Both the decay curve and the apparent resistivity curve are shown; the dotted lines show the noise envelope ( $\pm$  one standard deviation). The slope of the steep decay curve is relatively constant until the first slope break around 0.1 msec. Here the signal is whitened, extending the system's dynamic range, while noise is suppressed by stacking and averaging. Around 1 msec, the sounding encounters the second slope break, characterized by a rise in noise. Note the steep, artificial resistivity decline associated with the first slope break.

The key to interpreting late-time TEM data is to recognize where the slope breaks occur. Equation A-2 can be written from Spies and Frischknecht (1991) to show that the time of signal depletion  $t_{\max}$  is:

$$t_{\max} = 1.9 \times 10^{-7} (IA)^{2/5} \rho_o^{-3/5} \eta_v^{2/5}, \quad (\text{B-2})$$

where  $\rho_o$  is the resistivity of the overlying material (assumed to be homogeneous). Since  $I$ ,  $A$ , and  $\eta_v$  are constants, they are grouped for convenience as constant  $K$ , and one has  $t_{\max} = K\rho_o^{-3/5}$ . By plotting the times of the first slope break versus the resistivity at that break for a large data set, one can test the data for effects of signal depletion.

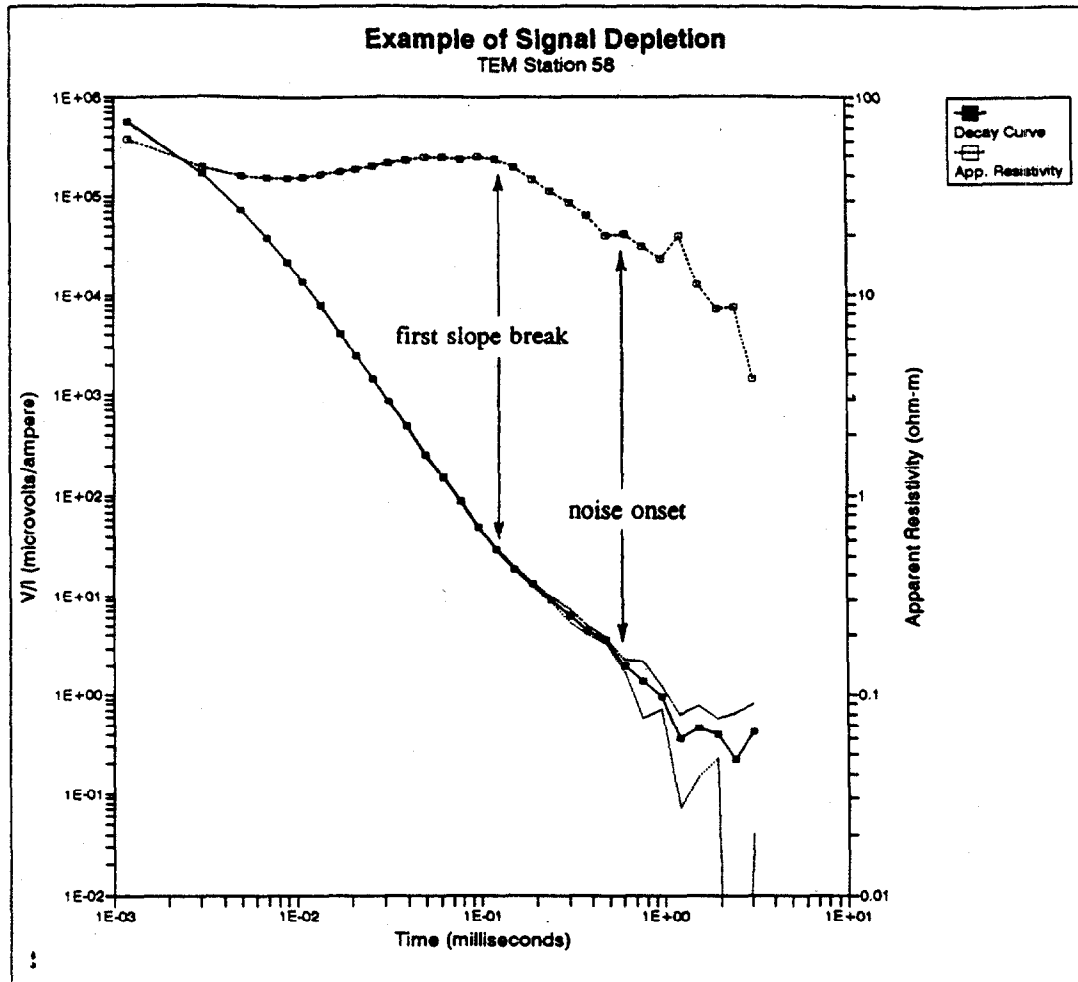


Fig. B-10. Field example of signal-depletion effects.

Figure B-11 shows a time-versus-resistivity plot of the first break for data at NAS Memphis. The plot includes only stations where the break was well defined and which are thought to be free of cultural effects (44 stations). A power curve fit yields  $t_{max} = 12.39\rho_o^{-1.59}$ , which differs significantly from the theoretical  $\rho_o^{-0.6}$  response. There is a good deal of scatter in the data (the correlation coefficient  $r$  is -0.56). Part of this is undoubtedly the result of errors in picking the exact time of the slope break (about  $\pm 50$  percent), modest errors in model-determined resistivity, and the fact that the overburden resistivity is not uniform. In addition, the data have the appearance of having more than one population, and a slight skewing of the points is observed

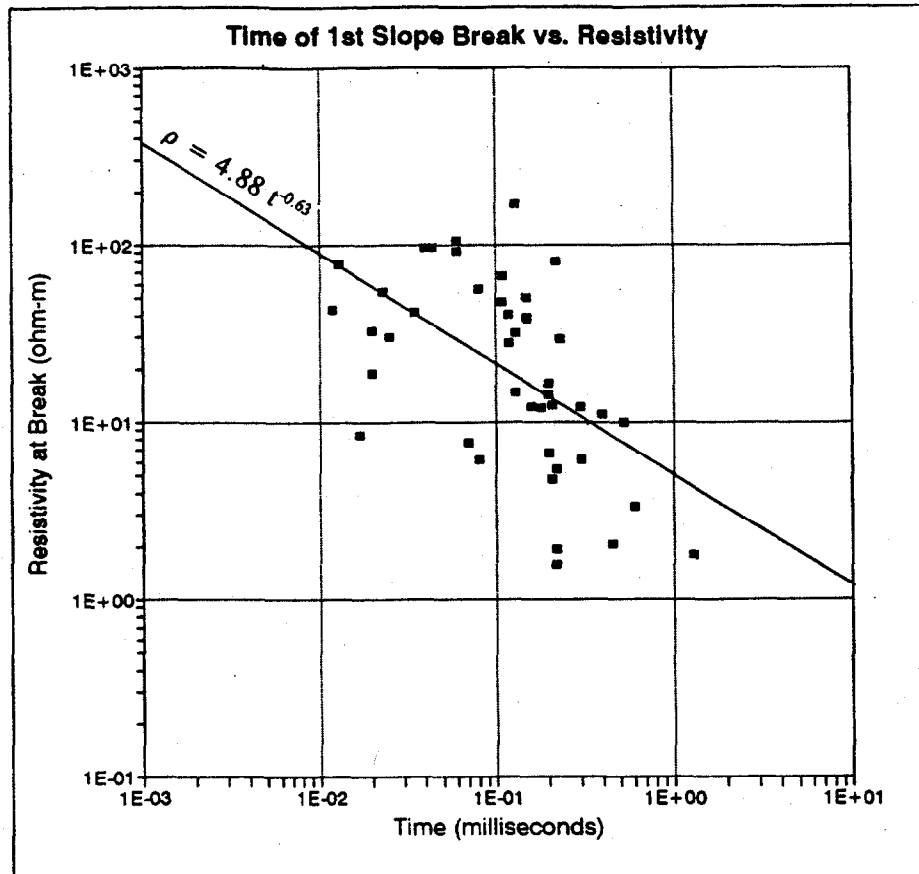


Fig. B-11. Time of the first slope break versus resistivity. The fit to the data is close to the theoretical relationship, but there is considerable scatter in the data. The conclusion is that deep TEM data at NAS Memphis are affected by signal-depletion, but many soundings still accurately identify deeper conductors. See text for explanation.

depending on the vertical separation between the depth of the Cook Mountain conductor and the depth at which signal is lost. However, the mismatch and the scatter are still larger than one might expect from these types of errors, suggesting that real geologic changes, not just signal-depletion effects, are being measured. The success in picking the Cook Mountain top, described in Section 4 of the report, supports this conclusion.

A similar plot for the second slope break is unreliable because the resistivities are artificially biased by the effects accompanying the first slope break.

Assuming one accepts that the first break is primarily influenced by geology, and that data at the second break are purely noise, the effective maximum penetration depth lies somewhere between the first and second slope breaks. Since there is no firm guideline to selecting the maximum depth, the determination is somewhat arbitrary. To maintain consistency, a strategy was devised to select the lower limit of each sounding. The lower limit was constrained to the shallowest of three criteria: (1) the second slope break/noise onset; (2) layer resistivity less than  $0.1 \Omega \cdot \text{m}$ ; (3) curve irregularities or noise that jeopardize model stability; (4) unacceptably poor range of equivalence in depth or resistivity parameters. All data parameters used for this report are terminated at the shallowest depths where one of these criteria are met. The cross-sections (Figures 8 to 10) illustrate the maximum penetration depths obtained by the above strategy.

**This page intentionally left blank.**

## **6.0 References**

Goldman, M., Tabarovsky, L., and Rabinovich, M. (1994). On the influence of 3-D structures in the interpretation of transient electromagnetic sounding data. *Geophysics* 59, 889-901.

Newman, G.A., Anderson, W.L., and Hohmann, G.W. (1987). Interpretation of transient electromagnetic soundings over three-dimensional structures for the central loop configuration: *Geophysical Journal of the Royal Astronomical Society (Geophysical Journal International)*, 89, 889-914.

Spies, B.R., and Frischknecht, F.C. (1991). Electromagnetic sounding: in Nabighian, M.N., Ed., *Electromagnetic Methods in Applied Geophysics*, v.2A: Society of Exploration Geophysicists, 285-425.